GHT CONSULTING SCIENTISTS

Tutuka Power Station
ASH STACK POLLUTION PLUME MODEL
FINAL REPORT
AUGUST 2010

for

Eskom

TUTUKA POWER STATION

by

GHT CONSULTING SCIENTISTS

PROJECT TEAM
L.J. van Niekerk
S. Staats

Project no.:	002-18-mod.571	Start Date:	November 2009
Report no.:	RVN 571.1/1014	Report Date:	August 2010

05 August 2010   Our ref.:   RVN 571.3/1072
The Manager
Tutuka Power Station
Private Bag 2016
Standerton
2430

FOR ATTENTION: Mr E Janse van Rensburg

Dear Sir

Ash Stack Pollution Plume Model - 2010

It is our pleasure in enclosing the report RVN 571.3/1072 "TUTUKA POWER STATION, Ash Stack Pollution Plume Model - 2010"

We trust that the report will fulfil the expectations of the Power Station and we will supply any additional information if needed.

Yours sincerely

Louis J van Niekerk (Pr.Sci.Nat.)

Copies: 1)   2 Copies to E Janse van Rensburg – Engineering Department
                        Tutuka Power Station, Private Bag 2016, Standerton 2430.

Table of Contents

1 INTRODUCTION

1.1 BACKGROUND

A dry ashing system is currently in operation at Tutuka Power Station, a coal fired power generation facility located approximately 20 km north-northeast of Standerton, Mpumalanga Province. Brine from the SRO plant is generally added to the ash at the power station site so that the quantity of material lost from wind action during transport along conveyors to the pile is minimized.

The ash stack at Tutuka Power Station has been a source of concern for the past few years, with respect to leachate generation potential. A large monitoring borehole field has been established around the ash stack and the pollution control dam system during the life of the power station (refer Appendix A Map 1). Previous studies that were done in an attempt to evaluate groundwater contamination and hydraulic properties in the ash stack area are Rudolph, van Niekerk and Associates 1993; SRK 1996; Blight 1998, GHT Consulting Scientists 1998, Hodgson 1999, GHT Consulting Scientists 2000, GHT Consulting Scientists 2002 and GHT Consulting Scientists 2007.

In the past ten years, the disposal of brine from the SRO plant at Tutuka has increased on the front and back stack, as a result of increased volumes of mine water inflow at New Denmark Colliery. This has led to an increased salt and water loading on the ash stack. Flow through experiments with fly ash has indicated that this material is not suitable for retarding the movement of water. Despite the fine particle size of the ash, the physical and chemical structure and surface physical properties are very different to clays, thus resulting in a lower potential for retardation of fluid flow, relative to clays.

The combined issues of ash and brine disposal are of concern to Eskom management due to cost concerns and the potential negative effects inappropriate disposal methods can have on the environment. This study attempts to use all available data, along with field observations, to determine what the true extent of the pollution plume is.

Modelling of groundwater flow and pollution transport through the substrata is commonly done to predict the outcome of specific scenarios. Groundwater modelling is based on a sound understanding of the geology, geohydrology and hydrochemistry of systems, also considering topographic variations and the amount of recharge to the groundwater system.

Site Layout Plan
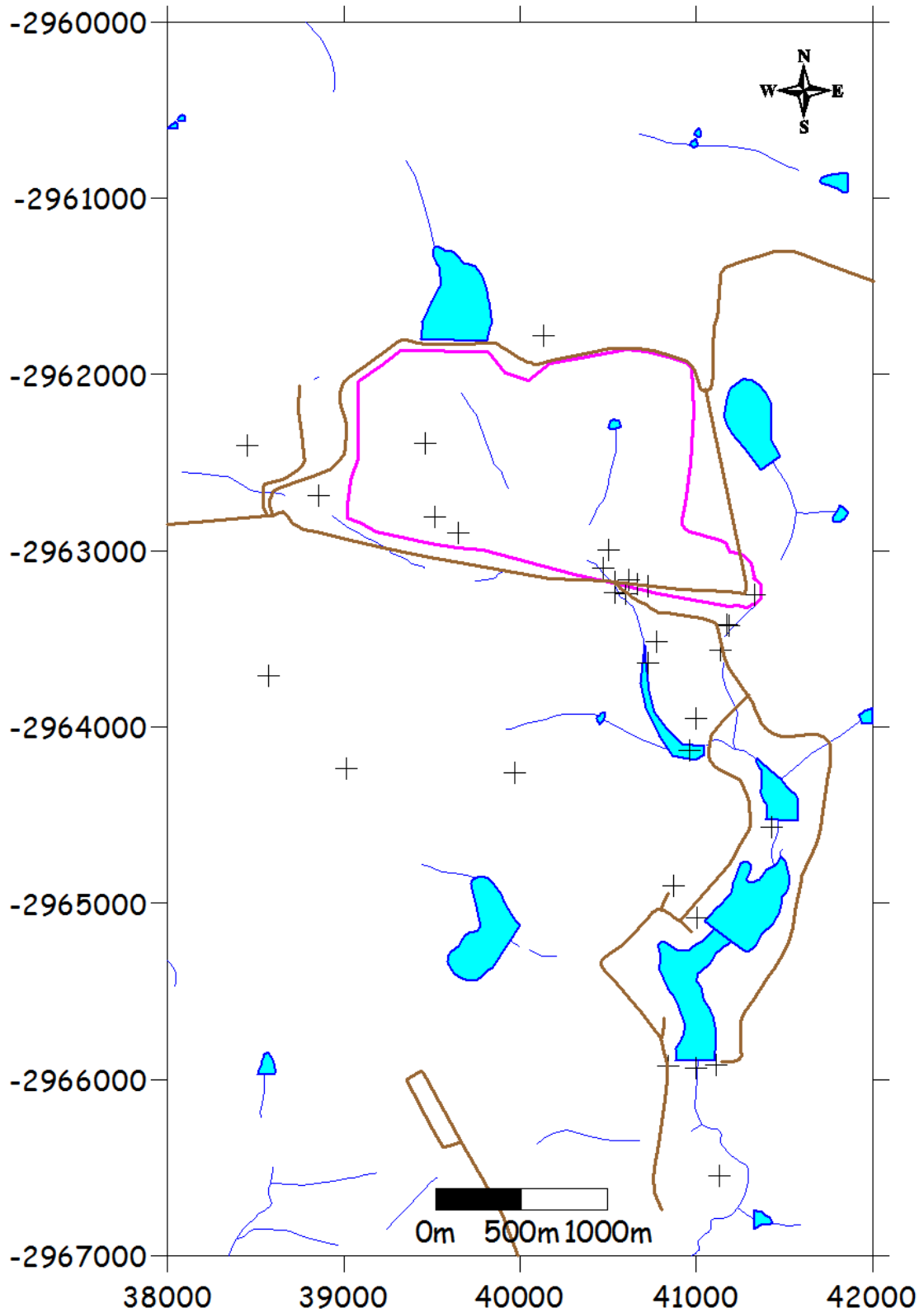
Figure 1.   Site layout plan of the area under investigation.
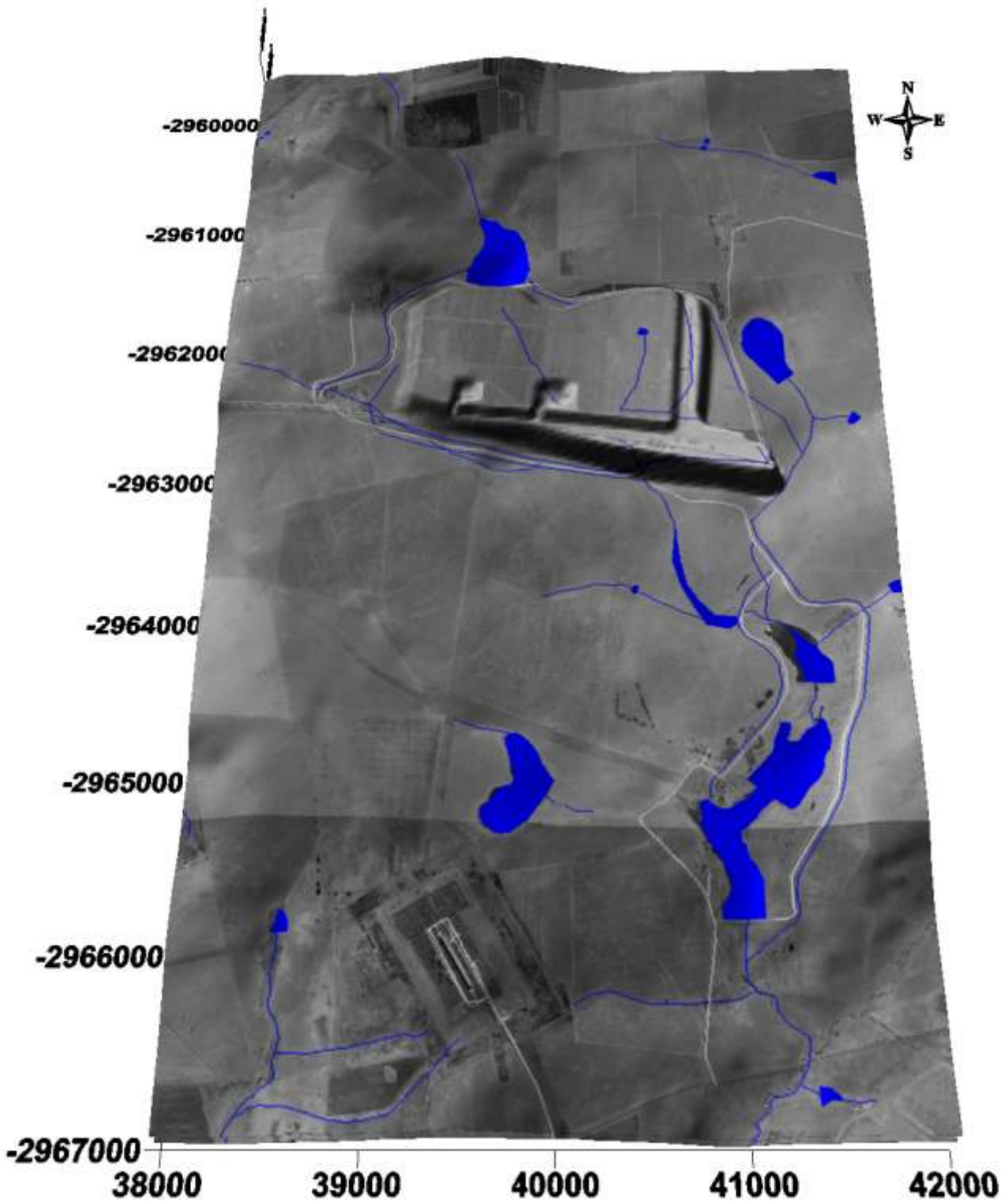
Figure 2.   3D Site layout plan of the area under investigation.

1.2   AIM

GHT Consulting Scientists was commissioned by Eskom to investigate the feasibility of the intersection of the pollution plume that occurs in the valley south of the ash stack. Specifically, GHT was commissioned to determine the following:

- The groundwater depths flow directions and rates;

- The depth of the pollution in the vicinity of the ash stack and downstream towards the Wolwe Spruit;

- The groundwater flow directions;

- The migration of the pollution plume to the south of the ash stack and the impact on the Wolwe Spruit;

- The ideal position and site of the interception scheme to be implemented;

- The optimal method for plume interception, with reference to establishing a dewatering trench or well field adjacent to the ash stack.

1.3 SCOPE

The most recent field investigations were undertaken in February, March and April 2010, and can be regarded as a continuation of previous studies undertaken at the site. Field investigations were commenced during the first week of February 2010, and subsequently completed by the 24th March 2010. All aspects of the investigation undertaken to date are reported here.

The scope of the current investigations was restricted to:

- A detailed magnetic survey to detect and delineate magnetic structures that may influence the groundwater regime by forming preferential pathways or barriers to groundwater flow. The results of the magnetic survey were to be used to site a number of monitoring boreholes in the vicinity of the ash stack;

- The installation of additional monitoring bores to use as pump and observations wells during pump tests;

- Determine the flow rates and permeabilities of the natural geology and ash stack by evaluating existing data, generate during previous investigations, and by performing permeability and pump tests on four newly drilled boreholes in the vicinity of the ash stack;

- EC profiling of the column of water of the four newly drilled boreholes to identify horizons along which preferential contaminant migration may be taking place. It is also done to correlate the different water strikes with zones of higher electrical conductivity to determine the optimal sample horizon which must be used during future monitoring events.

- Evaluate existing and current chemical and sampling data of boreholes and surface water sites in the vicinity of the ash stack to determine the extent and depth of the current pollution plume;

- Developed a conceptual numerical model of the ashing area and the ash stack;

- Use the conceptual model to test different rehabilitation and interception scenarios for the pollution plume.

2 FIELD INVESTIGATIONS

2.1 MAGNETIC SURVEY SOUTH OF THE ASH STACK

During March 2010 GHT Consulting conducted a magnetic survey in an area south of the Ash Stack at Tutuka Power Station. The purpose of the magnetic survey was to obtain information on the intrusive dolerite bodies known to occur in this part of the power station in order to site investigative, monitoring and high-yielding production boreholes. The investigative and monitoring boreholes will yield information on the geological and hydrogeological conditions at the site and will allow monitoring of contaminant plumes that may exist to the south of the Ash Stack. The production boreholes may in future be utilised to form a hydraulic gradient towards the Ash Stack in order to limit contaminant migration away from the Ash Stack.

2.1.1 Approach to the Magnetic Survey

As part of the magnetic survey to the south of the Ash Stack, the following actions were taken:

- Aerial photographs of the area under investigation were studied in order to identify any natural features that could indicate the presence of variations in the local geological conditions. Such features could include visible changes in the vegetation, the presence of rock outcrops and prominent topographical changes.

- An airborne magnetic map covering the area of interest was obtained and studied to identify large-scale magnetic features that may be indicative of the presence of geological structures in the area.

- Reports on past geohydrological investigations conducted in the area of interest were obtained and studied to allow better insight into the geological conditions that could be expected during the survey.

- A report on a two-dimensional resistivity survey across and in the vicinity of the Ash Stack was obtained and studied to identify changes in the subsurface resistivity distribution that may be indicative of the presence of geological structures.

- Ground magnetic data were recorded along four traverses to the south of the Ash Stack.

- The magnetic data recorded during the survey were interpreted in terms of the local geological and geohydrological conditions.

- Based on the interpretation of the geophysical data, targets for the drilling of investigative, monitoring and production boreholes were identified.

2.1.2 Geological Setting

The Ash Stack and study area occur within in an area underlain by rocks of the Karoo Supergroup, heavily intruded by dolerites of Jurassic age (refer to Figure 3). The Karoo rocks predominantly consist of sandstones, shales and coal beds of the Vryheid Formation, Ecca Group. The Ash Stack and study area are located in an area where a large dolerite sill extends to surface. A number of lineaments with south-west/north-east strikes have been mapped to the south-east of the study area,

the closest of which runs past the study area at a distance of approximately 1.5 km. These lineaments are in all likelihood due to prominent dolerite dykes.

Figure 3. Geological setting of the area under investigation.

2.1.3 **Geophysical Investigations**

During March 2010 GHT Consulting recorded magnetic data along four traverses within the study area, south of the Ash Stack. A report on a two-dimensional (2D) resistivity survey conducted during 2006 across and in the vicinity of the Ash Stack by Mr M. de Klerk was also studied as part of the geophysical investigations. The 2D resistivity data were recorded as part of an investigation by the Groundwater Group of the Department of Earth Sciences, University of the Western Cape (Towards the Development of Sustainable Salt Sinks: Fundamental Studies on the Co-Disposal of Brines within Inland Ash Dams and Dumps, December 2007). Some of the results of the resistivity survey are included in the current investigations.

The principles on which the magnetic and resistivity techniques operate are briefly described below:

Description of the magnetic method

Many earth materials contain magnetic minerals such as magnetite, ilmenite and pyrrhotite. When geological units contain such magnetic minerals, these units may become magnetised by the earth's magnetic field, and then have magnetic fields associated with them. These local magnetic fields that are due to the magnetised geological units will be superimposed on the earth's regional magnetic field. Measurements taken in the vicinity of magnetised geological units will therefore

show local variations or departures from the undisturbed magnetic field of the earth (called the regional field). These departures are referred to as anomalies. The shapes of the anomalies are dependent on a number of factors regarding the physical properties and dimensions of the magnetised geological units. By incorporating existing knowledge on the geological conditions at the site being surveyed, the magnetic anomalies recorded during a survey may be interpreted in terms of the local geological conditions.

The magnetic survey at the Ash Stack was conducted by GHT Consulting using the G5 proton magnetometer manufactured by Geotron.

Description of the resistivity method

The resistivity method is a non-invasive geophysical tool that can provide cost-effective answers to geological questions. The method is based on the fact that different geological units are more or less resistive to electrical current flow. A DC or slowly varying AC current is injected into the earth by means of pairs of grounded current electrodes. The voltage drops between pairs of grounded potential electrodes is then measured at selected positions. These voltage drops are dependent on the resistivities of the materials through which the electrical currents are flowing.

By assuming that the earth is homogeneous and isotropic, measurements of the injected electrical current and measured voltage drops, as well as the distances between the different electrodes, may be used to calculate an apparent resistivity for the earth at a specific position and (pseudo-)depth. The apparent resistivities recorded during a survey may be inverted to obtain a model of the resistivity distribution within the subsurface. The model resistivity distribution may now be interpreted in terms of the local geological conditions by incorporating known information on the geology of the site.

The resistivity surveys in the across and in the vicinity of the Ash Stack were conducted by Mr. M de Klerk using the Lund Imaging System with a Schlumberger geometry and a unit electrode spacing of 10 m.

2.1.4   Study of ortho-photographs

As part of the geophysical investigations overlapping ortho-photographs of the area under investigation were studied to identify any natural features that could indicate the presence of variations in the local geological conditions. Such features could include visible changes in the vegetation, the presence of rock outcrops and prominent topographical changes. The ortho-photographs of the study area are shown in Figure 4. Due to extensive agricultural and industrial activities, the near-surface material in the vicinity of the Ash Stack has been greatly disturbed. This precluded the identification of natural features at surface that could be indicative of changes in the near-surface geology.

Figure 4.   Ortho-photographs of the area under investigation.

2.1.5   **Study of airborne magnetic map**

An airborne magnetic map covering the area of interest was obtained from the Council for Geoscience. The airborne magnetic map is shown in Figure 5. A large number of prominent magnetic lineaments may be identified in the vicinity of the study area. These lineaments predominantly have west-south-west/east-north-east and north-west/south-east strikes, although some features also display south-west/north-east strikes. These lineaments are in all likelihood due to large-scale magnetic dykes.

The study area does not appear to lie on top of a dyke-like magnetic feature. The variable magnetic response within the study area is typical of an area underlain by an extensive dolerite sill.
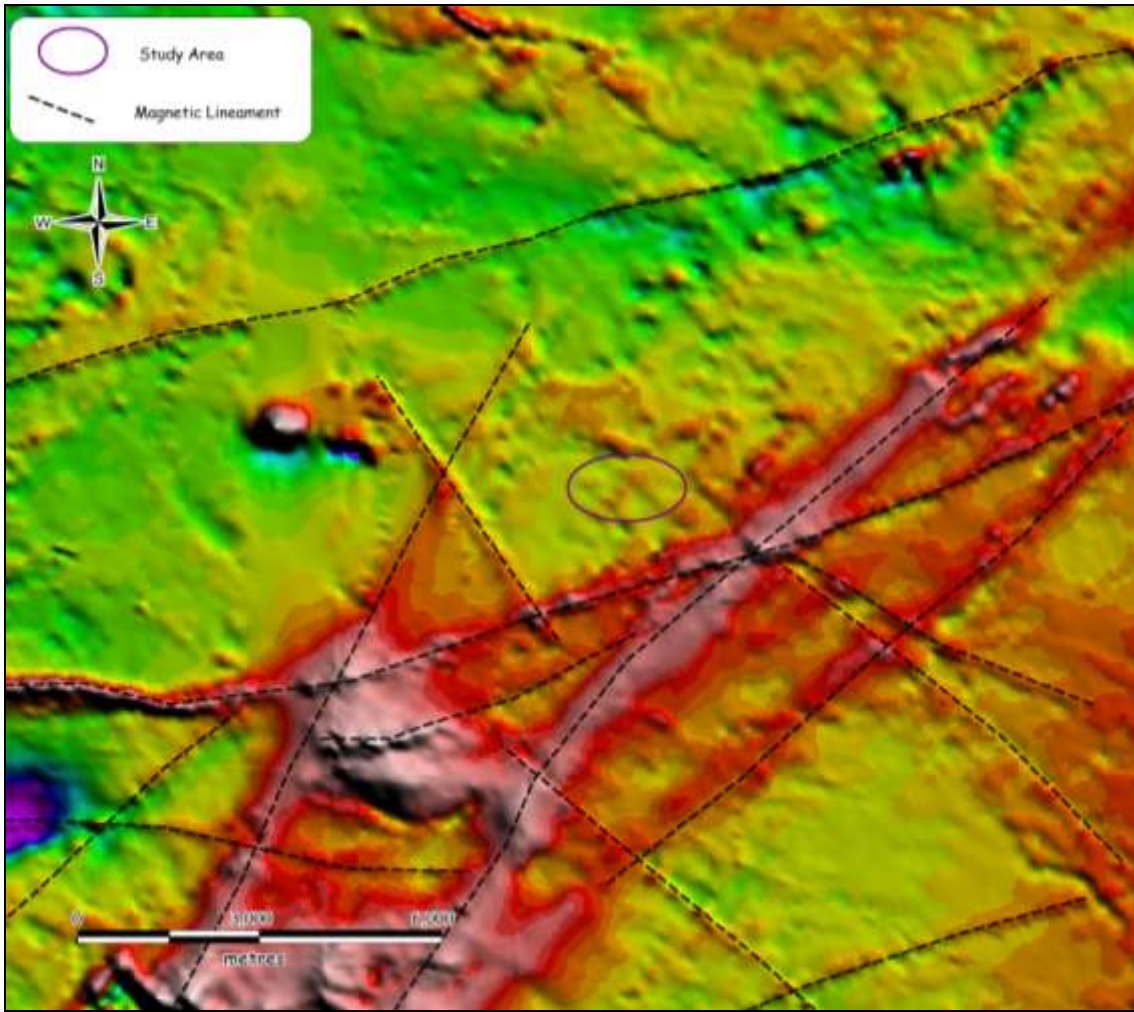
Figure 5.   Airborne magnetic map covering the area under investigation.

2.1.6   Two-dimensional resistivity survey

A two-dimensional resistivity survey across and in the vicinity of the Ash Stack was conducted by Mr. M de Klerk during 2006. The positions and orientations of the two resistivity profiles (P01 and P02) are shown in Figure 6.
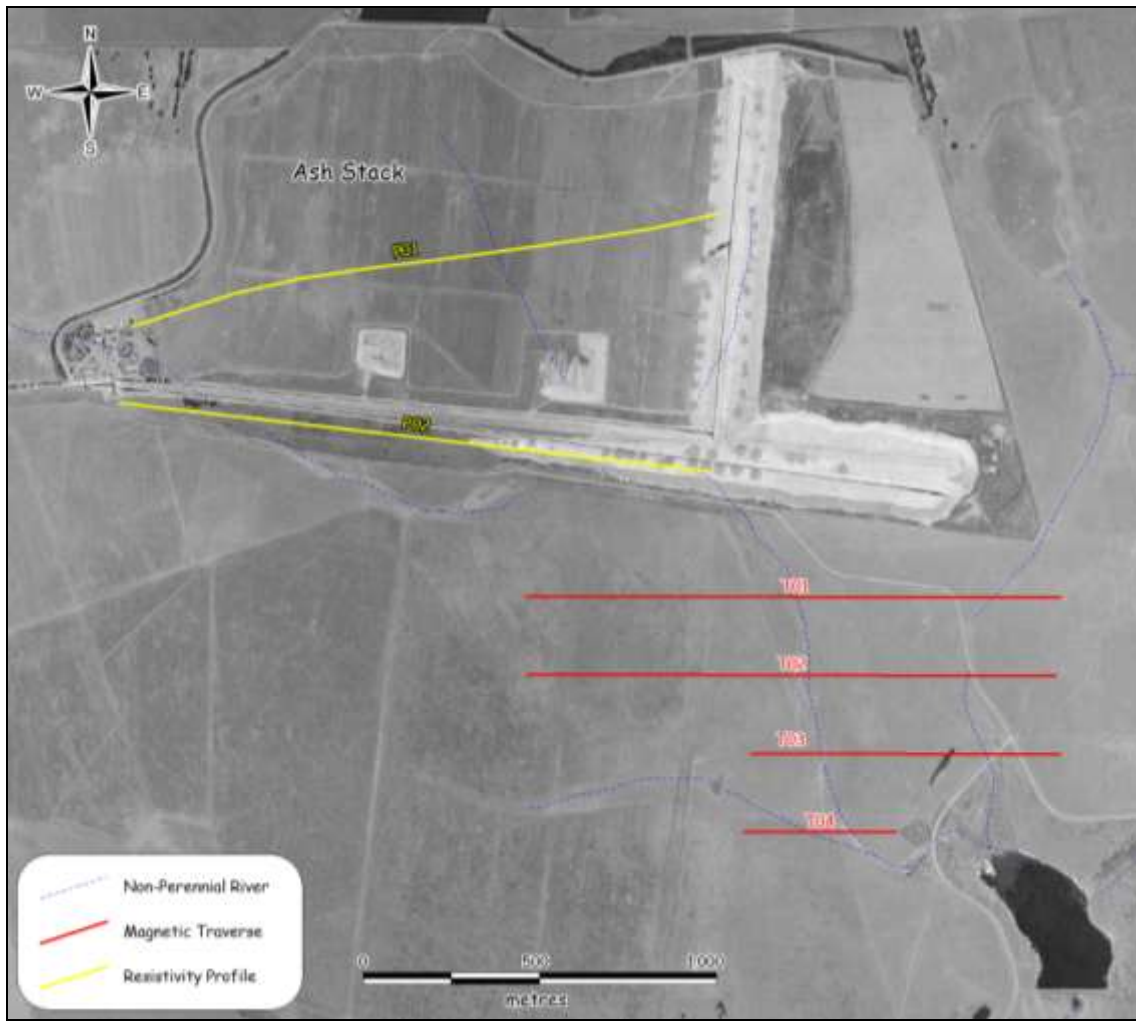
Figure 6.   Positions and orientations of the ground geophysics traverses and profiles relative to the existing infrastructure.

The inverted resistivity models compiled for profiles P01 and P02 are shown in Figure 7 and Figure 8, respectively. Of relevance to the current investigations is the apparent deepening of the bedrock near the position of the non-perennial river that is overlain by the Ash Stack (indicated by vertical dashed blue lines in Figure 7 and Figure 8). It therefore seems that the river may be associated with a geological feature that manifests itself as an increase in the bedrock depth. One possible geological feature could be a graben-like slump structure in the dolerite sill due to parallel faults.
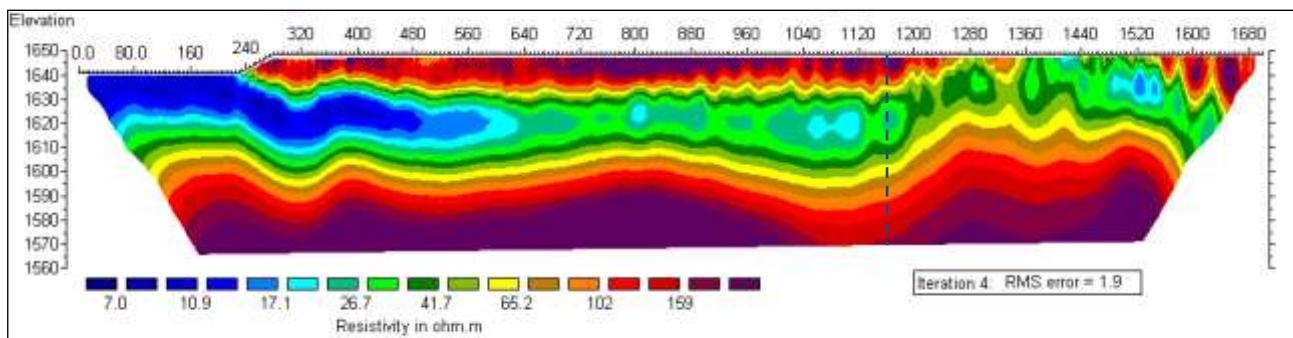
Figure 7.   Inverted resistivity profile P01.
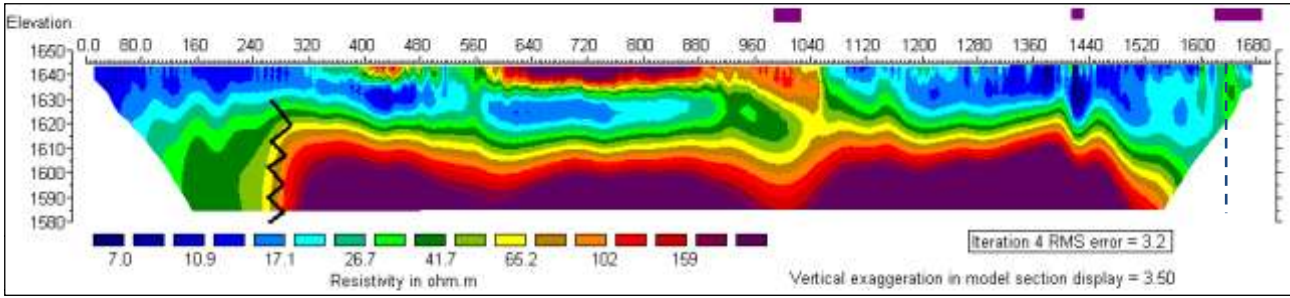
2.1.7   Ground Magnetic Survey

Magnetic data were recorded along four traverses with west/east strikes to the south of the Ash Stack. The positions of the four ground magnetic traverses relative to the Ash Stack and existing infrastructure are shown in Figure 6. Data were recorded at a station spacing of approximately 11 m in order to have a high spatial density to allow the detection of even thin magnetic structures. The results of the magnetic survey are displayed as profile plots in Figure 9.

The magnetic field displays large variability (variations in excess of 50 nT) on all four traverses. This type of response is typical of the response that can be expected from an extended dolerite sill. However, on traverses T01 and T02 much larger anomalies (150 – 200 nT) are observed on either side of the non-perennial river. These anomalies suggest that the dolerite sill was in some way disturbed in the vicinity of the non-perennial river. The above observation seems to confirm the suggestion made from the resistivity data that the non-perennial river follows a geological feature that has given rise to an increase in the bedrock depth, such as parallel faults within the dolerite sill.
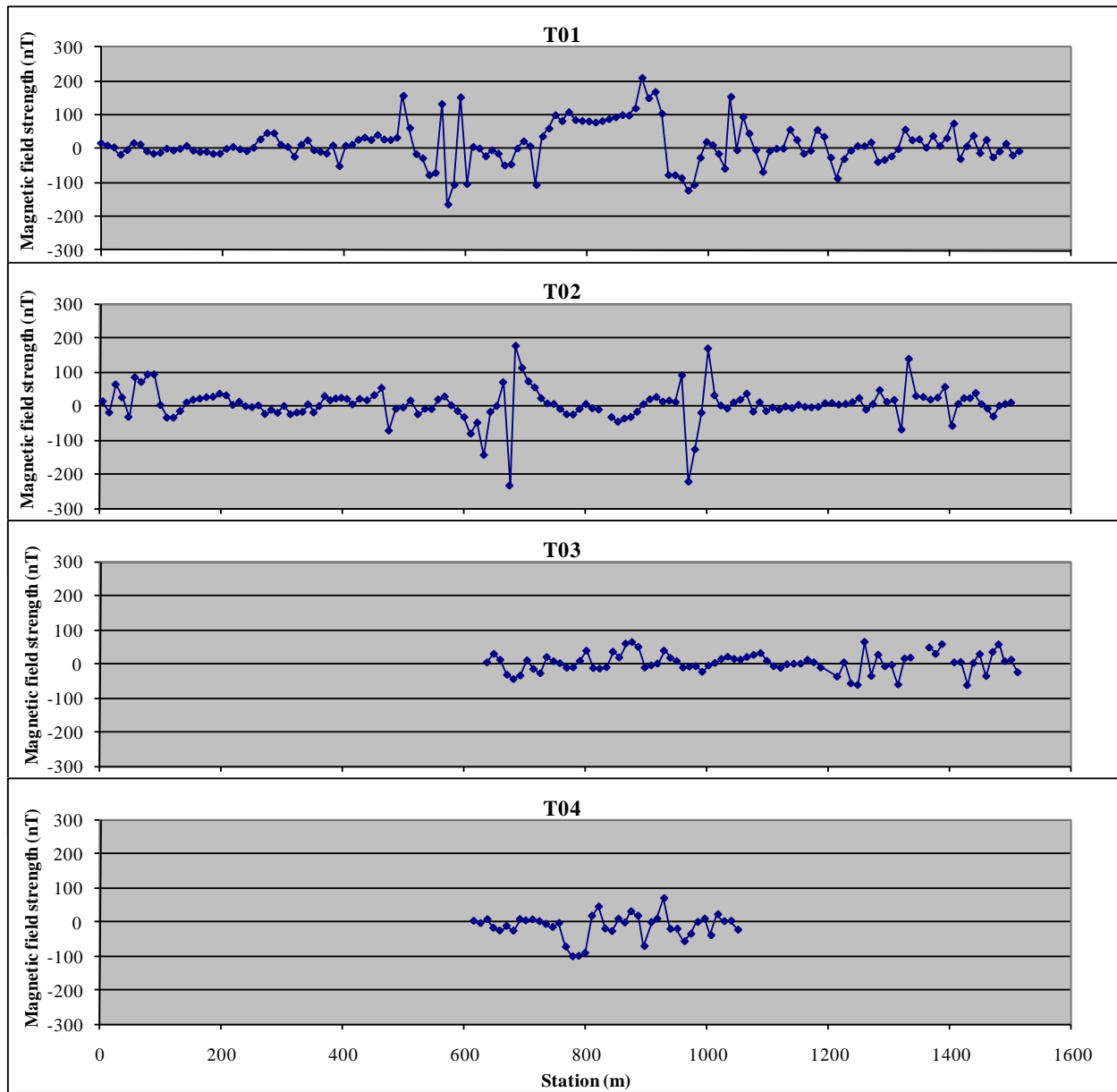
Figure 9.   Profile plots of the magnetic anomalies recorded along traverse T01 to T04 south of the Ash Stack.

2.1.8   Proposed target zone for the installation of boreholes

The results of the geophysical investigations suggest that a zone of increased bedrock depth occurs in the vicinity of the non-perennial stream. This zone may be due to a graben-like structure caused by parallel faults in the dolerite sill. Extensive fracturing can be expected in the vicinity of and between the faults. Since the fractured zone is likely to be associated with increased hydraulic conductivities, mobilisation of contaminant along this zone can be expected. Boreholes drilled within this zone may also be high-yielding. It is therefore suggested that investigative, monitoring and production boreholes target the possible fractured zone, as demarcated in Figure 10
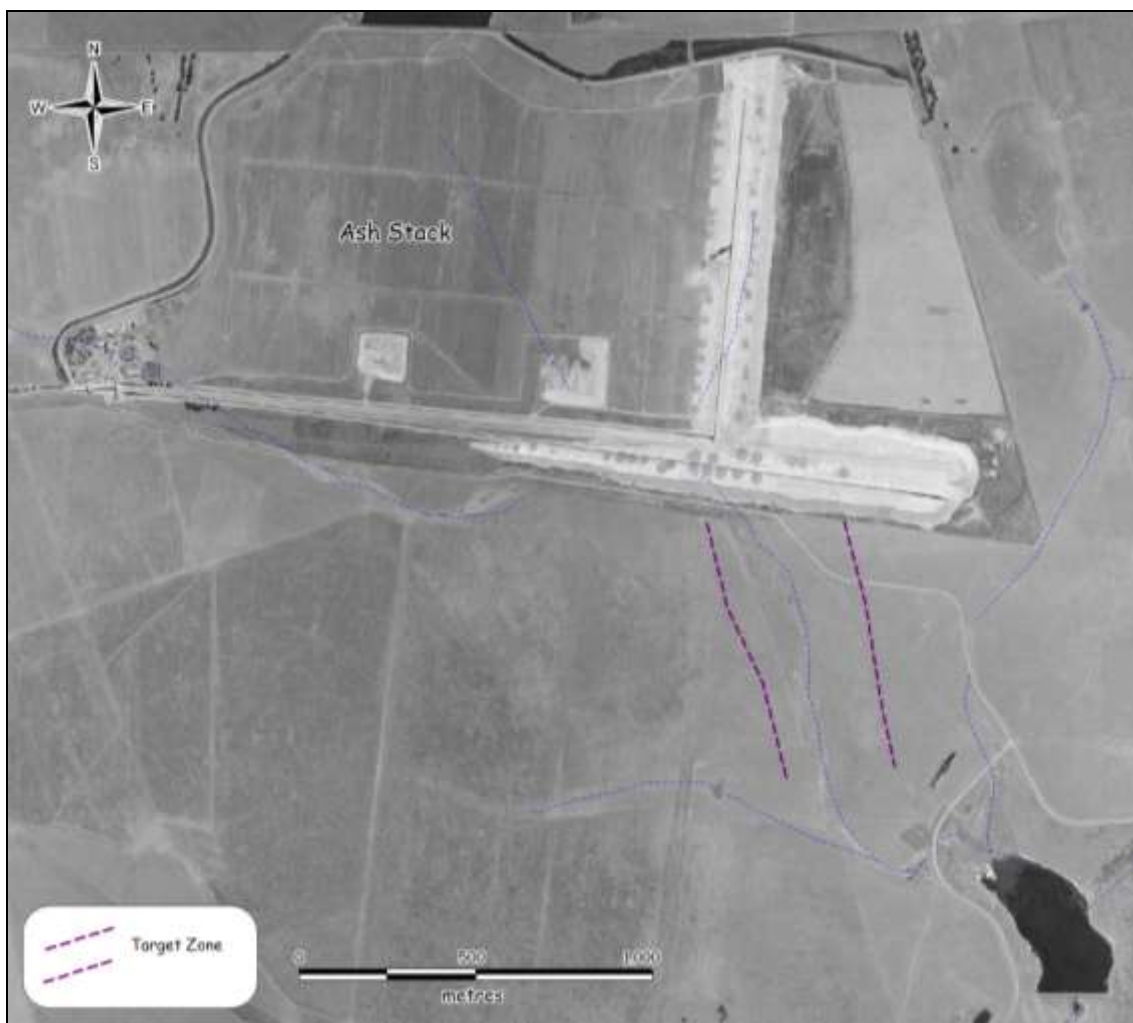
Figure 10. Target zone suggested for the installation of investigative, monitoring and production boreholes.

2.2   DRILLING DETAILS

Five additional boreholes were drilled as part of this investigation to be used as routine monitoring boreholes, pumping boreholes and observation bores during the pump tests. These bores will be incorporated into the monitoring program. AMB90 and AMB92 were sited ±50 m south of the ash stack on the eastern and western side of the stream respectively. AMB91 and AMB94 were sited ±100 m south of the eastern point of the ash stack west of Wolwe Spruit. AMB94 was drilled to a depth of approximately 50 m when the hole was abandoned due to the instability of the top 14 m of the geological formation encountered in the borehole.   AMB93 was drilled ±400 m south of the ash stack east of the stream in the direction of AMB02. The bore logs of the newly drilled bores are presented in Figure 11 to Figure 15. Dark coloured, highly plastic (CH) site soils of limited thickness (<1m) typically overlie in situ weathered dolerites and Karoo Basin sediments at the site. In the vicinity of the ash stack, site soils are typically underlain by extreme to moderately weathered fractured dolerite. Beyond depths of 15 m, intercepted doleritic material was typically slightly weathered to fresh, and resistant to drilling, with the total thickness varying from 25 to 45 m. Karoo Basin sediments (predominantly sandstones) occur beneath the sill, generally having a baked appearance where in contact with the overlying dolerite.

Shallow seepage was inferred at most recently installed monitoring bore sites, which suggests that a perched, weathered zone aquifers are of significance across the ashing area, although probably more

so in the weathered and fractured doleritic profiles. In terms of yield, however, by far the most water was derived from the deeper baked zone that has developed at the interface between the dolerite sill underside and the Karoo sediments, with blow yields of more than 2 L/s measured.
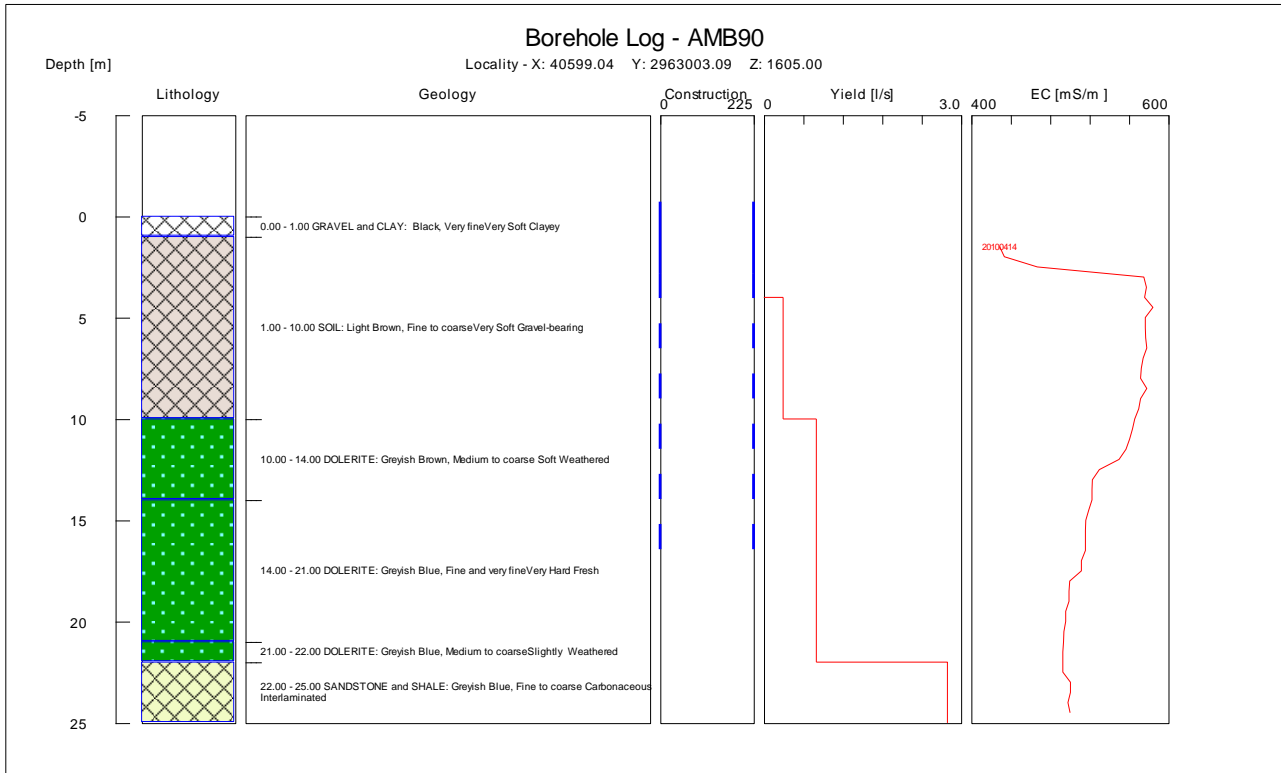

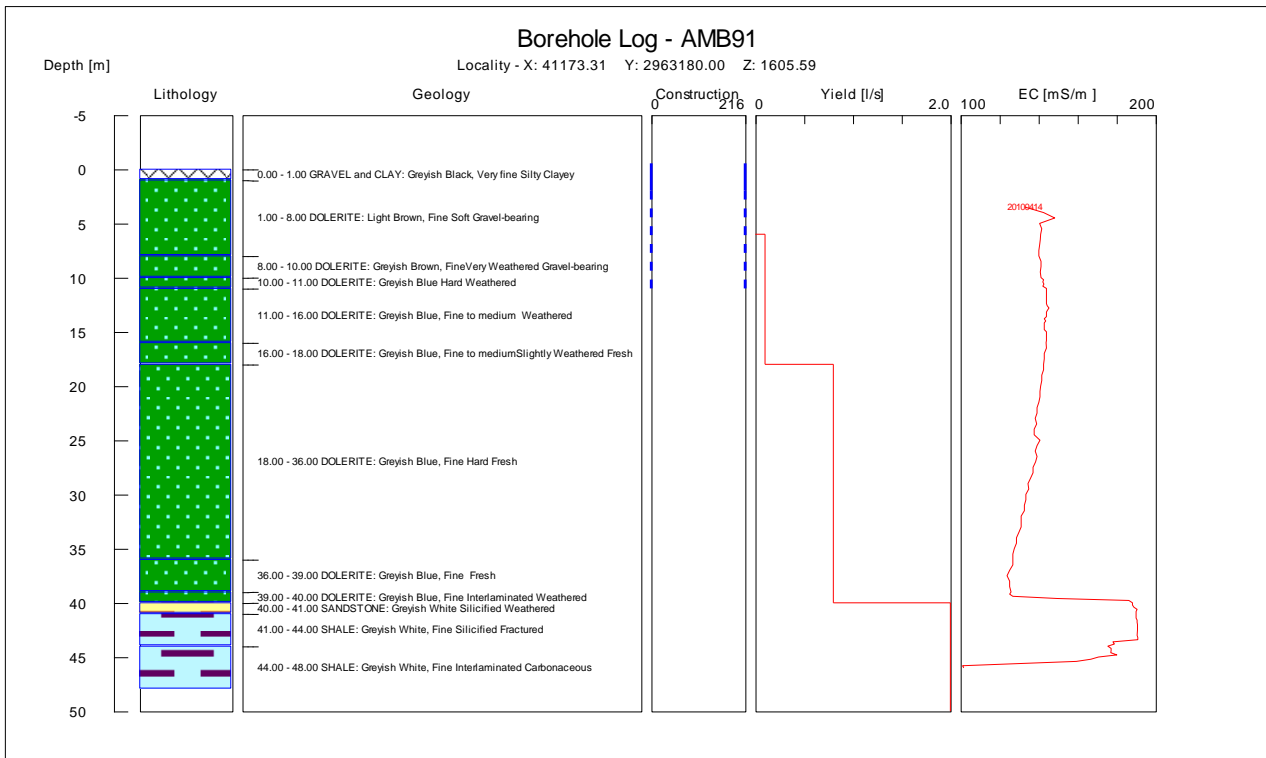*Figure 11. Geological log of borehole AMB90.*
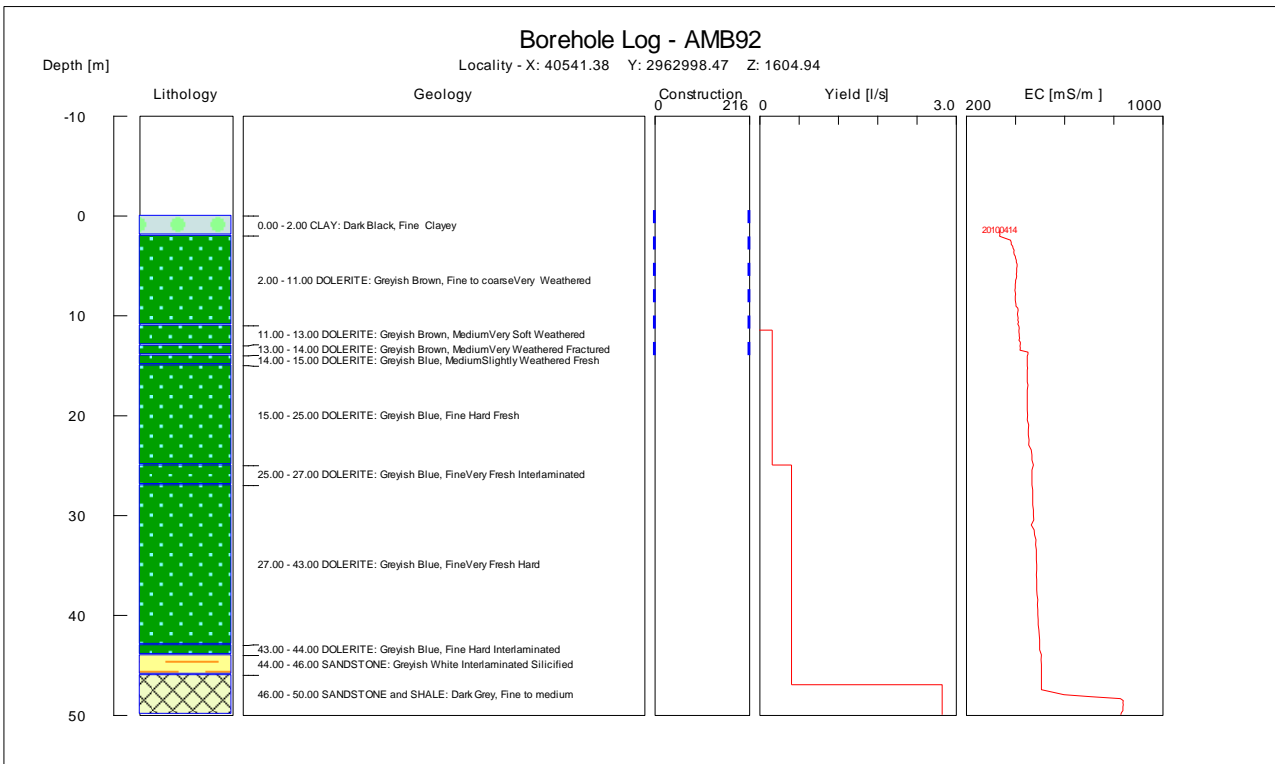

Figure 12. Geological log of borehole AMB91.
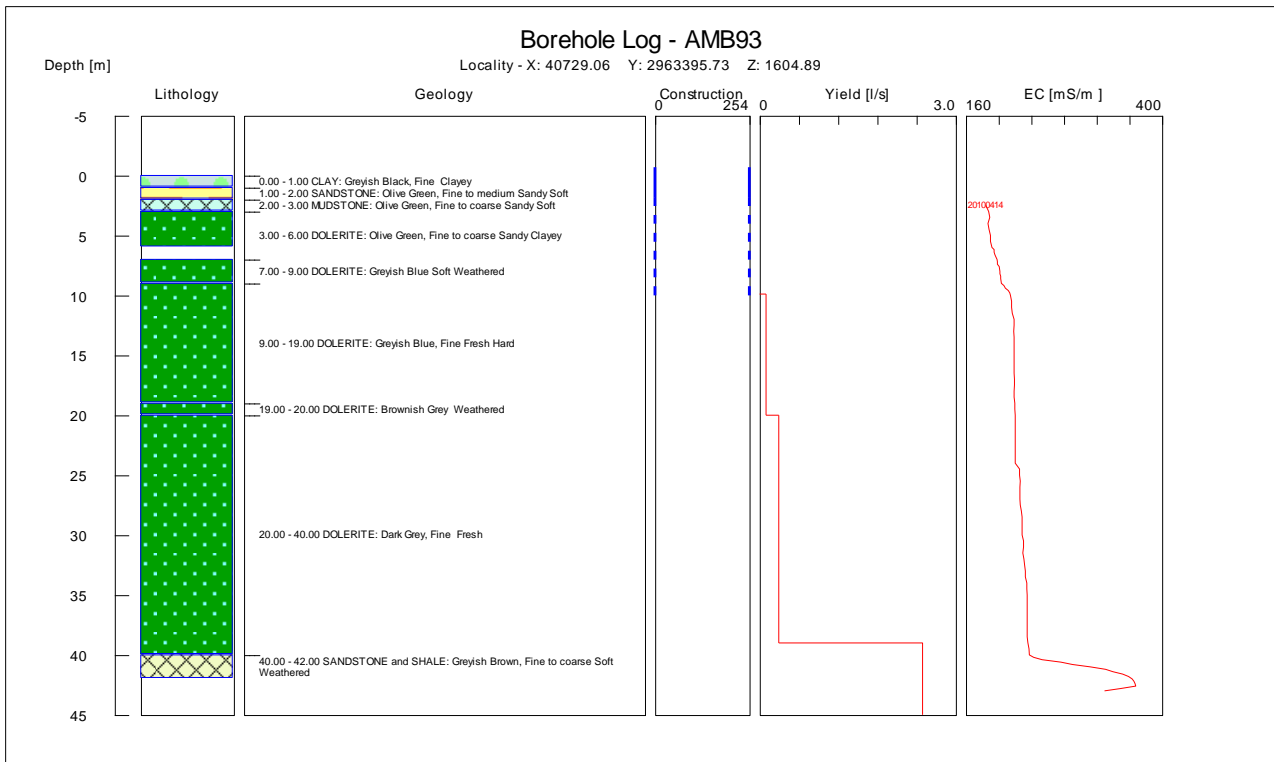
Figure 13. Geological log of borehole AMB92.

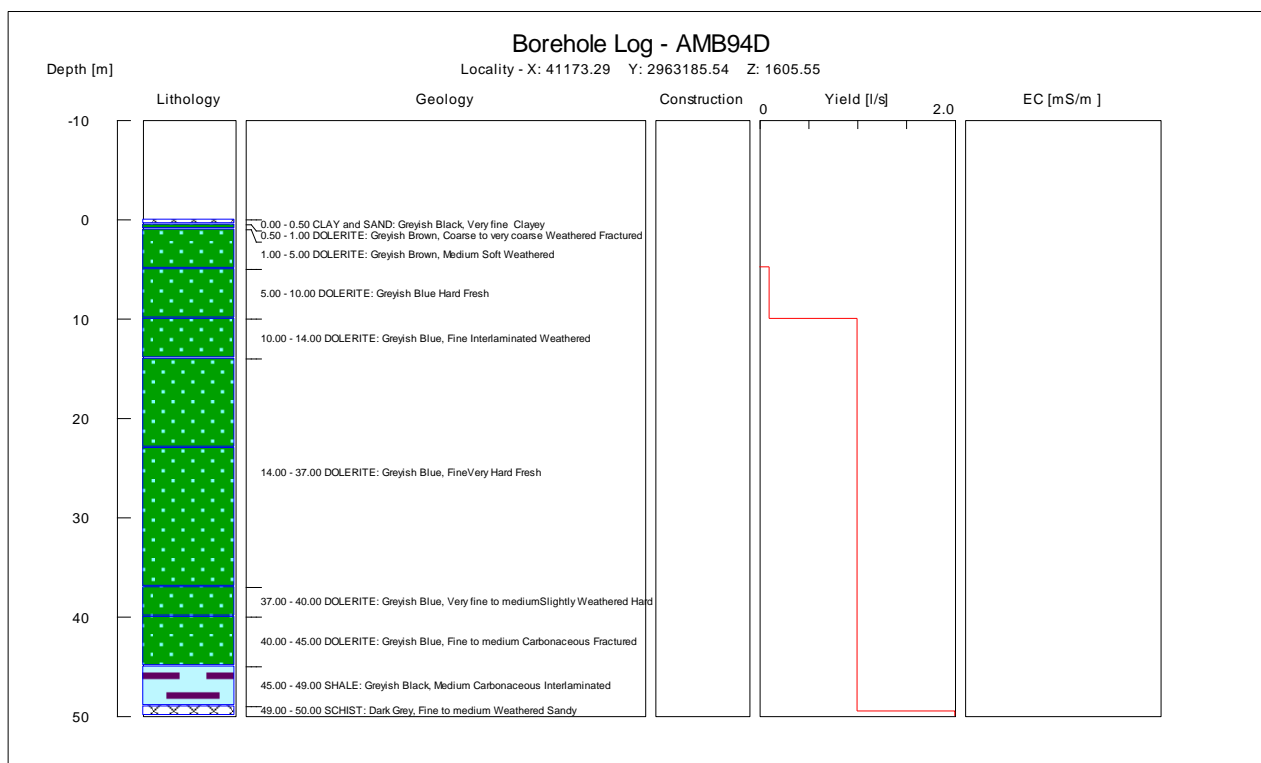*Figure 14. Geological log of borehole AMB93.*

Figure 15. Geological log of borehole AMB94.

2.3 AQUIFER TESTING DETAILS

Four pump tests, with the use of 2 observation level monitoring boreholes for each test, were done during this investigation to determine the hydraulic properties in the vicinity of the ash stack. The following tests were performed on borehole AMB90, AMB91, AMB92 and AMB93 at the ashing area;

- Permeability Tests (Slug tests)

- Yield (Calibration),

- Constant-rate and

- Recovery Tests.

The slug test graphs are displayed in Figure 16 to Figure 19 and the pump test graphs are displayed in Figure 20 to Figure 23. Analyses of the pump tests that were conducted between the 27th of March and the 10th of April 2010, indicate some hydraulic conductivity between boreholes B93 and B67, as well as between boreholes B90 and B92.

2.3.1 Permeability Tests (Slug Tests)

Slug tests were performed at all the monitoring bore sites during different detailed investigation from 1994. The field measurements obtained during the slug tests were analysed using the Bouwer and Rice (1976) method. This method provides an indication of aquifer permeability in the immediate vicinity of a tested borehole. In this instance, the line of best fit through slug test data was taken through later values to allow for drilling induced increases in aquifer permeability in the area immediately adjacent to the borehole.

2.3.2   Yield (Calibration) Test

This type of test involves the determination of the actual rate of inflow into the borehole from the surrounding geological formations. It is obtained by abstracting all the water which is flowing into the borehole. Eventually, when the borehole is empty, it is only the water that flows into the borehole which is pumped out. If this rate of abstraction is measured, it represents the rate by which the water enters the borehole from the aquifer, i.e. the actual yield of the aquifer.

The calibration tests were conducted over a 60-minute period at AMB90, AMB91 and AMB93 and over a 120 minute period at AMB92 with abstraction rates of 3.3 l/s : AMB90, 1.9 l/s : AMB91, 3.8 l/s : AMB92 and 2.2 l/s : AMB93. All the boreholes were recovered for 60 minutes.

2.3.3   Constant-rate Test

The rate of the constant discharge test is determined by evaluating the behaviour of the borehole during the yield test.

The decision of how long a borehole should be pumped during the main constant discharge test depends upon the degree of certainty that is required regarding the sustainable yield of a borehole or a pumping scheme.

The abstraction of groundwater at a constant rate for a longer period, e.g. 24 hours, gives information on the hydraulic properties of the aquifer over a greater area around the borehole. This enables one to determine the hydraulic characteristics of the aquifer on a much larger scale than is the case with a step test.

A discharge rate of approximately 60% of the aquifer yield is usually chosen so that the pumping water level is not drawn down to pump intake during the test period.

The Constant rate test at AMB90 was conducted over a 24 hour period with an abstraction rate of 2.2 l/s during which the water level lowered from 1.15 mbgl to a depth of 12.56 mbgl . The pump inlet was installed 21 mbgl. (Figure 20)

The Constant rate test at AMB91 was conducted over an 18 hour period when pump inlet was reached with an abstraction rate of 1.4 l/s during which the water level lowered from 3.15 mbgl to a depth of 40.0 mbgl . The pump inlet was installed 40 mbgl. (Figure 21)

The Constant rate test at AMB92 was conducted over a 24 hour period with an abstraction rate of 3.6 l/s during which the water level lowered from 1.44 mbgl to a depth of 18.42 mbgl . The pump inlet was installed 44 mbgl. (Figure 22)

The Constant rate test at AMB93 was conducted over a 24 hour period with an abstraction rate of 1.4 l/s during which the water level lowered from 2.38 mbgl to a depth of 26.25 mbgl . The pump inlet was installed 40 mbgl. (Figure 23)

2.3.4   Recovery Test

The rate, at which the static water level recovers to its normal level, is monitored from the moment the pump is stopped at the end of the constant discharge test. This recovery is allowed to continue until the normal static water level is reached, or at least for a period as long as the constant discharge took place if it does recover within that period of time. The rate of recovery determines the optimum ratio between the length of the period of abstraction and the period that must be

allowed for recovery once the borehole is in production. For example, it can be that a borehole must be left alone for recovery for a period of 14 hours per day after the pump has been switched off. This means that, for the specific abstraction rate for the borehole, the pump can run for 10 hours per day after which 14 hours must be allowed for the borehole to recover. Evaluation of the recovery data can also be used to confirm the aquifer parameters determined from the main test.

Borehole AMB90 recovered to 90% of the original water level within twelve hours of the recovery time. (Figure 20)

Borehole AMB91 recovered to 90% of the original water level within twenty minutes of the recovery time. (Figure 21)

Borehole AMB92 recovered to 90% of the original water level within forty minutes of the recovery time. (Figure 22)

Borehole AMB93 recovered to 90% of the original water level within eighteen hours of the recovery time. (Figure 23)

Figure 16. Water level observations during slug testing – AMB90
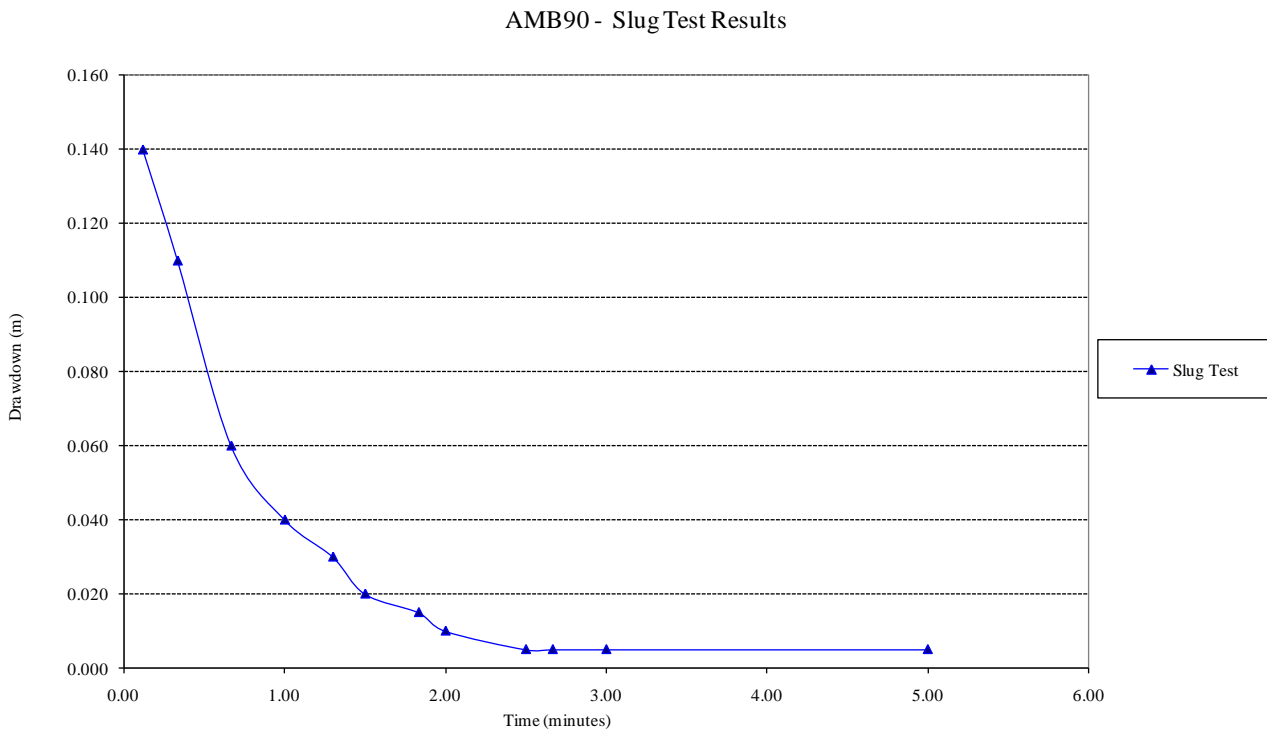
AMB91 - Slug Test Results

Figure 17. Water level observations during slug testing – AMB91

AMB92 - Slug Test Results

Figure 18. Water level observations during slug testing – AMB92

AMB93 - Slug Test Results
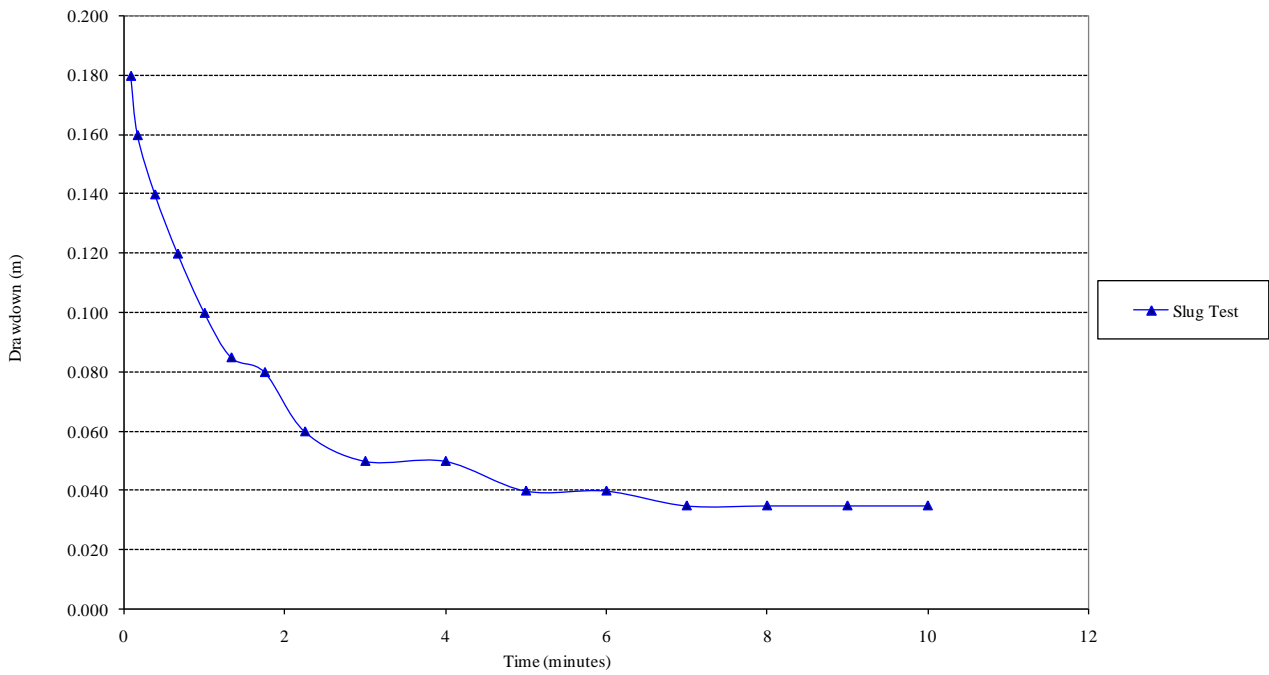
Figure 19. Water level observations during slug testing – AMB93

AMB90 - Pumptest Results
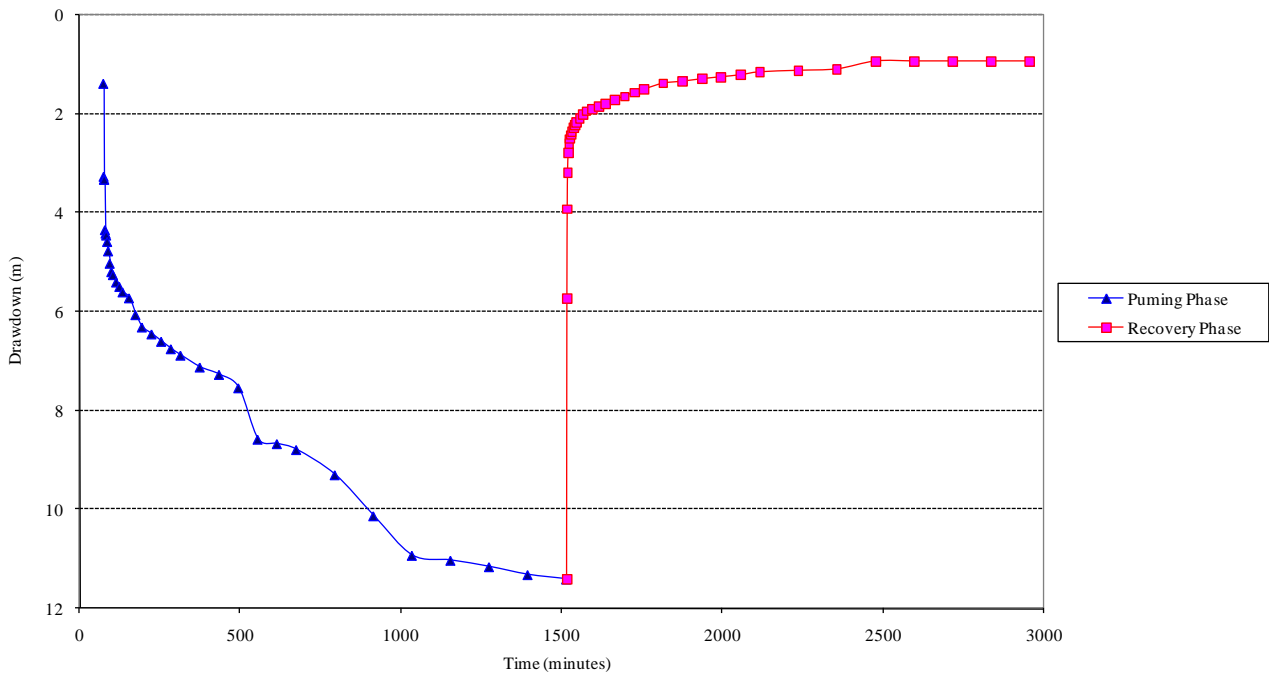
Figure 20. Water level observations during pump testing – AMB90.

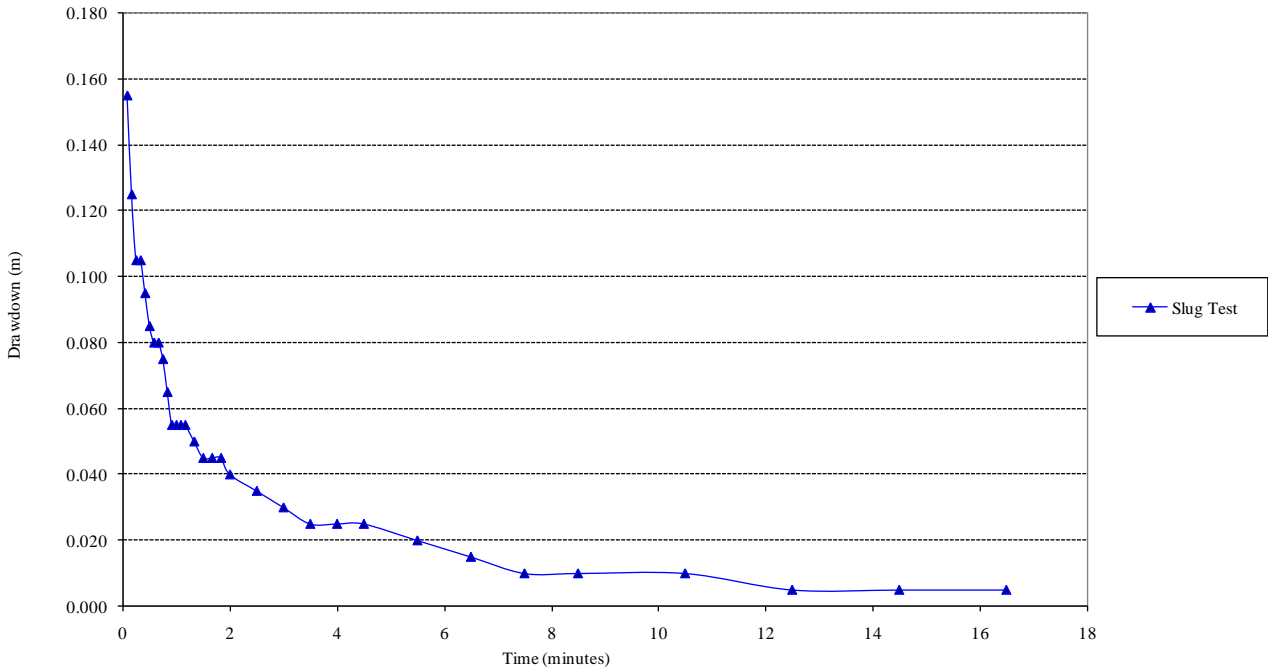AMB91 - Pumptest Results
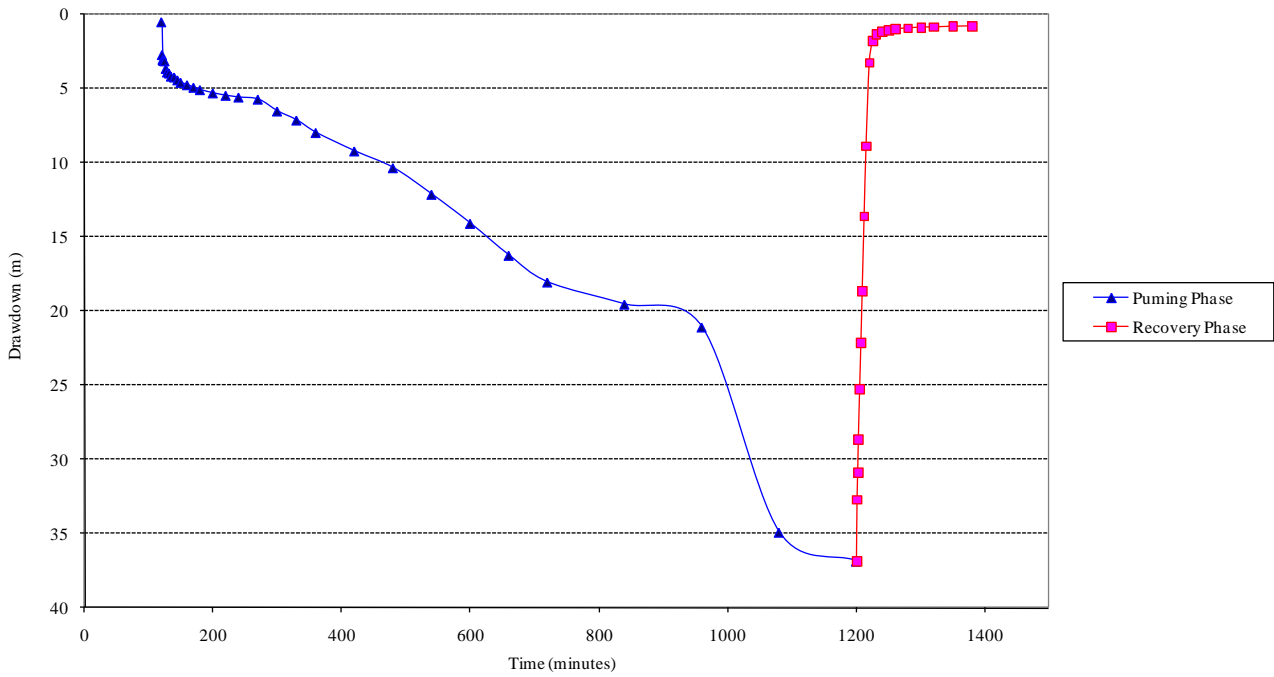
Figure 21. Water level observations during pump testing – AMB91.

AMB92 - Pumptest Results

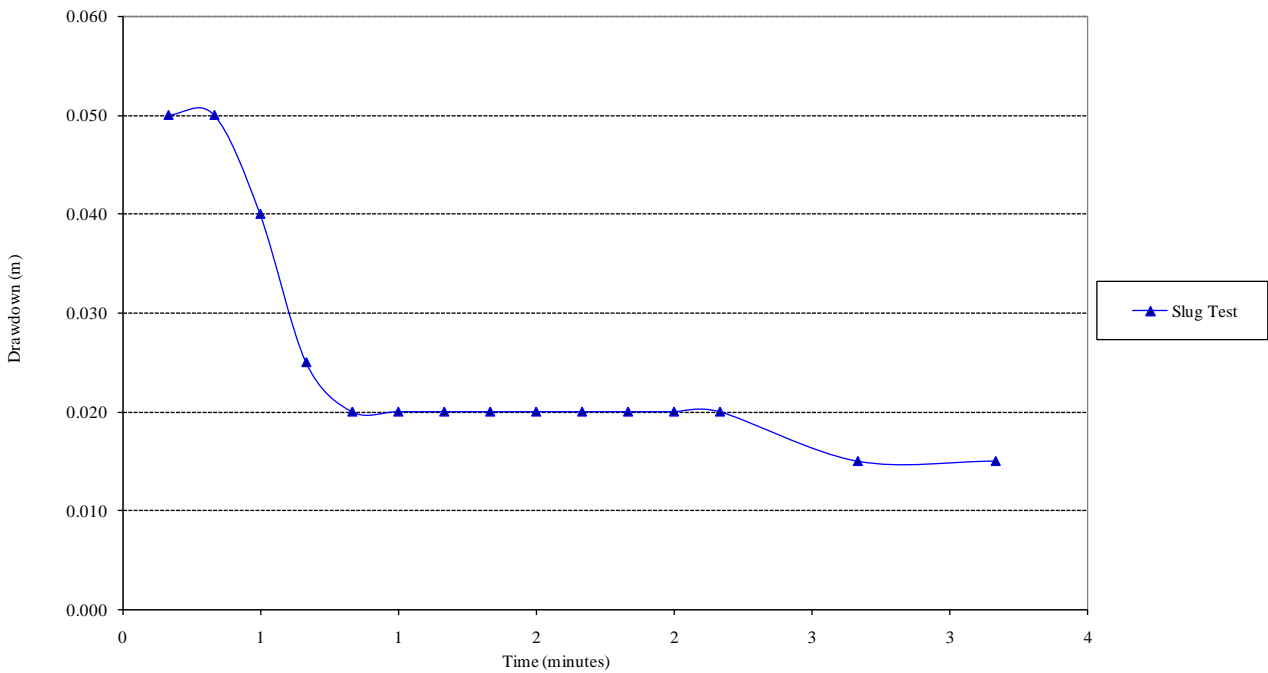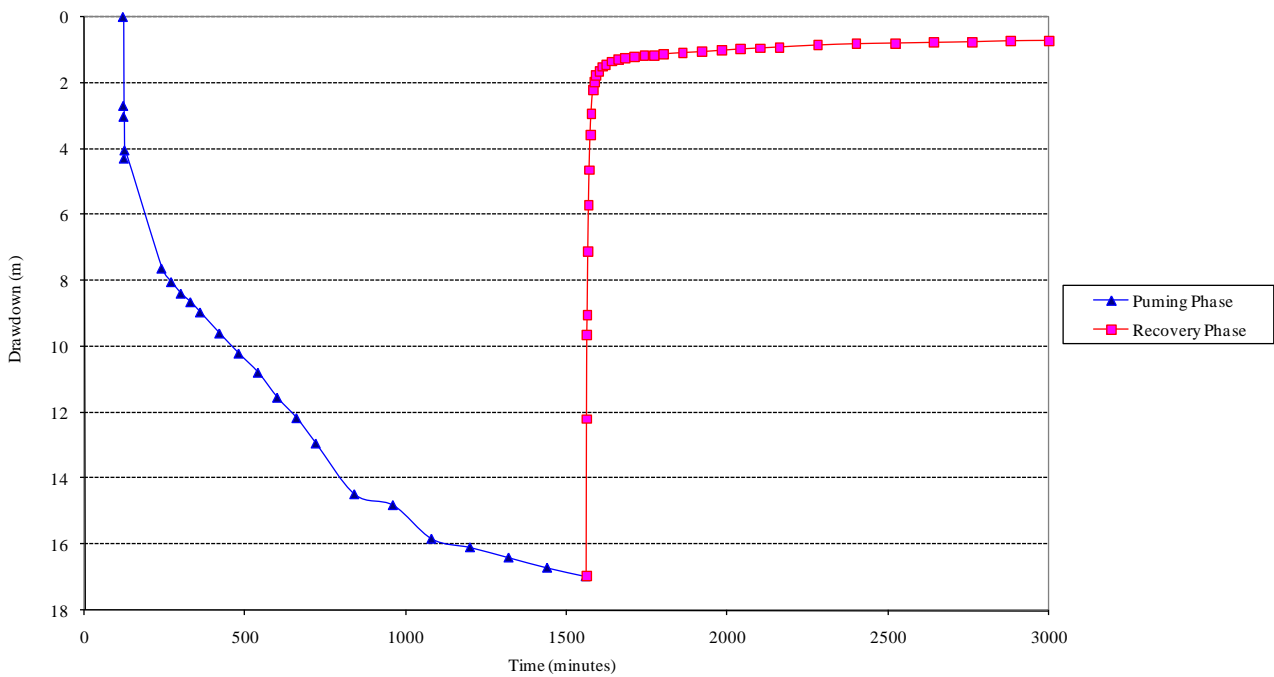*Figure 22. Water level observations during pump testing – AMB92.*

AMB93 - Pumptest Results
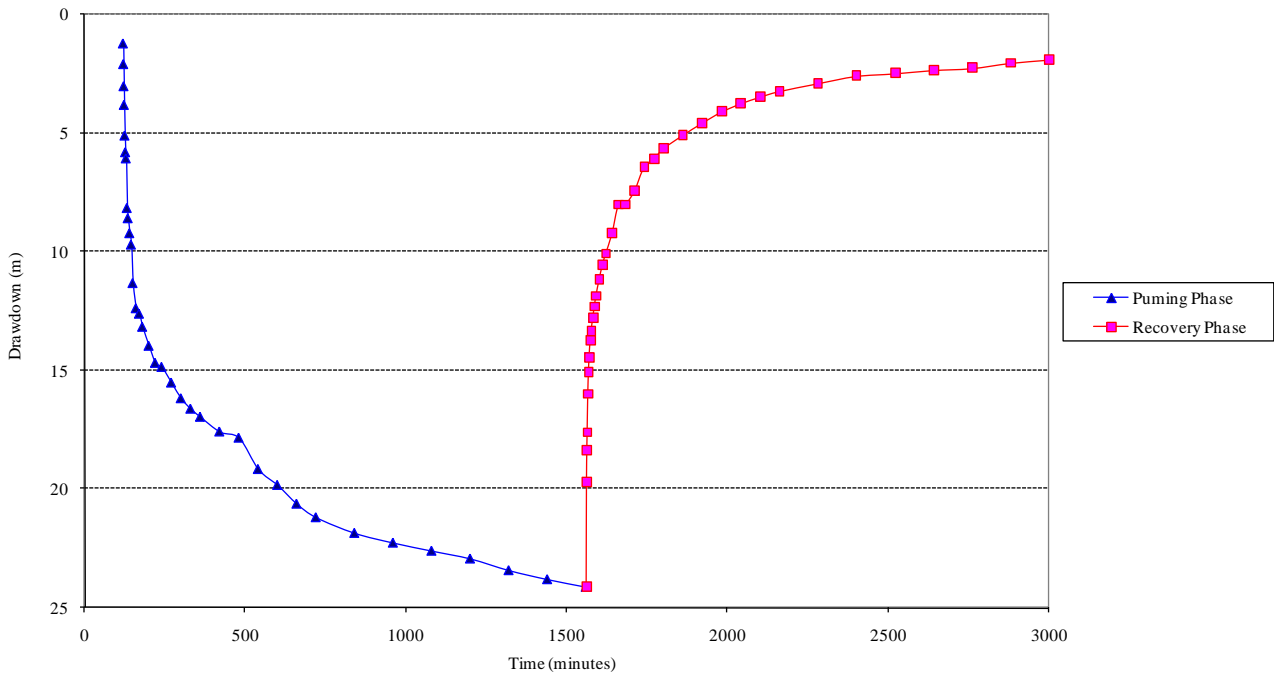
Figure 23. Water level observations during pump testing – AMB93.

2.3.5   Results

The data obtained from the pump tests were analysed with the latest FC-method developed by Prof. G van Tonder from the IGS at UFS and Aquitest developed by Waterloo. The test results can be viewed in Figure 24 to Figure 27 and Table 3.
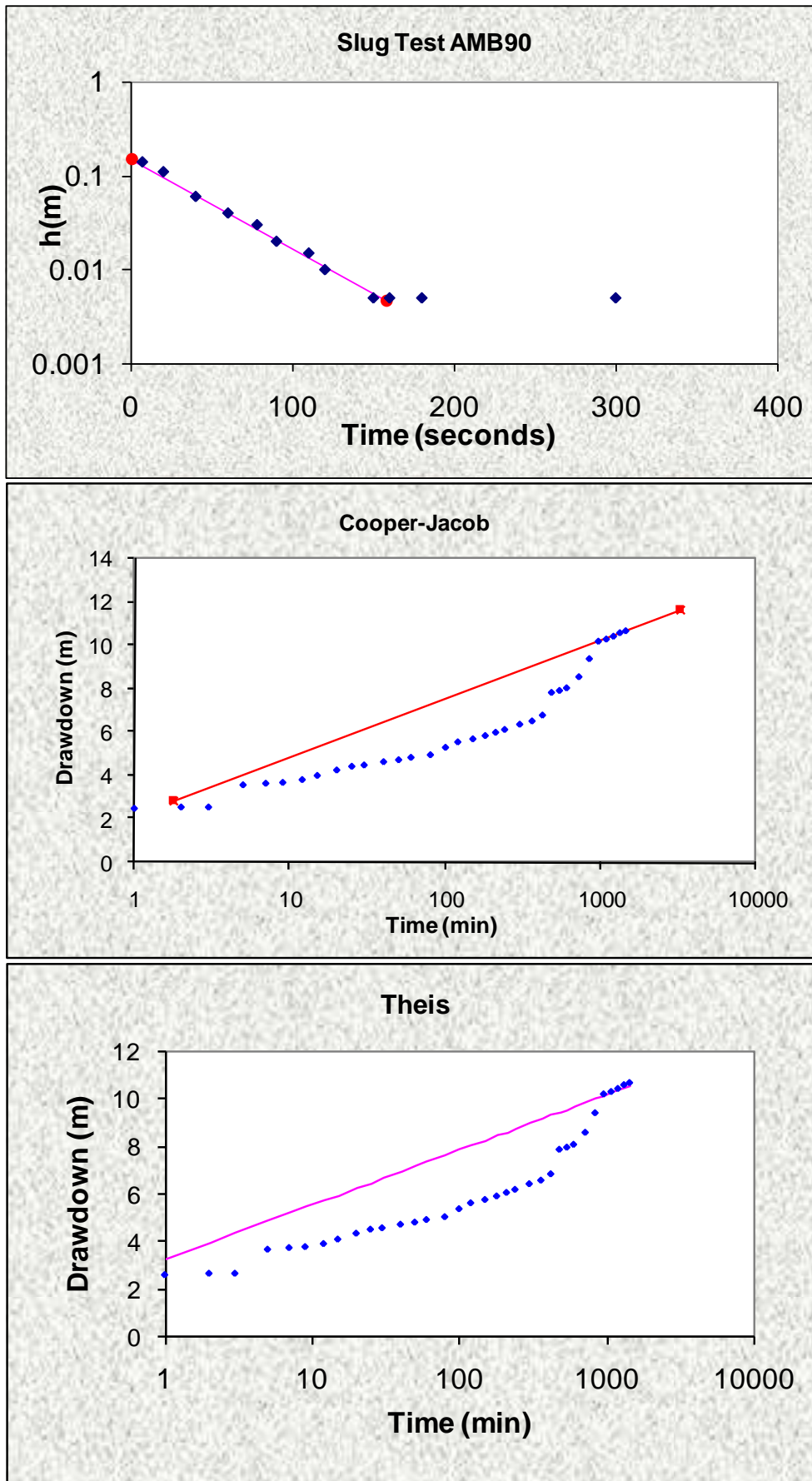
Figure 24. AMB 90 determination of aquifer parameters

Slug Test   K = 1.935 m/d   FC Method Sust. Yield = 2.08 l/s for 8h/day
Cooper Jacob: T = 12.8 m²/d;   S = 4.06E-03
Theis: T = 15 m²/d;   S = 1.27E-03
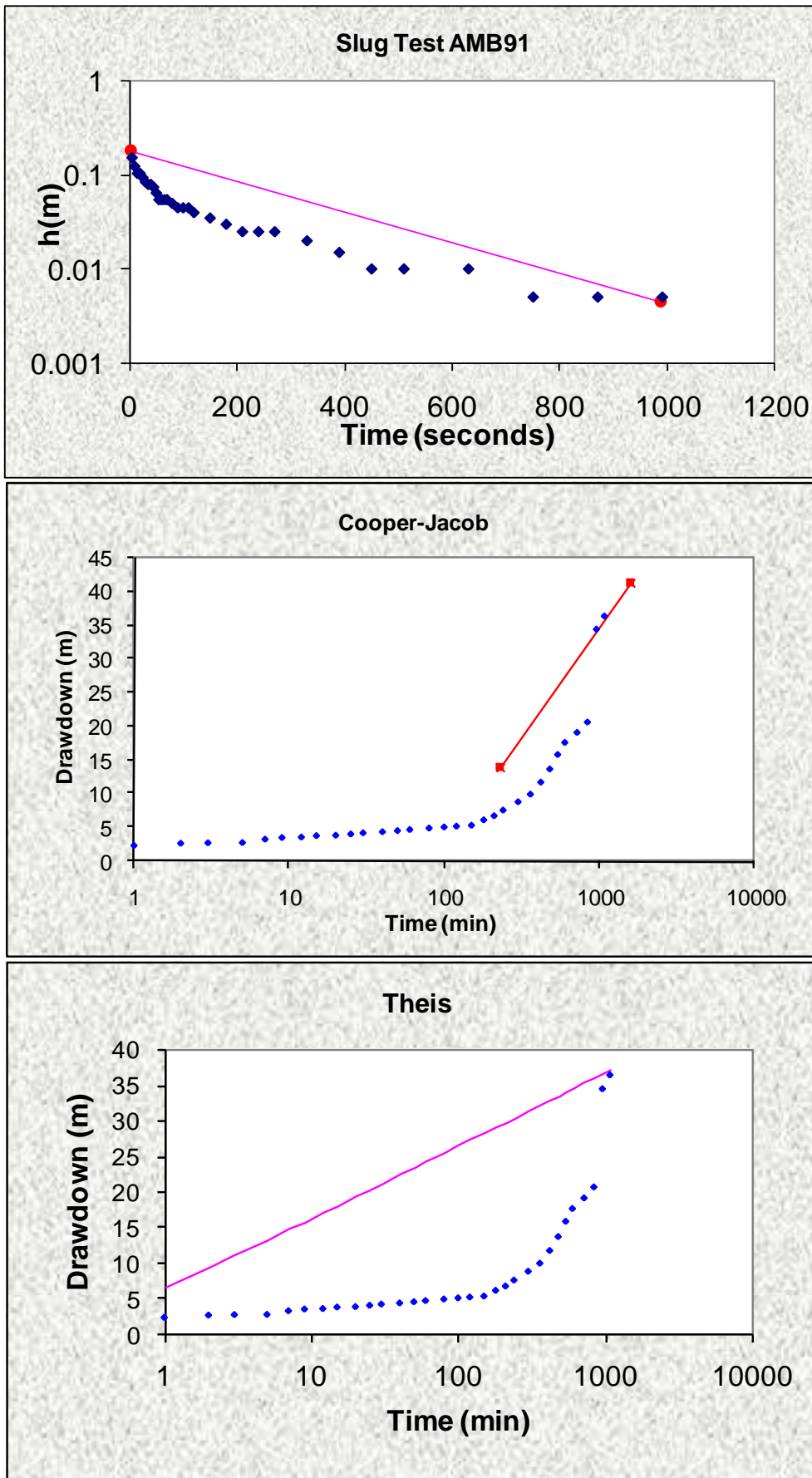
Figure 25. AMB 91 determination of aquifer parameters
Slug Test   K = 0.203 m/d   FC Method Sust. Yield = 0.29 l/s for 8h/day
Cooper Jacob: T = 0.6 m²/d;   S = 4.74E-02
Theis: T = 2 m²/d;   S = 4.74E-04

Figure 26. AMB 92 determination of aquifer parameters

Slug Test	*K = 0.315 m/d*	*FC Method Sust. Yield = 3.1 l/s for 8h/day*
Cooper Jacob:	*T = 9.3 m²/d;*	*S = 1.33E-02*
Theis:	*T = 9 m²/d;*	*S = 1.6E-02*

Figure 27. AMB 93 determination of aquifer parameters
*   Slug Test   K = 0.172 m/d   FC Method Sust. Yield = 1.04 l/s for 8h/day*
*   Cooper Jacob: T = 3.18 m²/d;   S = 8.16E-04*
*   Theis: T = 3 m²/d;   S = 9.45E-04*

3 CONCEPTUAL MODEL

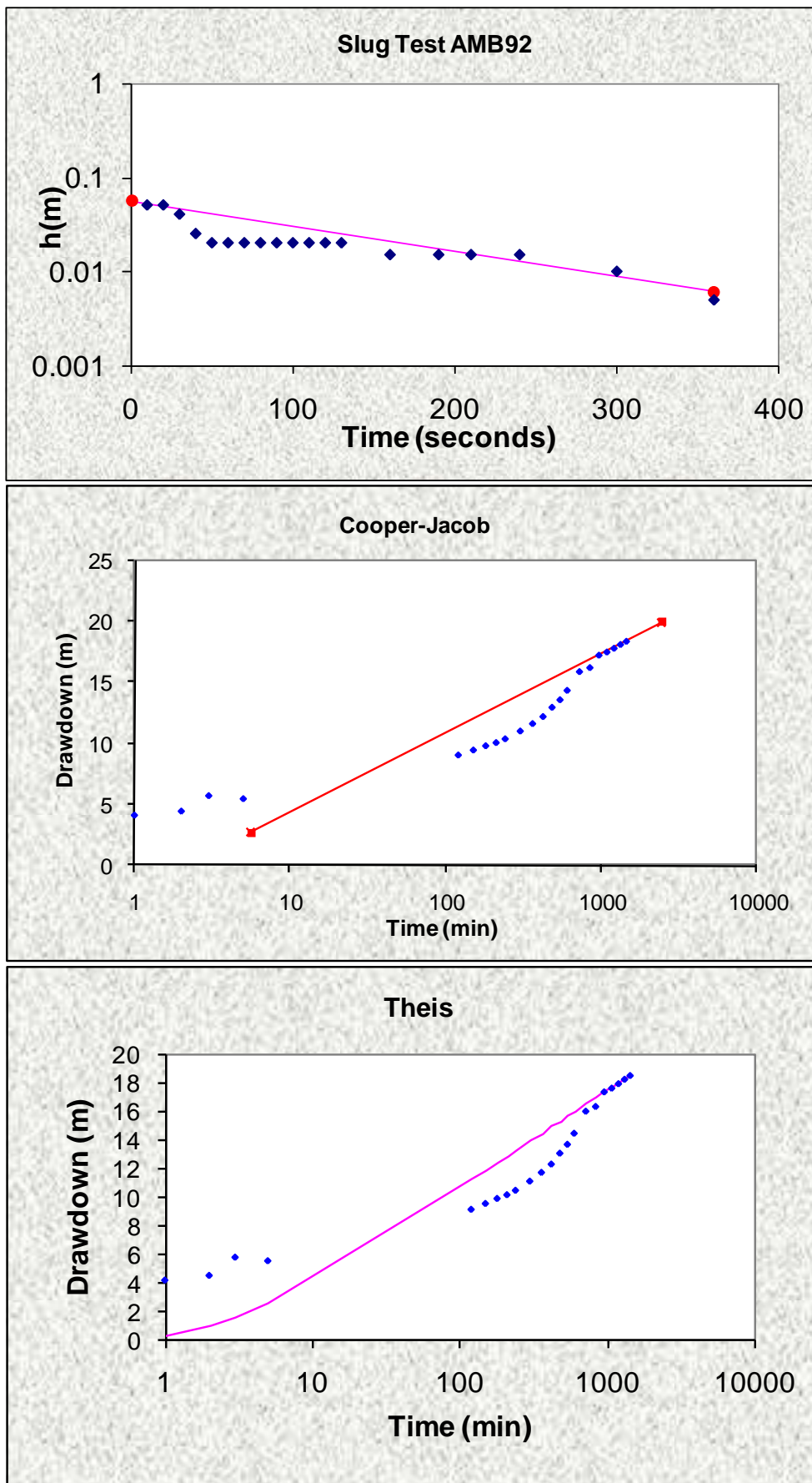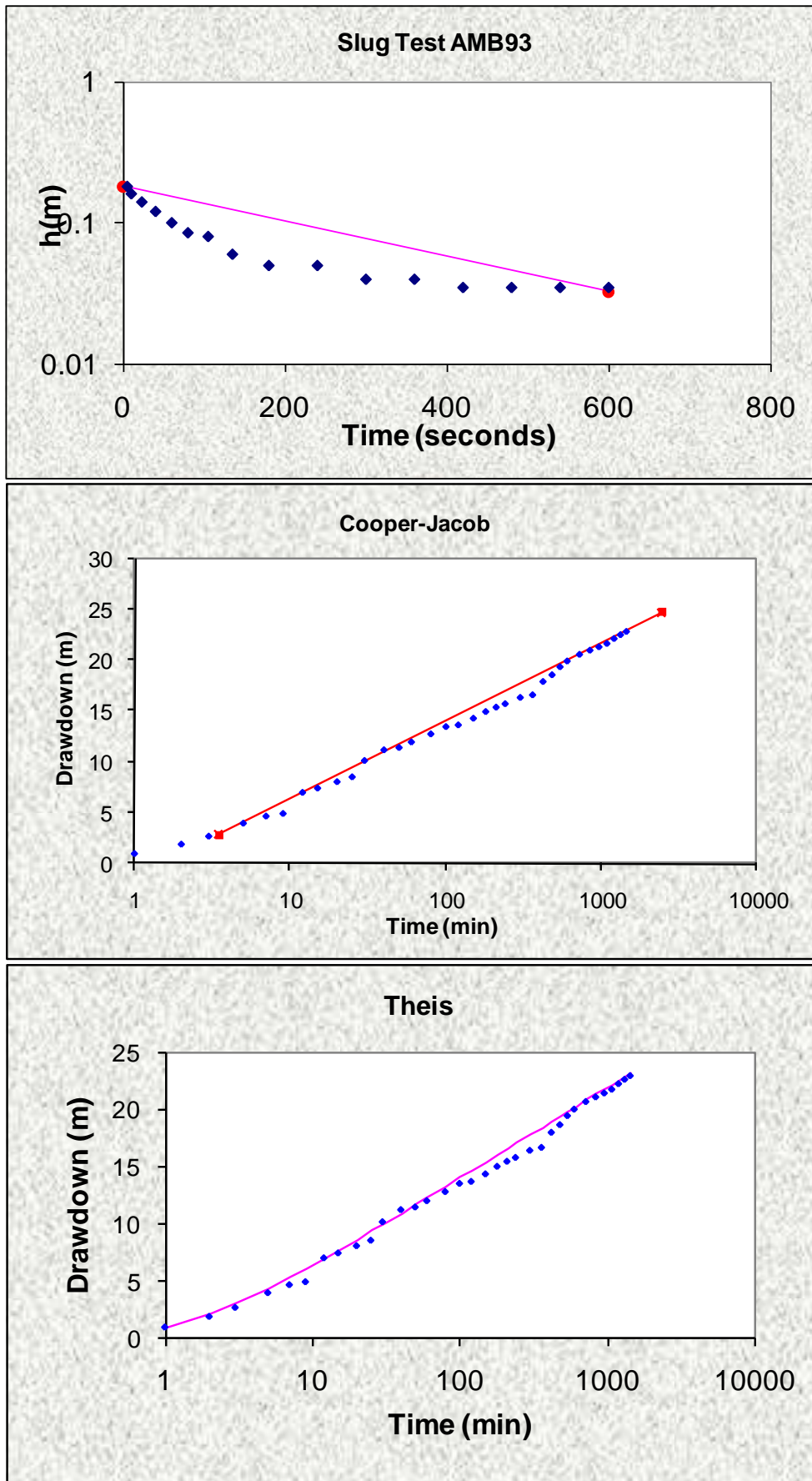The first step in constructing a model is the subdivision of the area to be modelled into smaller areas (elements) within which the characteristics are similar. Considerations for subdivision of the Tutuka Ashing Area were typically:

- The surface geometry, such as topography, streams and positions of waste management facilities;

- The hydraulic characteristics of the ash stack;

- The hydraulic characteristics of the underlying aquifer;

- Current groundwater quality distribution;

- The impact of the brine irrigation on the ash stack;

- Model potential pollution plume migration through local aquifers and test different scenarios of rehabilitation of the local aquifers.

The crux of any modelling exercises rests on the proper conceptual design of the model. This design incorporates all the information available on the system and simplifies it via several assumptions. In this way the system can be adequately summarised and different scenarios simulated.

All relevant monitoring results, results from hydraulic tests, material analysis, natural topographical and geological characteristics, etc. was integrated into the following conceptual model. Consequently, the following conceptualisation for groundwater flow and mass transport within the ashing area was done.

Several man-made features are also of significance at the site. Ash is applied to the pile via two systems; an ash stacker, and an ash spreader. Most of the ash is applied using the ash stacker, with the ash spreader only operating along the southern edge of the pile as a standby system when the stacker is not in use. The area between the toe of the pile batter slope and the ash stacker is referred to as the front stack, and this currently defines the eastern face of the pile. The back stack occurs to the west of the stacker and abuts the rehabilitated area. The ash stack currently extends over 1.84 km^2 (refer to Table 1), with heights in excess of 40m in some instances.

Numerous dams have been constructed for a variety of purposes, but mainly for pollution control. To date, five of these dams have been constructed, which form part of the pollution management of surface run-off at the ashing area. These dams currently extend over 0.7 km^2 (refer to Table 1).

Table 1.   *Surface extends of the surface water structures in the ashing area.*

Site no.	Description	Area (km^2)	Perimeter (km)
	Ash Stack	2 322	6.881
AMD06	Farm dam	0.1246	1.412
AMD07	Clean Water Dam	0.2127	1.985
AMD08	Dirty Water Dam	0.1376	1.838
AMD09	Settling Dam	0.1209	1.697
AMD14	North Dam	0.1040	1.448

The following site layout plan, with the most important and general power generation structures was used for the modelling exercise and for identification purposes for the simulation figures:

3.1 PHYSICAL GEOGRAPHY

Tutuka Power Station is located on a topographic high about 20 km north of Standerton, Mpumalanga Province. The facility occurs within drainage region C311, and can be sub-divided into secondary drainage regions comprised of smaller streams and creeks. The surface topography of the area is typical of the Mpumalanga Highveld, consisting in the main of a gently undulating plateau. The flood plains of the local streams are at an average elevation of approximately 1600 meters above mean sea level (mamsl).

Altitudes varies from $\pm$ 1660 mamsl at the higher parts plume the contour line of the $\pm$ 1590 mamsl which defines the base of the different Spruit areas. The ash stack area is situated between the contour lines of the 1610 – 1635 mamsl.

Topographic maps of the area show a recurring block type drainage pattern that seems particularly well developed in the region, characterized by stream sections orientated northeast-southwest and northwest-southeast. Drainage of this type is often structurally controlled, and thus may provide some insight into the orientation of regional and convergent stresses.

The ashing area has been developed upon gradual slopes and a semi-developed drainage system (refer Figure 11). The Wolwe Spruit drains the area to the east of the ash pile to the Grootdraai Dam, an artificial impoundment constructed across the Vaal River approximately 10k m from the site.

Several drains and dams have been constructed around the ashing area. Of importance in terms of preventing water quality degradation off-site are the Dirty Water (D8) and Settling (D9) Dams, constructed to the southeast of the site across the Wolwe Spruit. All surface water runoff from the ashing area is diverted to these reservoirs. Surface water run-off that has been diverted around the ash pile flows to the Clean Water Dam (D7) downstream of D8.

The North Dam (D14) and a dam adjacent to workshops near B55 have been constructed across minor gullies trending approximately north-south and west-northwest to east-southeast, respectively, up hydraulic gradient of the ash pile. The ash pile itself has been, in part, constructed over these surface features. Previous work undertaken by Geo Hydro Technologies (2000) concluded that the North Dam (D14) is leaking at a rate roughly estimated at 1.2 m^3/d, with water tracking along the ash/in situ interface within the palaeochannel that underlies the middle of the pile. This leakage can be expected to reduce the moisture retention capacity of the ash in the vicinity of the palaeochannel, resulting in the leaching and redistribution of brine.

Surface run-off from the area is in the order of 8% of the annual rainfall. Groundwater recharge in undisturbed areas is in the order of 3% of the annual rainfall.

The following figure (refer to Figure 28) represents the local topography of the area under investigation. Data obtained from several topographical maps were combined and interpolation was used for mapping.
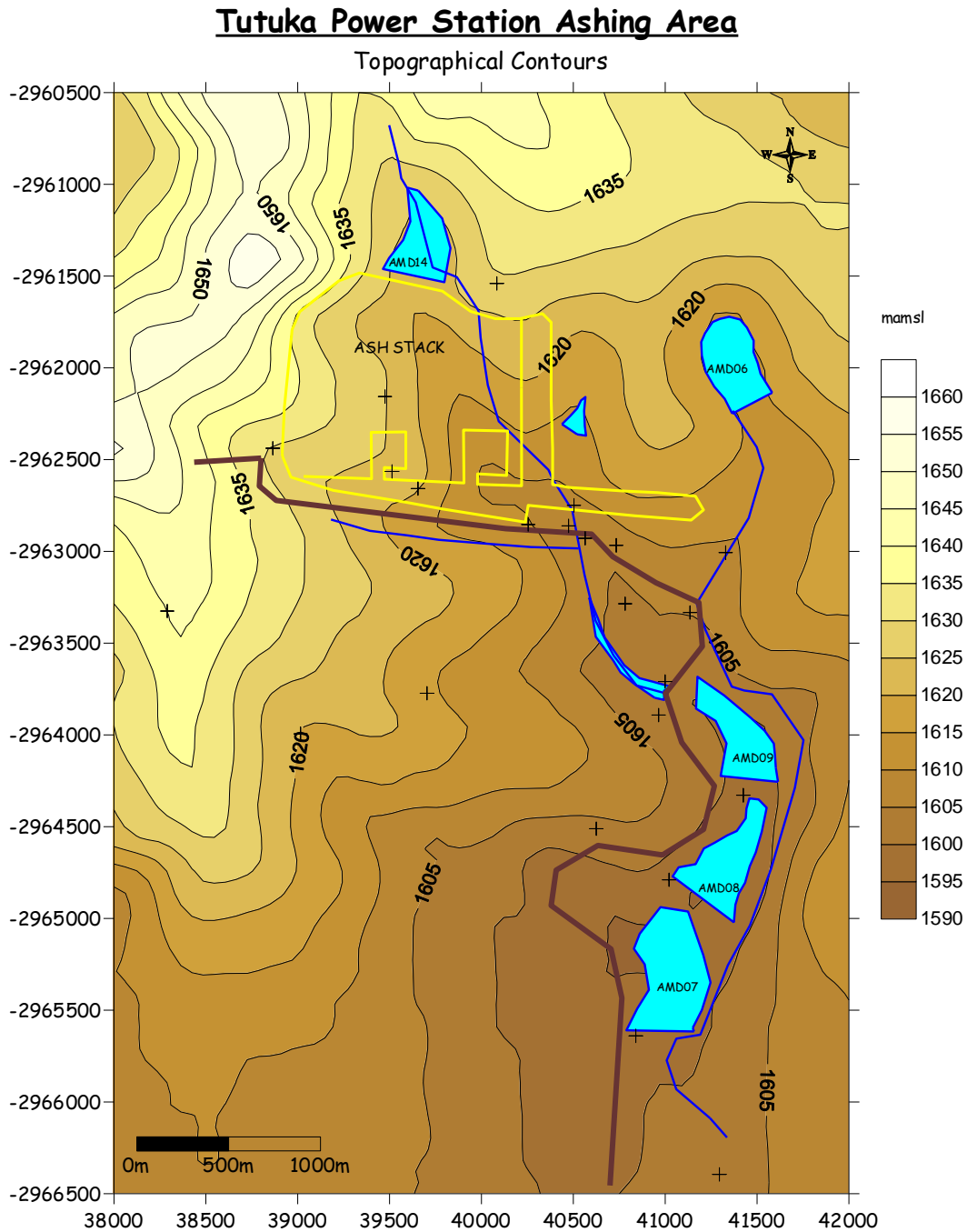
Figure 28. Topography of the area under investigation.

3.2   GEOLOGY

The site falls within the Carboniferous to early Jurassic aged Karoo Basin, a geological feature that covers much of South Africa. Sediments in this part of Mpumalanga Province fall within the Permo-Triassic aged Northern facies of the Ecca Series (Truswell, 1977). Typically, shales define the lower and upper levels of the series, with coal measures and associated coarser detrital sediments present between. Coal measures currently mined in the area form part of the Highveld Coal Field.

Late Triassic to Middle Jurassic aged Dolerite dykes and sills are common in the Karoo Basin, and occur throughout the power station area. Previous investigations identified the presence of a near surface, slightly weathered to fresh dolerite sill beneath the ash dump. The extent of the sill beneath, and in the vicinity of, the dump is unknown, however.

Soil cover surrounding the site appears relatively thin, particularly in the vicinity of the ash pile where soil has been removed for rehabilitation purposes. The type and distribution of site soils appears to be, in part, controlled by parent rock material. Soils overlying doleritic material are typically highly plastic, and dark brown to black in colour, while those on Karoo sediments are typically lighter in colour and moderate to highly reactive in character. Shrinkage cracks can, however be expected to develop in site soils irrespective of parent material during periods of prolonged dry weather.

All the boreholes used in this investigation, geological logs were discussed and plotted during previous investigations and are also available on a comprehensive database. Two additional boreholes were drilled as part of this investigation to be used as observation bores during the pump tests. These bores will be incorporated into the monitoring program. The typical geological sequence at the investigation area are indicated in Figure 29 and Figure 30, these two figures represents the top 40 to 50 m of in-situ material of monitoring boreholes B03 and B66.
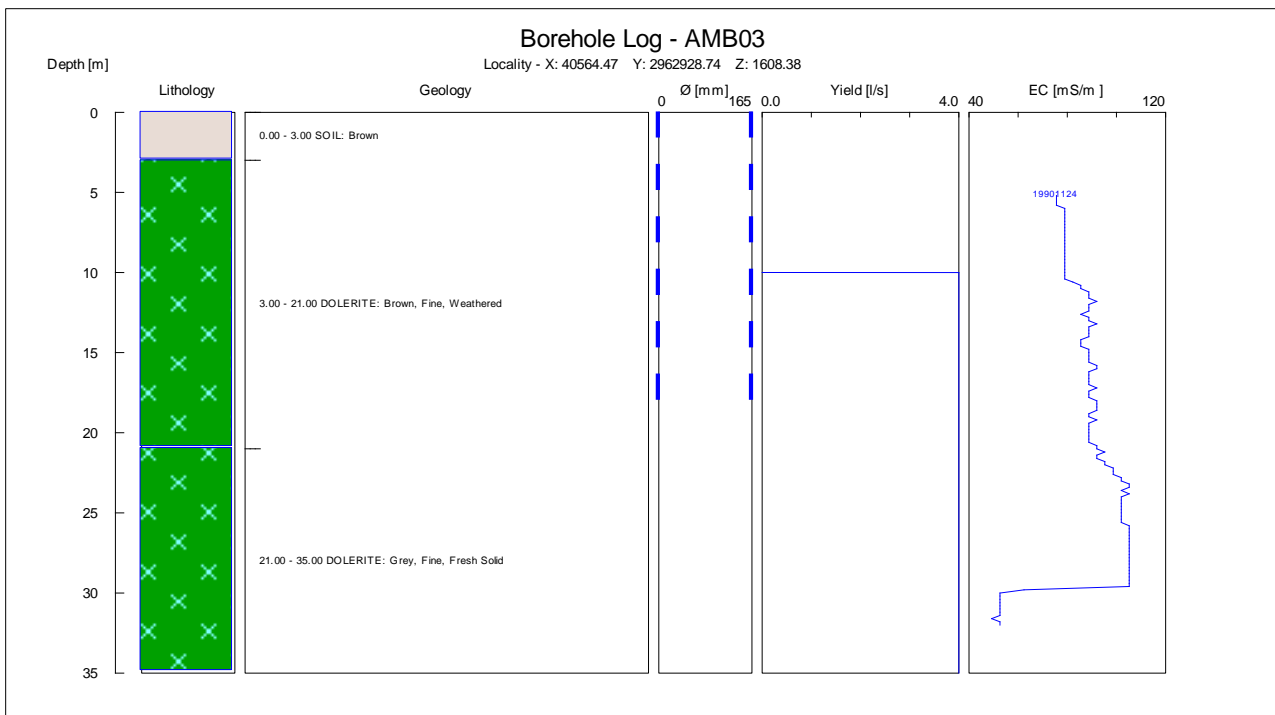

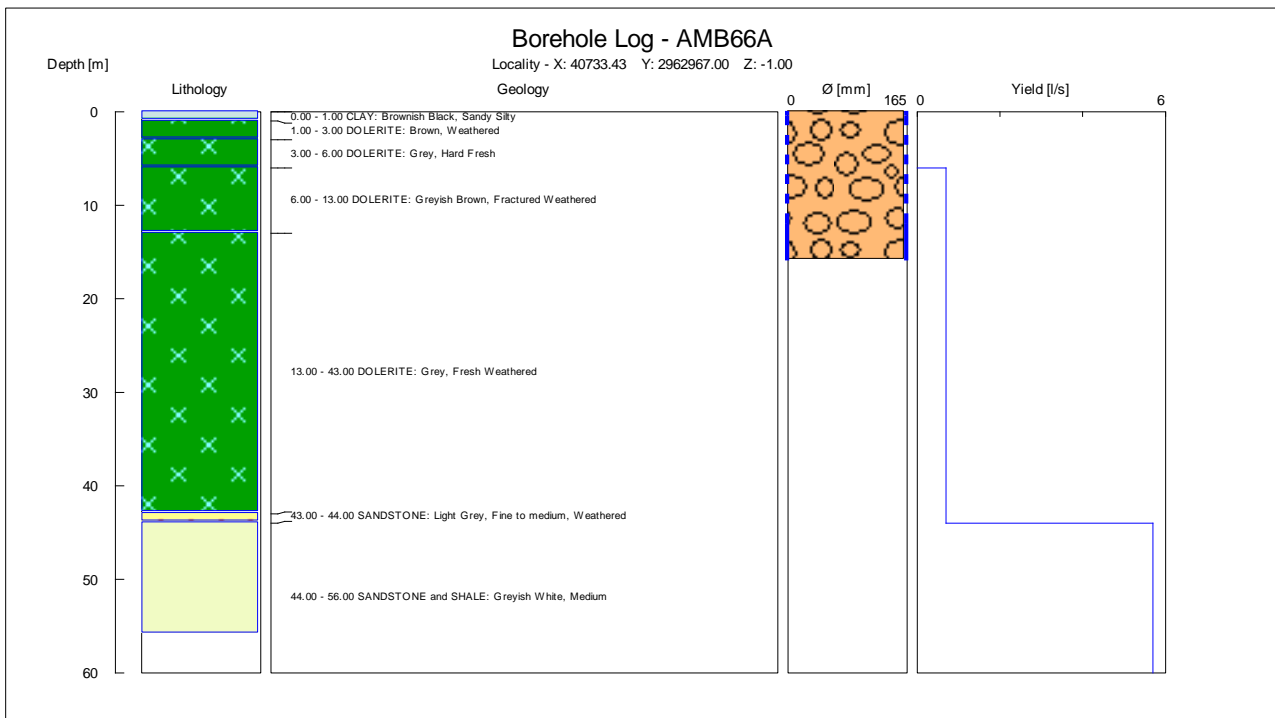*Figure 29. Geological log of monitoring borehole B03*

Figure 30. Geological log of monitoring borehole B66

3.3   GEOHYDROLOGY

The main water bearing aquifers in the vicinity of the ash stack are fractured rock aquifers. The term fracture refers to cracks, fissures, joints and faults, which are caused by (i) geological and environmental processes, e.g. tectonic movement; secondary stresses; release fractures; shrinkage cracks; weathering; chemical action; thermal action and (ii) petrological factors like mineral composition, internal pressure, grain size, etc.

From a hydrogeological point of view, a fractured rock mass can be considered a multi-porous medium, conceptually consisting of two major components: matrix rock blocks and fractures. Fractures serve as higher conductivity conduits for flow if the apertures are large enough, whereas the matrix blocks may be permeable or impermeable, with most of the storage usually contained within the matrix. Actually, a rock mass may contain many fractures of different scales. The permeability of the matrix blocks is in most cases of practical interest a function of the presence of micro-fractures. A rock mass which consists only of large fractures and some matrix blocks with no micro-fissures (or smaller fractures) lead to a term called purely fractured rocks. In this case, the domain takes the form of an interconnected network of fractures and the rock matrix, comprising the blocks surrounded by fractures, is impervious to flow. However, there may still be porosity. In the case where the domain is a porous medium (or a micro-scaled fractured medium) intersected by a network of interconnected fractures, the rock is termed a fractured porous rock and the domain is therefore characterized by at least two subsystems, each having a different scale of inhomogeneity (called scale effect).

3.3.1   Aquifer characteristics

Drilling data and work undertaken during previous investigations suggests that multiple aquifer types are represented at the site. These include:

- Unconfined aquifers present within soil horizons that have developed within colluvial and alluvial environments and the weathered upper levels of Ecca Formation sediments. These aquifers are generally perched on less permeable underlying in situ sediments;

- Unconfined aquifers along the trend of dolerite dykes. These may also act as recharge points for confined aquifers within the Ecca Formation at depth;

- Semi-confined aquifers within the Ecca Formation. These aquifers are commonly confined along essentially horizontal bedding interfaces between different lithologies, but can be locally unconfined along the trend of fractures zones, which allows the aquifers to recharge seasonally. The aquifers can therefore be regarded as a semi-confined, or leaky confined, aquifer on a regional scale if the definition of Fetter (1994) is considered;

- Deeper confined aquifers within basement lithologies.

From a pollution management viewpoint, the presence of a perched shallow aquifer is problematic due to resulting localised decreases in the bearing capacity of site profiles, and the increased potential for pollutant transport. In this instance, site aquifers are generally seasonal, which suggests that they either drain quickly (i.e. they are relatively permeable), have a low storage potential, or that stored water can be lost via evapo-transpiration processes. Contaminant movement away from pollution point sources can be reduced, or prevented entirely, through the construction of cut-off trenches and sub-soil drains to the confining layer at the base of the aquifer. This is not an option at the Tutuka ashing area site where pollutants are entering the underlying regional aquifers through cracks, fractures and highly weathered zones as in the vicinity of borehole AMB74 which intercepted weathered dolerite from surface to a depth of more than 24 meters.

All the available geological and geohydrological data (as described above) were considered and the following conclusions were made:

The model area was divided into four different layers, each with specific hydrological characteristics.

- The top layer represents all manmade structures like the ash stack, cut of drains and open pits. As part of this layer the top part of the unsaturated zone comprising of clays and soil were also included.

- The second layer represents the thin weathered geological formations on top of the underlying dolerite sill. Aquifers in this layer are generally perched on less permeable underlying in situ sediments.

- The third layer represents in-situ matrix of the fractured dolerite sill. Layers of low permeabilities and low yielding fractured rock aquifers characterize this layer. Semi-confined aquifers within the Ecca Formation occurred in this layer as well.

- The fourth layer represents impermeable bedrock formations of the local Karoo sediments, also with low yielding fractured rock aquifers. Deeper confined aquifers within basement lithologies occurred in this layer.

3.3.2   Water level Interpolation

When evaluating groundwater levels, it is also clear from the boreholes in the ash stack that the phreatic level of the water within the western part of the ahs stack becomes lower as the brine

irrigation progresses to the east. The time and progress at which this lowering occurs is currently not well documented due to the limited number of boreholes in the ash stack. For the same reason, the influence of the streams on the natural water table below the ash stack is also not recorded. From the graphs it is also evident that the water table is at the bottom or below the ash stack and that very little water exists in the ash stack itself where the brine irrigation has stopped.
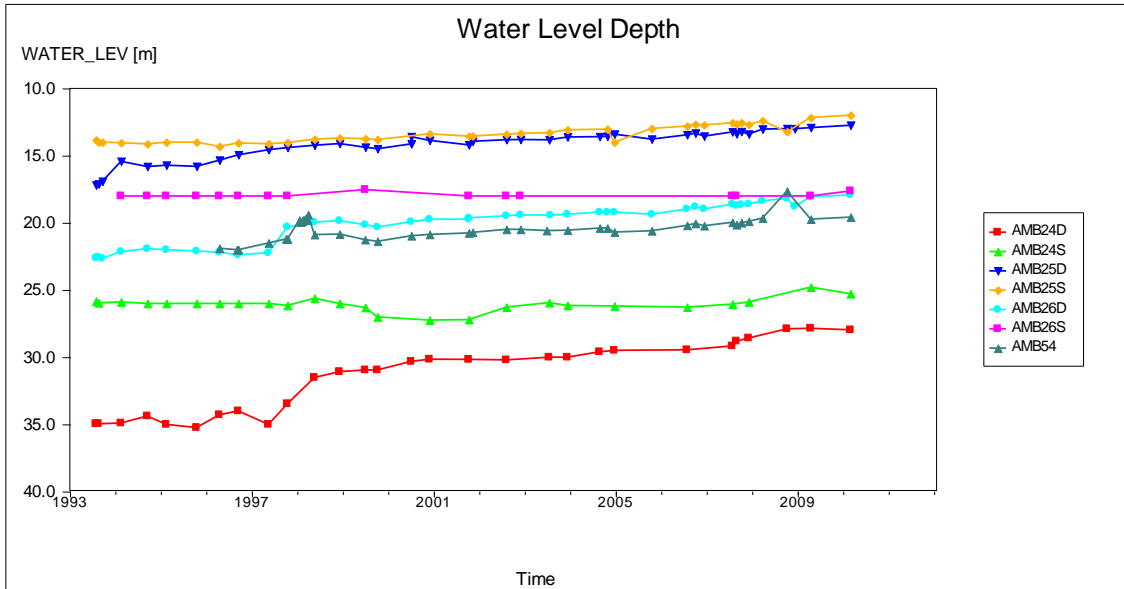
Figure 31. Water level depths of boreholes in or on the ash dump – measured in meters below ash dump surface.
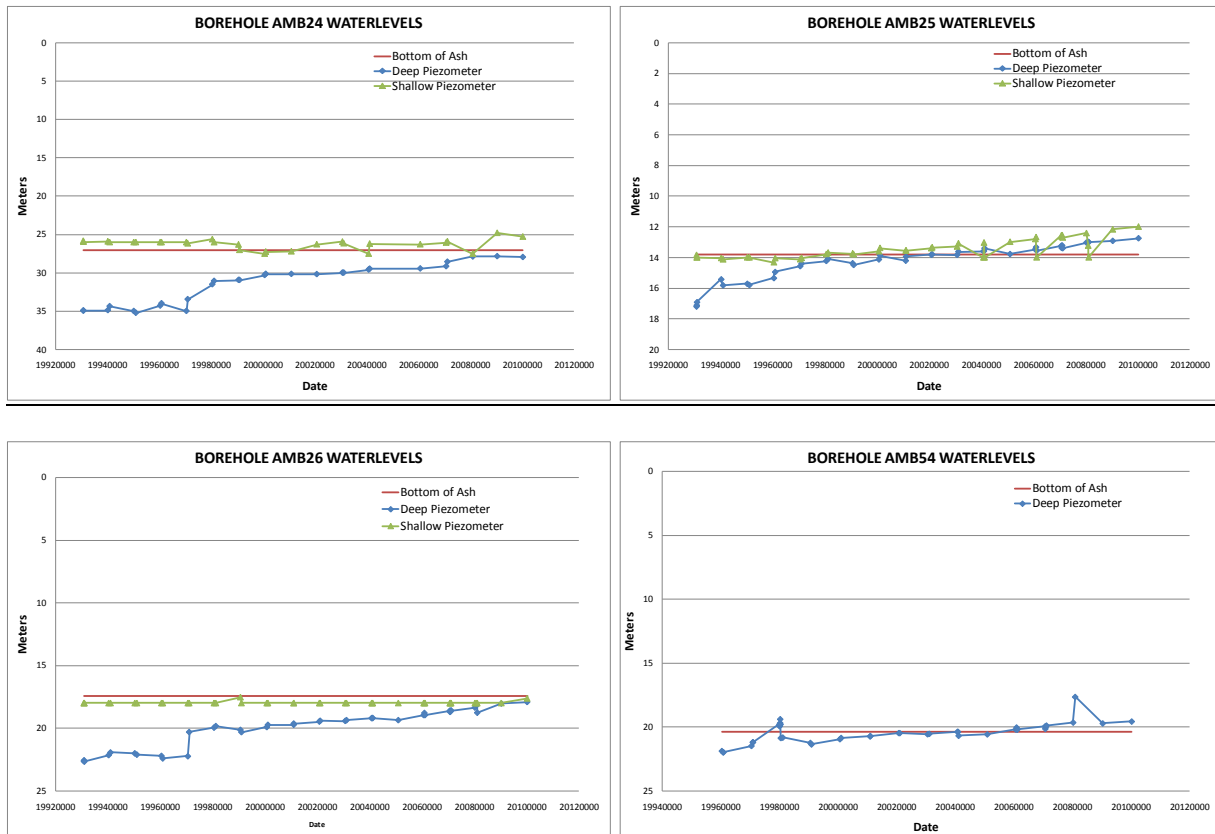
Figure 32. Bottom of ash stack and water level depths of boreholes in or on the ash dump – measured in meters below ash dump surface.

Due to the fact that the groundwater levels closely follow the topography in the region, the latter can be used to estimate groundwater levels at unknown points. Actual water level measurements taken at observation boreholes, were used as input data for the Bayes algorithm, while topographic contours were obtained from topographic maps and site plans from the mine and power station.

Bayesian Kriging is an interpolation method that uses this principle. In this approach, the classical statistical analysis of Ordinary Kriging is replaced by a Bayesian statistical analysis. The beauty of the Bayesian approach is that it allows one to express prior knowledge of the variable with a *qualified guess* that can be included in the estimation.

Bayesian interpolation is done with the estimator

$$Z*(\mathbf{x}_o) = \sum_{i=1}^{n} \alpha_i \left[Z(\mathbf{x}_i) - \mu(\mathbf{x}_i) \right] + \mu_0(\mathbf{x}_0)$$

where $\mu(\mathbf{x_i})$ is the qualified guess for site $\mathbf{x_i}$. The coefficients α_i , $i=1,...,n$ can again be determined from a system of linear equations and is a function of the parameters σ(Sigma) , k and ρ(Rho). These values can be estimated by the approximation of the semi-variogram with the theoretical $k\rho$ semi-variogram.

The following figure (refer to Figure 33) represents the local water level contours in meters above means sea level (mamsl).
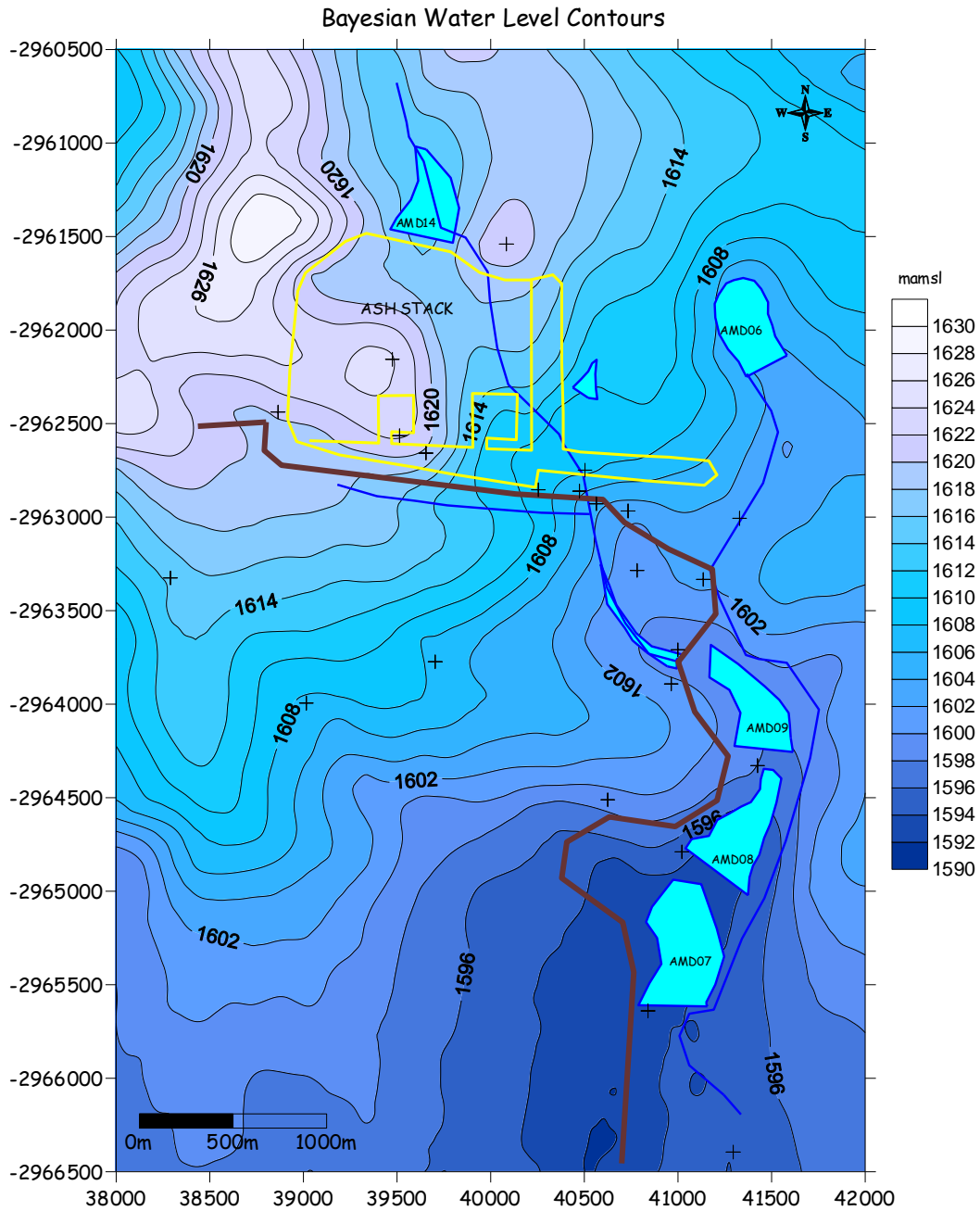
Tutuka Power Station Ashing Area

Bayesian Water Level Contours

Figure 33. Water level contours.

3.3.3 Hydraulic variables and constraints

Variables and constraints that act upon the movement of groundwater and pollutants through an aquifer are typically:

- The transmissivity and hydraulic conductivity of the underlying strata. The hydraulic conductivities of fractured systems vary considerably and are dependent on: aperture (distance between fracture walls), frequency or spacing (density), length, orientation (random or preferred), wall roughness (asperities, including skin factor), presence of filling material, fracture connectivity, channelling (preferred paths) and the porosity and permeability of the rock matrix

- The storage coefficient of aquifers in the Highveld Coalfields has been tested by pumping test methods, and an average value of 10^{-4} can be assumed for the fractured aquifer. The reason for this relatively low storativity value lies in the fact that only a small proportion of the pores and fractures in the un-weathered aquifer partake in water flow. In the upper, weathered aquifer the effective porosity is an order higher and a value of 10^{-2} can be achieved. This higher value is a result of the fact that almost all calcium and magnesium that normally binds the sedimentary grains together, has been leached from this horizon. Water can therefore permeate into and through the weathered matrix (Hodgson, 1999).

- The hydraulic gradient, dispersion and convection characteristics of the aquifer.

- Groundwater boundaries exist in various forms in nature and have to be accounted for in models. Typical boundaries are dolerite dykes and sills, which may act as impermeable barriers in the transverse direction, or as conductive zones along intrusive contacts. Close to surface, dolerite weathers and water permeates easily through it. The lateral propagation of pollution plumes is therefore not hindered by these structures. Other boundaries are, for instance, catchment boundaries, where a change in the direction of the water-table gradient may occur. Surface boundaries, above which the groundwater level cannot rise without decanting, should also be considered. Boundaries of this type can be accommodated in flow and mass transport models, with the prerequisite that knowledge about these boundaries must be available for the areas in question.

The following boundaries were incorporated in the flow model: *Constant head boundaries*: structures like the active ash dams were classified as constant heads. *River boundaries:* the Wolwe Spruit east and south of the ashing area.

- Other sources of water in the area such as streams, pans, dams and lakes. Sources of water may be incorporated in groundwater computer models. They may exist in the form of constant or specified flux sources. A good example of such a source in the modelling exercise to follow is the constant water supply (brine irrigation) at the ash dam. Another source is the rainfall that recharges the aquifer.

  A recharge of 3% of the annual rainfall was used for normal geological formations as well as the rehabilitated areas of the ash stack. A recharge of 20% of the annual rainfall was used for the un-rehabilitated areas of the ash stack where no irrigation is taken place. The average annual rainfall for the region under investigation is about 700 mm per year according to data obtained from various weather stations in the area.

  An additional 0.7 Ml/day of brine is irrigated onto approximately 0.1 km^2 or 100 hectares un-rehabilitated areas of the ash stack. The areas irrigated is approximately 0.1 km^2 or 100 hectares this result in 2555 mm per year of brine irrigated. The recharge used on the irrigated areas is 651 mm per year which is 20% of the rainfall and brine irrigated (20% of 3255 mm per year).

Table 2.   Recharge figures for the area under investigation

Area	Precipitation / Irrigation (mm/year)	Recharge %	Recharge (mm/year)
Undisturbed natural areas	700	3%	21
Rehabilitated ash stack	700	3%	21
Un-rehabilitated ash stack	700	20%	140
Front stack & back stack irrigation	2555	20%	511
Front stack & back stack precipitation & irrigation	3255	20%	651

- Sinks within the area where groundwater is abstracted or naturally emanates on surface in the form of fountains. Points where water is taken from the system, such as boreholes, drains or fountains, are referred to as sinks. The finite difference model to be used in this exercise can accommodate sinks at any position in the model, and the effect of water abstraction or water loss at these points can be simulated. This facility may be used to predict the response of a pollution plume during groundwater abstraction. Currently, there are no significant users of groundwater in the area that could impact on the movement of pollutants through the aquifer.

Different techniques were used to perform and evaluate aquifer tests at Tutuka Power Station during the last ten years. Point dilution, slug and constant discharge tests were used. Point dilution and constant discharge tests proved unfeasible at some sites due to the excessive water strike depth, the low apparent profile permeability suggested by slow seepage rates, and poor wet weather access. Given these site conditions, slug tests were thought to be a more appropriate method of assessing aquifer characteristics in some instances. All the results of the tests are listed in Table 3.

Table 3.   Aquifer parameters obtained from different methods.

BH no.	Test date	Method test	Permeability K (m/day)		Transmisivity T(m2/day)				Storitivity S				Velocity (m/d)	
			Bouwer & Rice	IGS FC Software	Cooper et al	Cooper & Jacob	Theis	Neuman	Cooper et al	Cooper & Jacob	Theis	Neuman	Darcy IGS Tracer Software	Seepage IGS Tracer Software
AMB01	Sep-93	Slug	6.040		95.00				0.0001					
AMB02	Sep-93	Slug	1.440		37.00				0.0003					
AMB03	Sep-93	Slug	1.830		54.00				0.0003					
AMB03	Dec-02	Constant disharge obs. bh						48.40				0.0004		
AMB23	Sep-93	Slug	0.243		4.00				0.0356					
AMB24	Sep-93	Slug	0.012		0.07				0.0513					
AMB25	Sep-93	Slug	0.008		0.07				0.0417					
AMB26	Sep-93	Slug	0.009		0.06				0.0910					
AMB63	Oct-01	Point dilution											0.04	0.73
AMB64 shallow	Oct-01	Point dilution											0.04	0.80
AMB64 deep	Oct-01	Point dilution											0.09	1.73
AMB65	Oct-01	Slug		0.729										
AMB66	Oct-01	Slug		0.573										
AMB66	Dec-02	Constant discharge pump bh				4.90	5.00			1.5100	0.0018			
AMB67	Oct-01	Slug		0.048										
AMB68	Oct-01	Slug		0.839										
AMB73	Dec-02	Constant discharge obs. bh						4.30				0.0001		
AMB74	Dec-02	Constant discharge pump bh				52.80	50.00			0.0001	0.0001			
AMB90	Apr-10	Slug		1.935										
AMB90	Apr-10	Constant discharge pump bh				12.80	15.00			0.0041	0.0013			
AMB91	Apr-10	Slug		0.203										
AMB91	Apr-10	Constant discharge pump bh				0.60	2.00			0.0470	0.0005			
AMB92	Apr-10	Slug		0.315										
AMB92	Apr-10	Constant discharge pump bh				9.30	9.00			0.0130	0.0160			
AMB93	Apr-10	Slug		0.172										
AMB93	Apr-10	Constant disharge pump bh				3.18	3.00			0.0008	0.0009			

Regardless of the test method used, results suggest that both groundwater flow rates through perched aquifers within the weathered zone, and deeper regional aquifers associated with fractured and baked zones, are relatively high (refer Table 3).

Consideration should be given to developing a well field in the vicinity of the ash pile for pollution management purposes, particularly given the relatively high permeability of site aquifers in this area. All the above parameters were used as input parameters into the groundwater model.

Different abstraction rates were also tested with the model at these boreholes to determine the effective interception of the pollution plume.

3.4 ASH HYDRAULIC CONDUCTIVITY

Falling head permeability tests undertaken on undisturbed samples indicate that sample hydraulic conductivity decreases with increasing dry density (refer Table 4), a characteristic observed previously by Geo Hydro Technologies (1998). Upon construction of a semi-log plot, however, a log-normal relationship is apparent, which suggests that there is little spatial variation in the physical characteristics of the ash.

Table 4.   Results of permeability testing undertaken on undisturbed ash samples.

Test Pit	Depth	Initial Dry Density	Initial Moisture Content	K	Porosity
	m	kg/m^3	%	m/d	%
1	0.3-0.45	1164	23.6	0.161	47
3	0.8-1.1	930	36.1	9.150	58
3	1.7-1.95	978	22.4	2.037	56
3	2.8-3	962	23.8	2.369	56
4	0.3-0.6	1112	21.7	2.101	49
5	0-0.4	889	39	7.323	60
5	0.5-0.8	1026	29.5	2.331	53
6	0.9-1.2	1070	43	0.772	51

Bouma et al. (1999) note that the hydraulic conductivity of a given soil increases with moisture content, and reaches a maximum when the sample is saturated. Thus, a plot was also prepared to determine whether there was a relationship between these two parameters (refer Figure 34). The resulting graph indicates that an exponential relationship does exist, further supporting the presence of a pile comprised of ash of consistent physical characteristics.

Table 4 also shows porosities for undisturbed samples calculated assuming an ash particle Specific Gravity (S.G.) of 2.2 (Kreuiter, pers. comm., 2000). As would be expected, a log-normal relationship is also apparent.
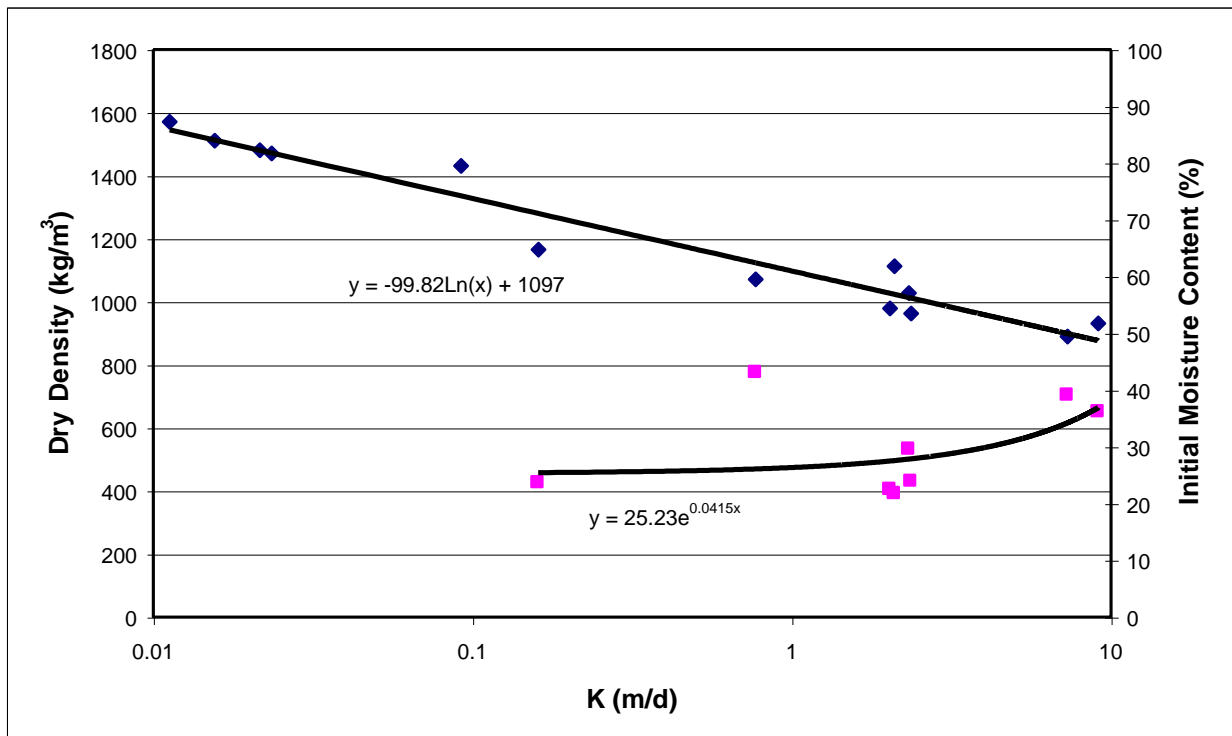
Figure 34   Plot of log-normal relationship between permeability and dry density. Note that an exponential relationship is also apparent between ash moisture content and dry density. Thus, the placement moisture content of the ash appears to influence the degree to which the ash will compact, be it by artificial or natural settling processes.

3.5   ASH MOISTURE RETENTION

Moisture retention testing undertaken in the laboratory indicates an approximately linear relationship between moisture content and induced soil suction between pressures of 10 and 300 kPa (refer Figure 35). Results suggest that the tested ash material had a high moisture retention capacity at low suction, with a progressive decrease in retention apparent with increasing negative head pressures. At head pressures of 30m, approximately 25% of moisture is retained.

Interpolation from the retention plot suggests a total porosity of 55 and 71% for ash material with a dry density of 889 and 930 kg/m^3, respectively, values consistent with those calculated assuming an ash particle S.G. of 2.2. However, the surface field capacity measured by Blight (1998) was about 40%, a significantly lower value comparable to the moisture content of an in situ surface sample taken within the irrigated area during this investigation (TP5: 0-0.4m=39%). Thus, it initially appears that laboratory derived moisture retention curves for Tutuka ash has little applicability.

Differences between the effective and total porosity of the ash may be one reason for the observed moisture retention response. In the laboratory, every pore has the opportunity to become filled with water, and thus testing is indicative of the total porosity of the sample, while under field conditions this may not be possible, and therefore the effective porosity is represented.
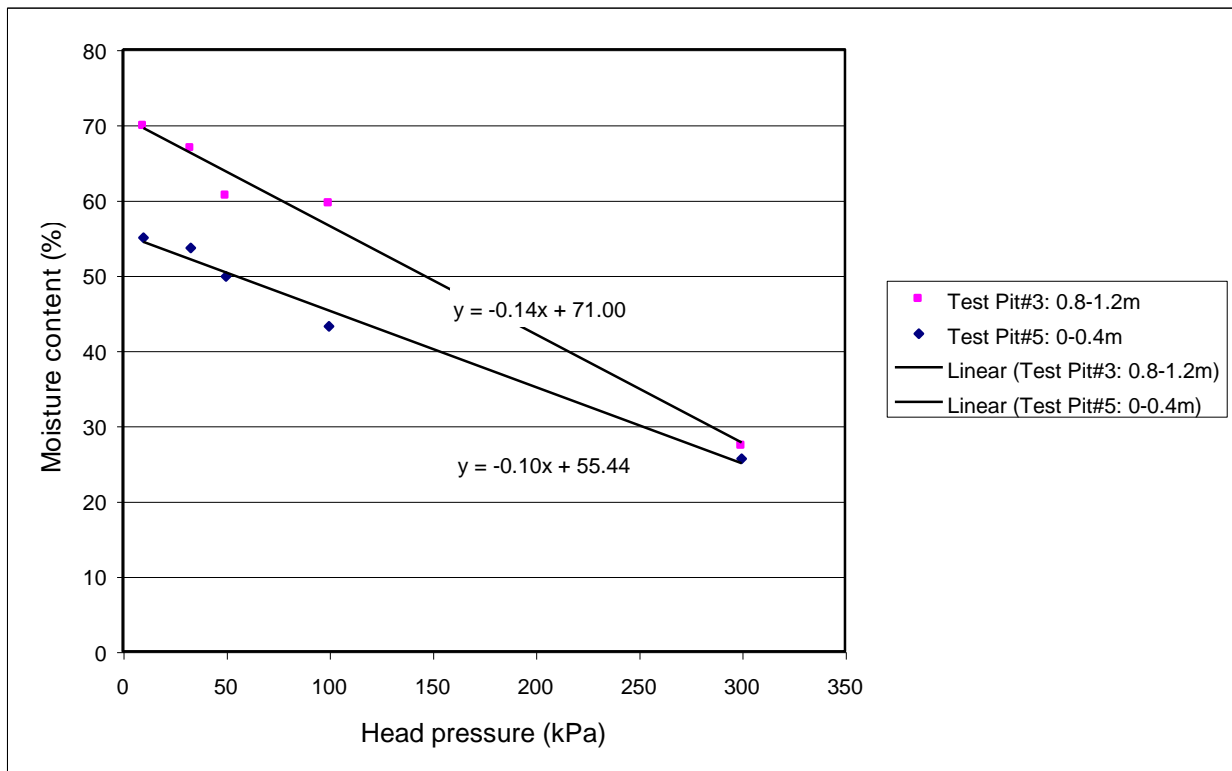
Figure 35. Laboratory derived moisture retention characteristics determined for in situ ash samples. These results do not, however, appear to relate to the moisture capacity measured in the field.

3.6 HYDROCHEMISTRY

Historical chemical trends, along with spurious values and the differences between chemical constituents with depth are discussed in detail in this section. This is necessary to determine the depth and extend of the pollution in the vicinity of the ash stack. This was done by using different presentation techniques and tables.

3.6.1 Background concentrations

By selecting water sampling sites that represents the least polluted water and assuming that this represents background conditions, a pollution index can be defined. Sites that fall under these specifications at the ashing area are AMB31, AMB36, AMB51, AMB52 and AMB53. Pollution indicator elements were determined by different statistical methods during previous investigations. From which

EC, Na, Cl, and SO_4

were selected as elements which will serve as good indicators of pollution. For this study only EC and SO^4 were selected for representation in figures. SO^4 concentrations were also used for the mass transport model and the determination of the pollution plume. The following figures represent the concentrations of the elements at the different background sites.
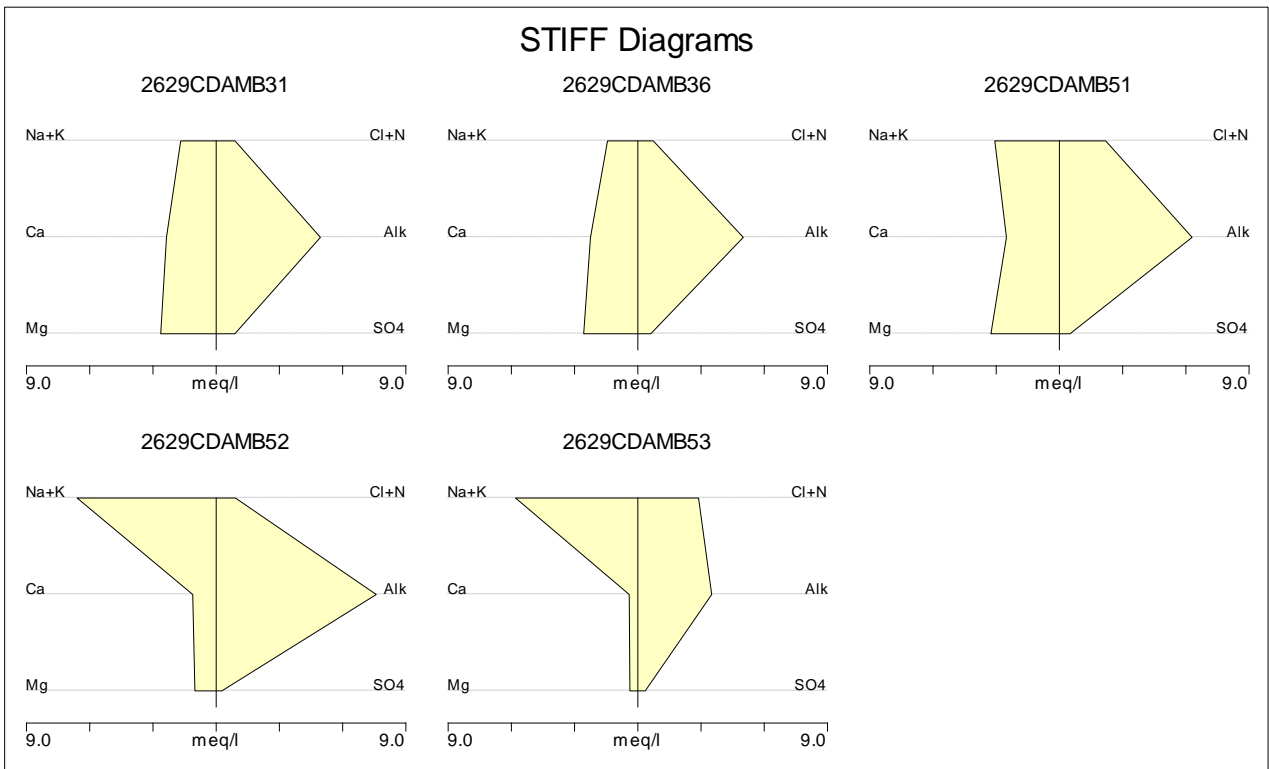
Figure 36. Stiff diagrams of unpolluted background boreholes
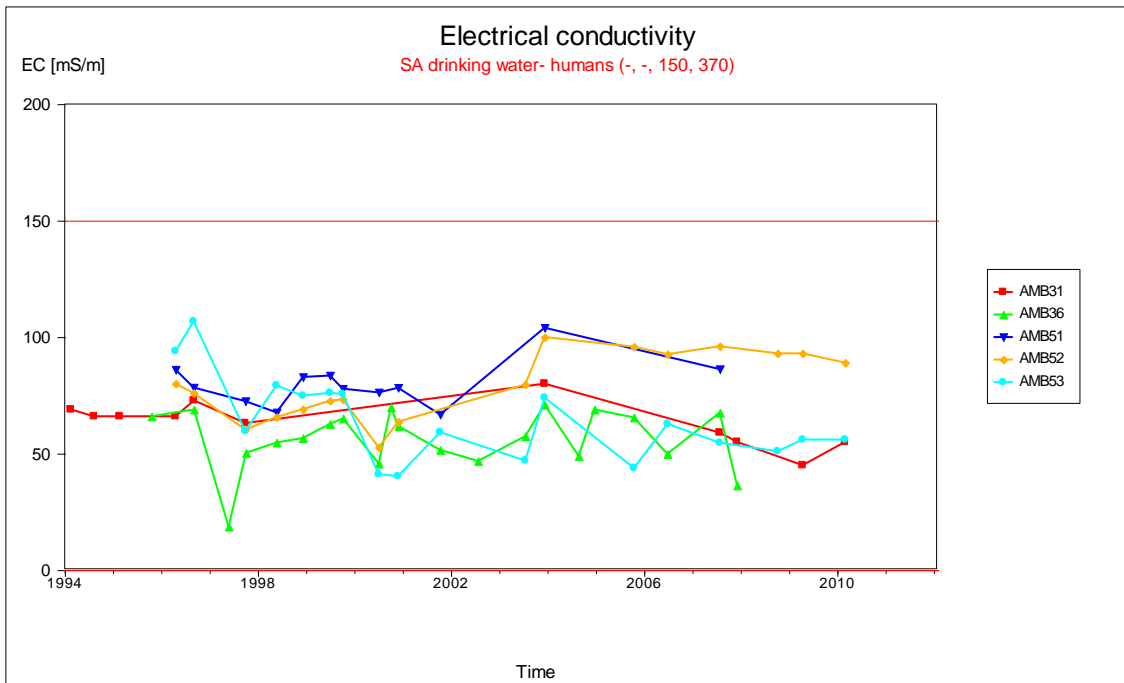
Figure 37. EC concentration of unpolluted background boreholes
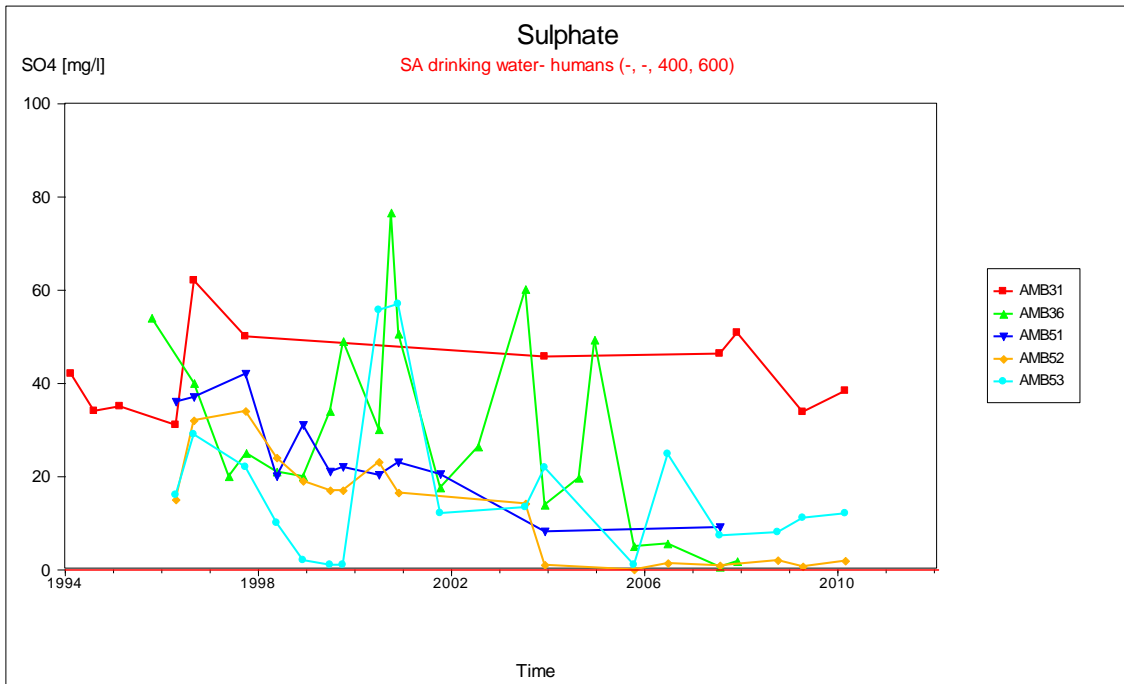
Figure 38. SO⁴ concentration of unpolluted background boreholes
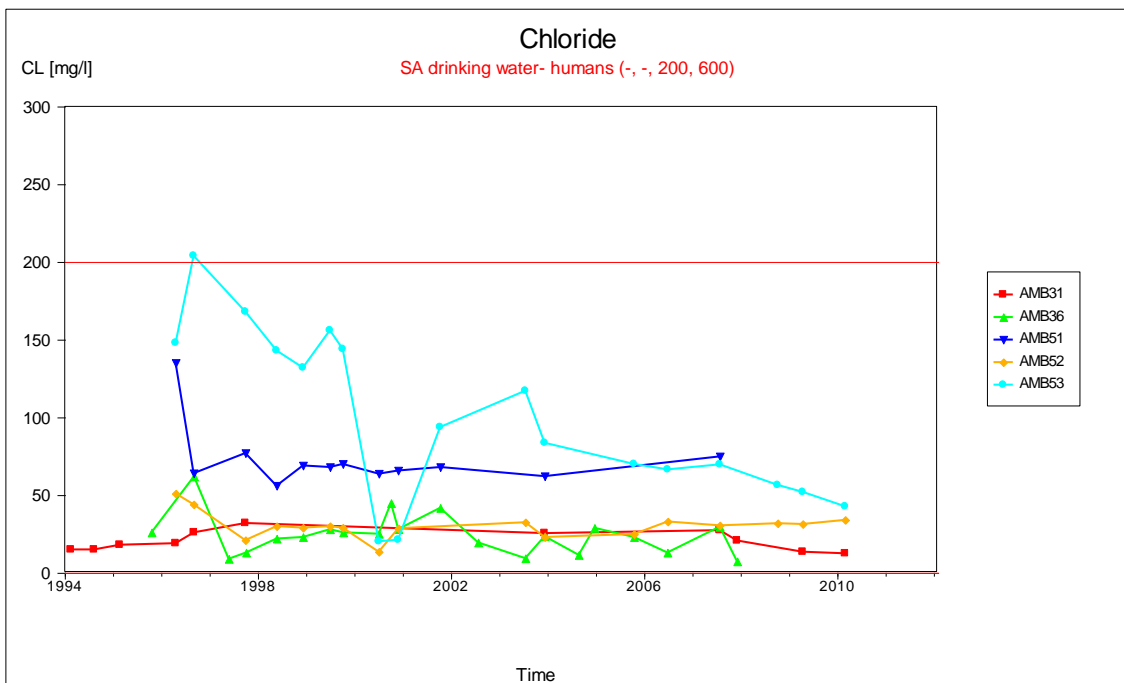
Figure 39. Cl concentration of unpolluted background boreholes
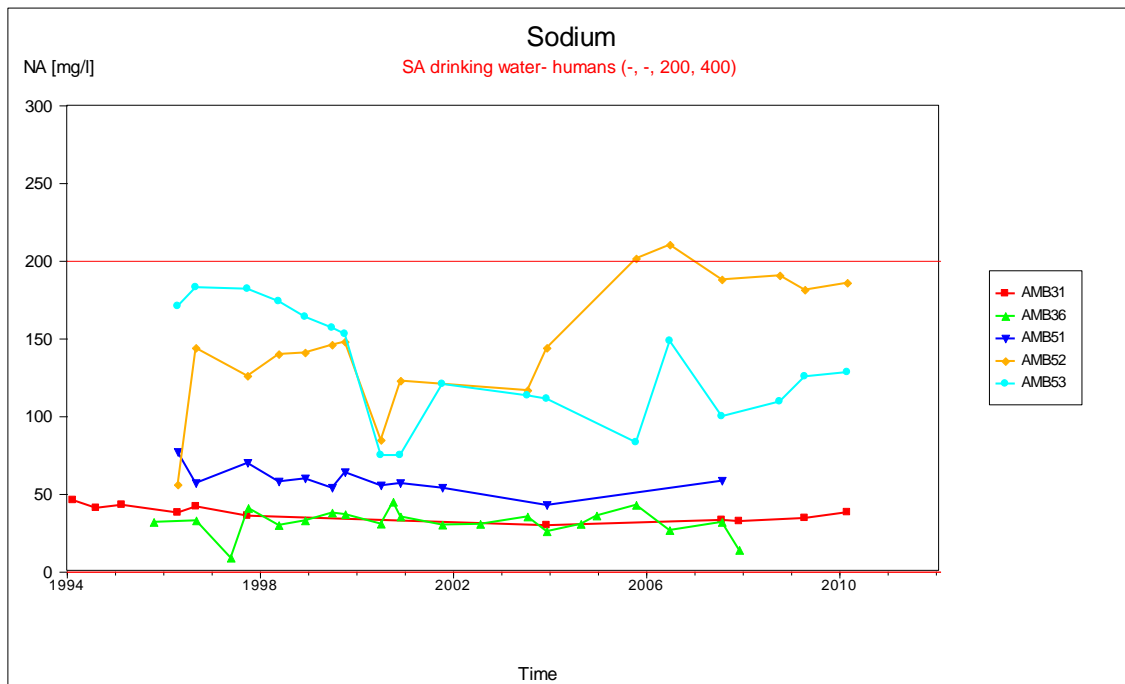
Figure 40. Na concentration of unpolluted background boreholes

Unlike all other boreholes constructed into regional doleritic aquifers at the site, AMB31, AMB36, AMB51, AMB52 and AMB53 are constructed up hydraulic gradient from the ash pile, which contained groundwater of the Mg-HCO$_3$ type characteristic for aquifers of basaltic composition (Bean, 1999). Further, the Cl content of groundwater sampled from these bores showed little temporal variation. It thus seems reasonable to assume that these sites could be used to provide some insight into background water quality.

From the above figures and discussion it can be concluded that selected sites represent the ambient unpolluted chemical concentrations of the ashing area.

3.6.2 Pollution index

The groundwater quality at the different boreholes in the ashing area was measured and evaluated by means of a local background groundwater quality as discussed in the previous section.

An average concentration of all the background boreholes was used as reference concentrations for the different indicator elements. The reference concentrations of the indicator constituents of the selected sites are then used as a standard for comparison. Comparison is made between these values and the values of the sites within the ash stack sphere of influence. This method provides an effective survey to gauge the impact of the ashing activities on the water quality of the surrounding aquifers.

The index value is calculated by dividing the concentration of each monitoring site by the reference concentration. Generally, index values greater than one indicate that the water quality is been impacted on.

Table 5.   Pollution indexes of the indicator elements.

	EC		Ca		Na		Cl		SO4	
	mS/m	Index	mg/l	Index	mg/l	Index	mg/l	Index	mg/l	Index
Background concentrations										
Minimum	19		6		9		9		4	
Average	65		34		80		55		29	
Maximum	107		75		183		204		102	
Deep aquifer concentrations										
AMB23	255	4	166	5	115	1	524	9	725	25
AMB24D	615	9	502.8	15	100	1	1051	19	1508	52
AMB25D	105	2	118	4	74	1	202	4	134	5
AMB26D	178	3	148	4	148	2	299	5	435	15
AMB30D	428	7	465	14	345	4	839	15	1547	53
AMB66A	271	4	325	10	71	1	531	10	721	25
AMB68A	74	1	4	0	164	2	50	1	2	0
Average	**275**	**4**	**247**	**7**	**145**	**2**	**499**	**9**	**725**	**25**
Shallow aquifer concentrations										
AMB24S	638	10	364.7	11	1055	13	1007	18	1747	60
AMB25S	380	6	244	7	550	7	382	7	1223	42
AMB30S	453	7	343	10	500	6	810	15	1463	50
AMB64B	67	1	10	0	141	2	51	1	30	1
AMB68B	74	1	4	0	160	2	59	1	8	0
AMB03	311	5	293	9	84	1	564	10	1129	39
Average	**320**	**5**	**210**	**6**	**415**	**5**	**479**	**9**	**933**	**32**
Down gradient deep and shallow aquifer concentrations										
AMB01	67	1	8	0	180	2	25	0	12	0
AMB02	60	1	69	2	32	0	14	0	44	2
AMB21	60	1	69	2	32	0	26	0	42	1
AMB36	47	1	39	1	31	0	20	0	26	1
AMB54	57	1	27	1	70	1	101	2	7	0
AMB55	42	1	31	1	53	1	19	0	4	0
AMB56	46	1	22	1	73	1	14	0	2	0
AMB63	178	3	104	3	72	1	319	6	204	7
AMB65	59	1	31	1	59	1	26	0	62	2
AMB67	34	1	17	0	49	1	9	0	14	0
Average	**65**	**1**	**42**	**1**	**65**	**1**	**57**	**1**	**42**	**1**

The following figures represent the concentration of the different boreholes on and in the vicinity of the ash stack. Note the different concentrations in the shallow and deep piezometers as well as the boreholes which have been sampled at different depths.
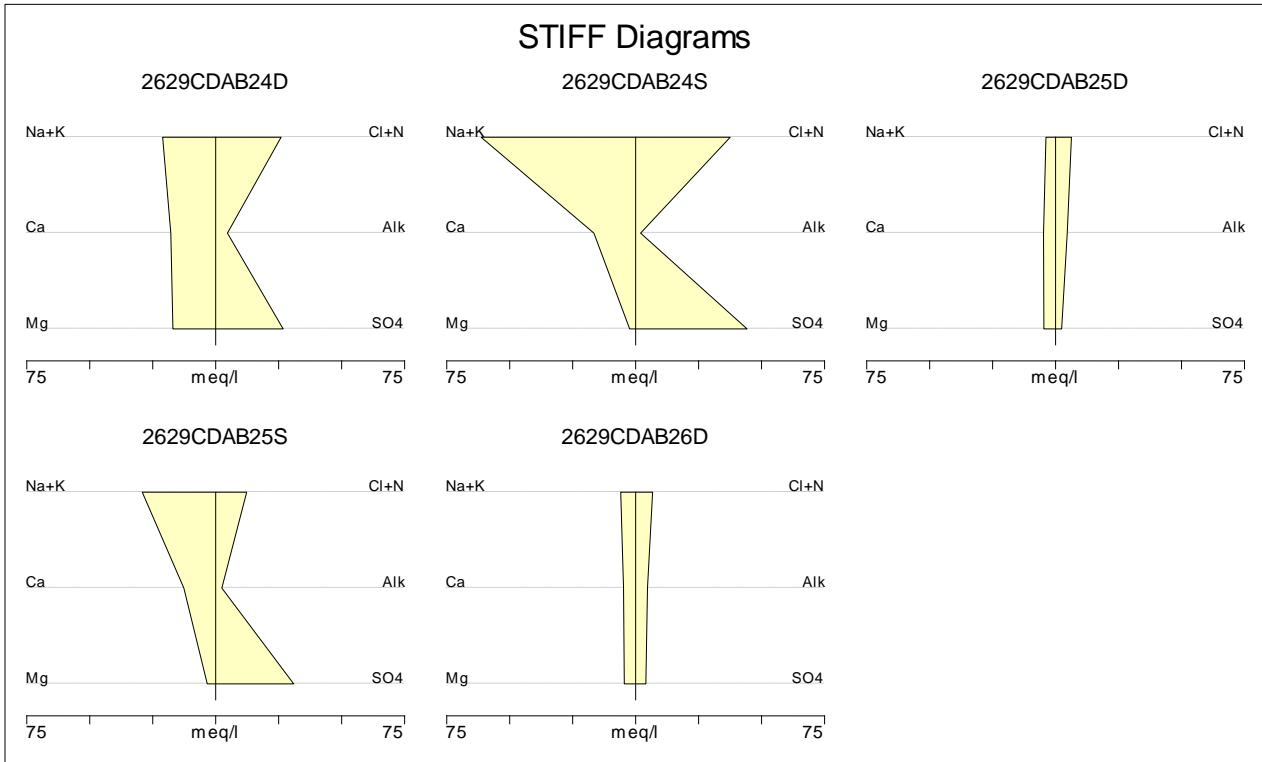
Figure 41. Stiff diagrams of polluted boreholes on the ash stack
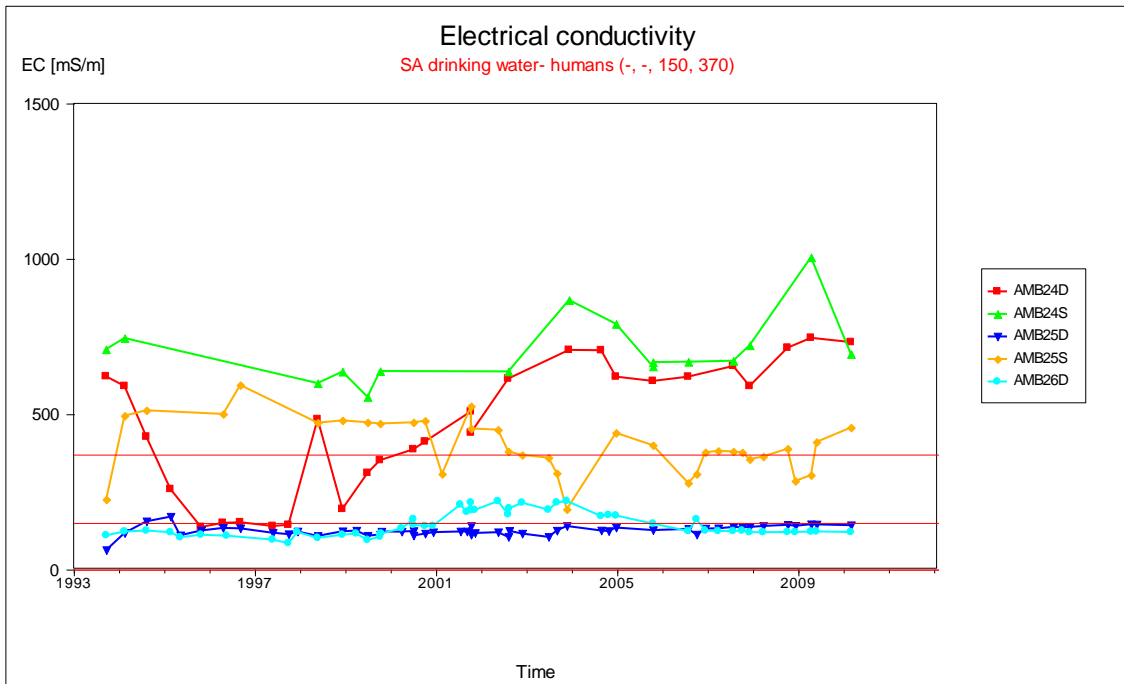
Figure 42. EC concentration of boreholes on the ash stack
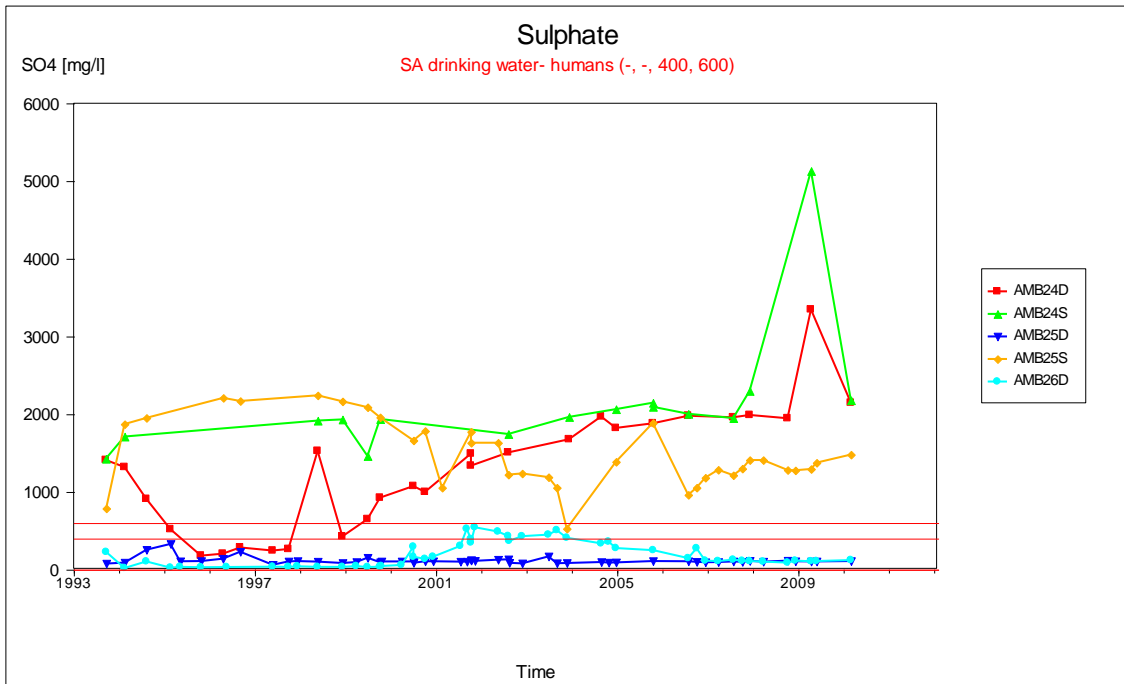
Figure 43. SO⁴ concentration of boreholes on the ash stack
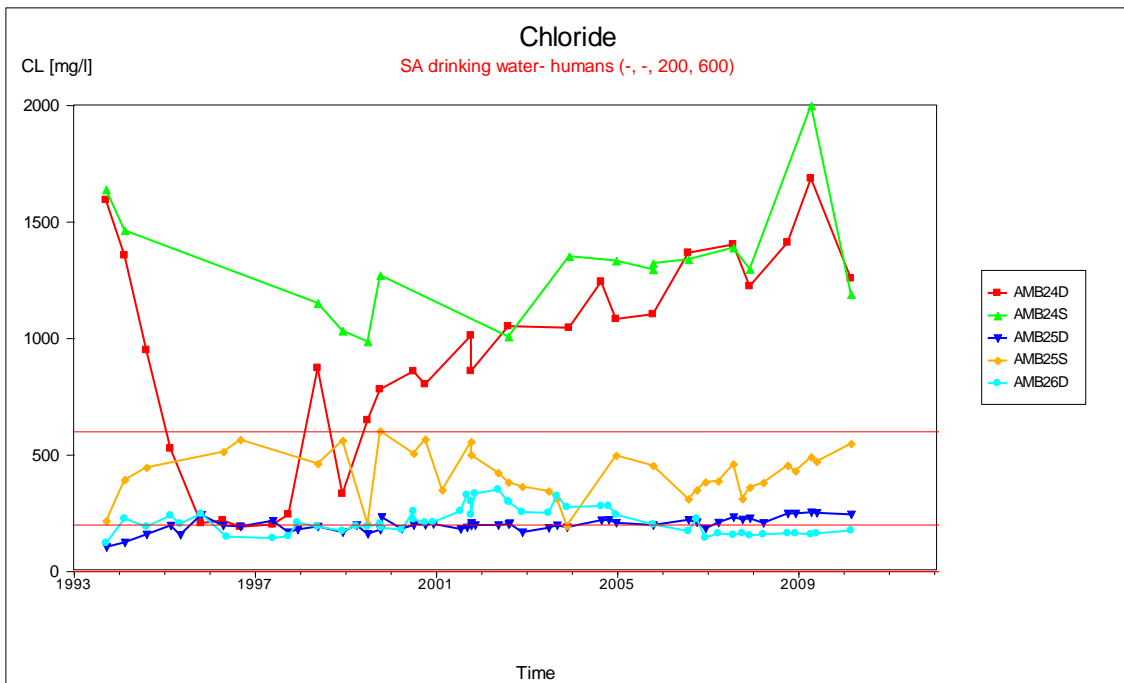
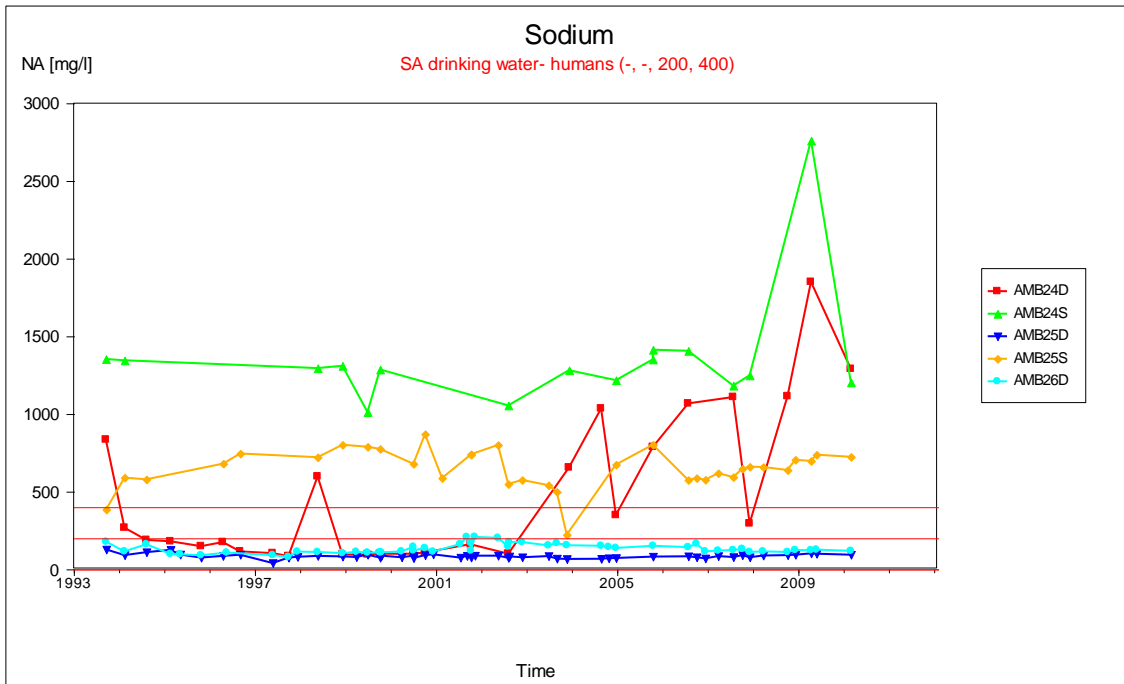

Figure 44. Cl concentration of boreholes on the ash stack

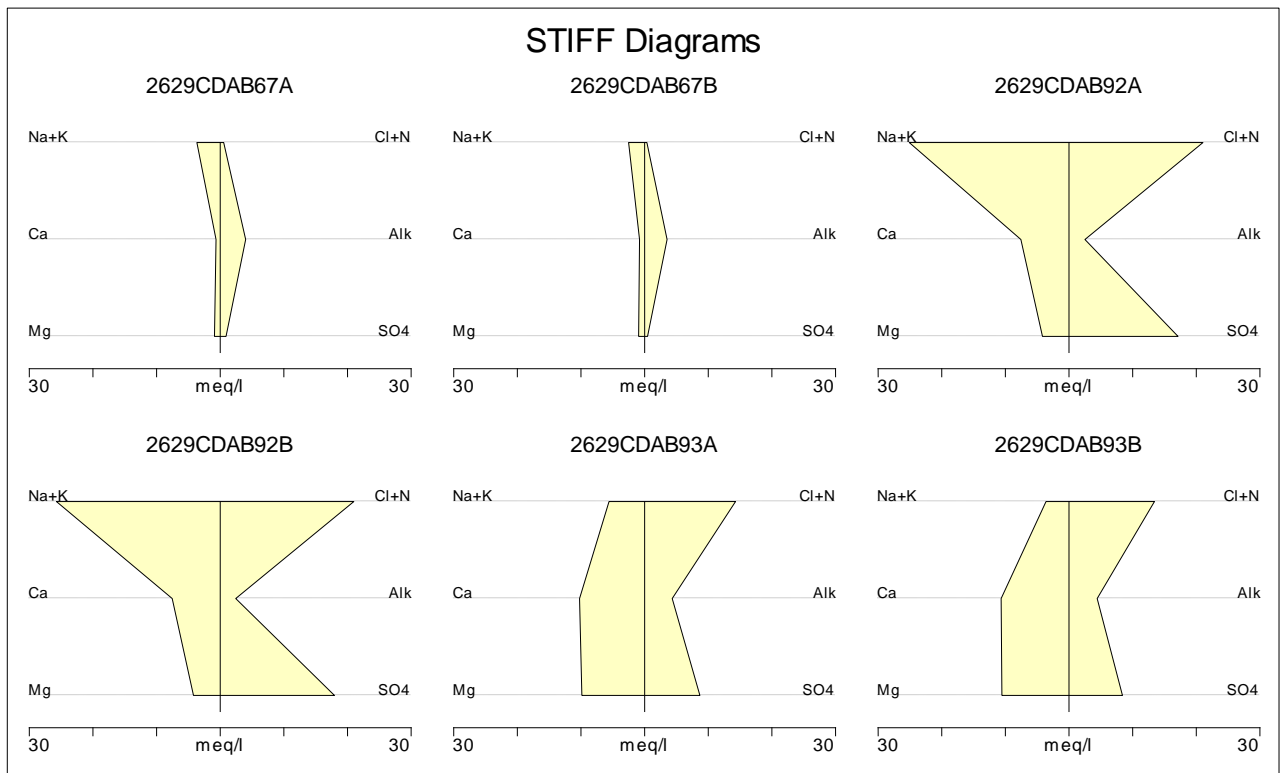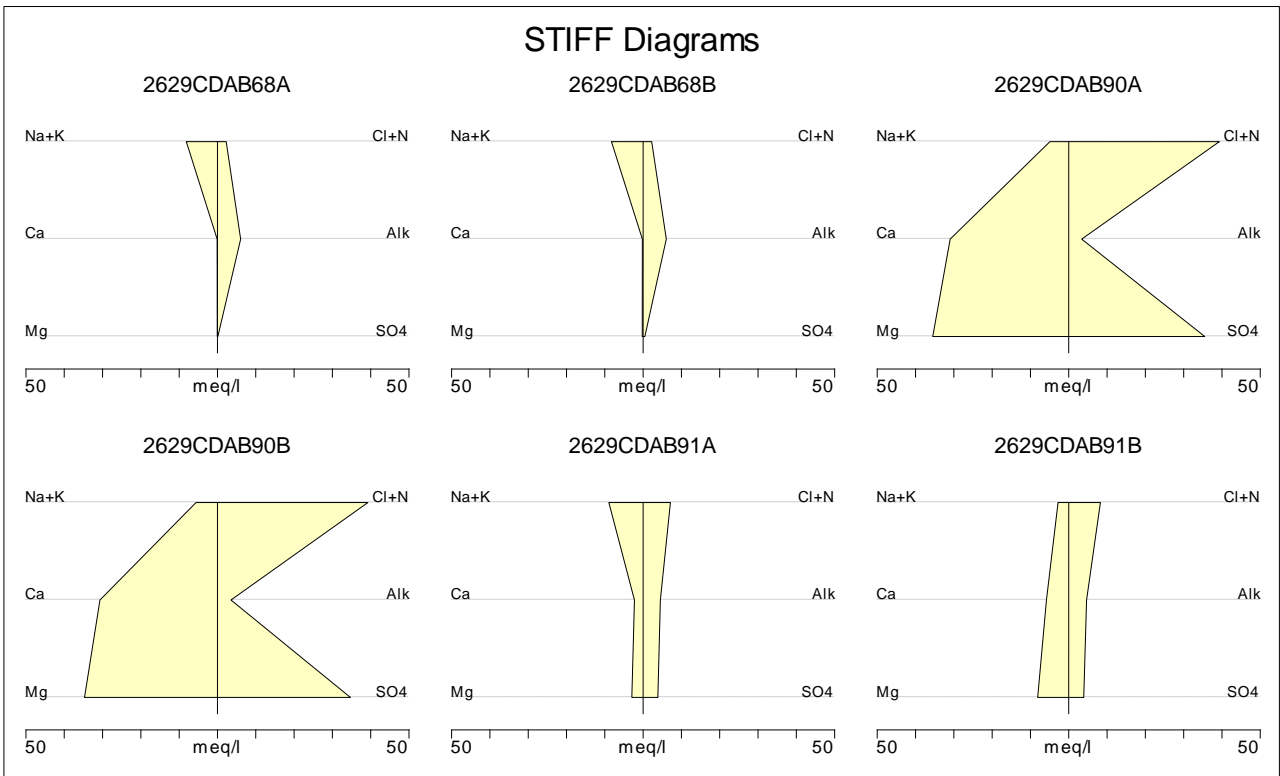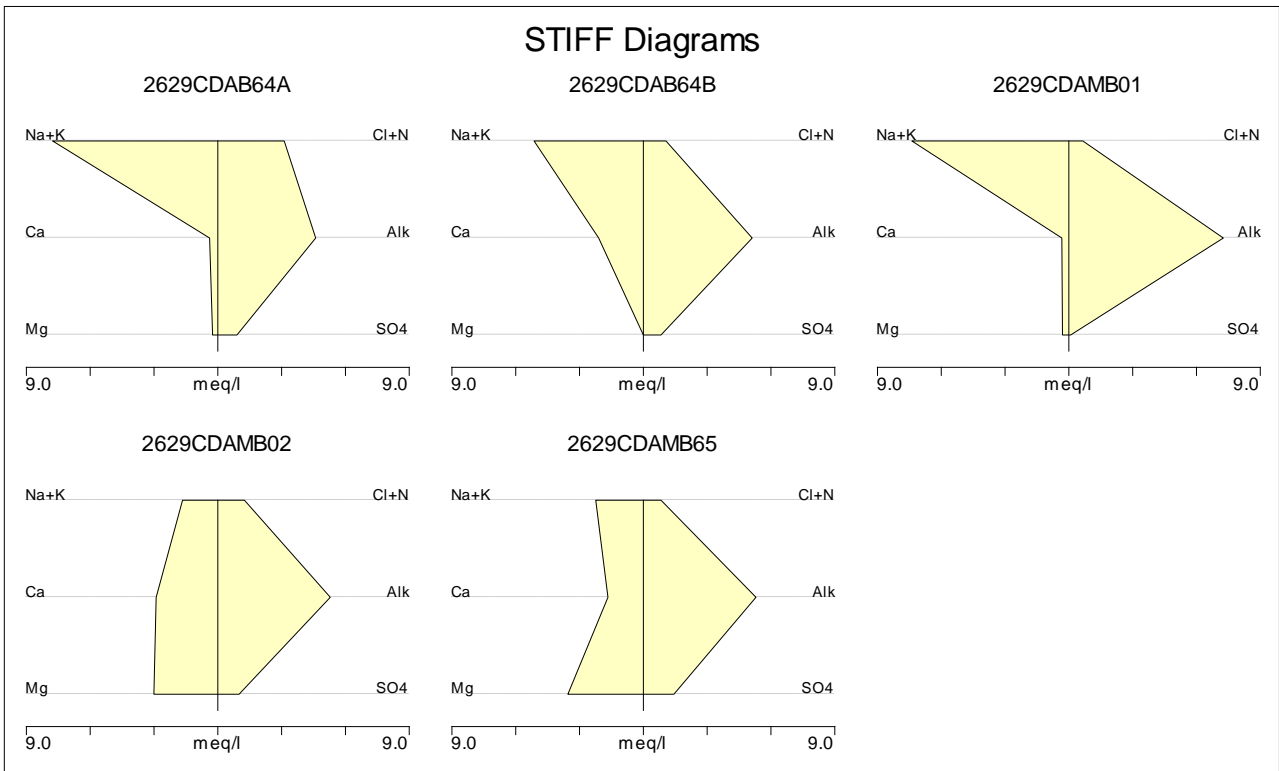*Figure 45. Na concentration of boreholes on the ash stack*

STIFF Diagrams

STIFF Diagrams

Figure 46.   Stiff diagrams of boreholes drilled to determine the extent of the pollution plume.
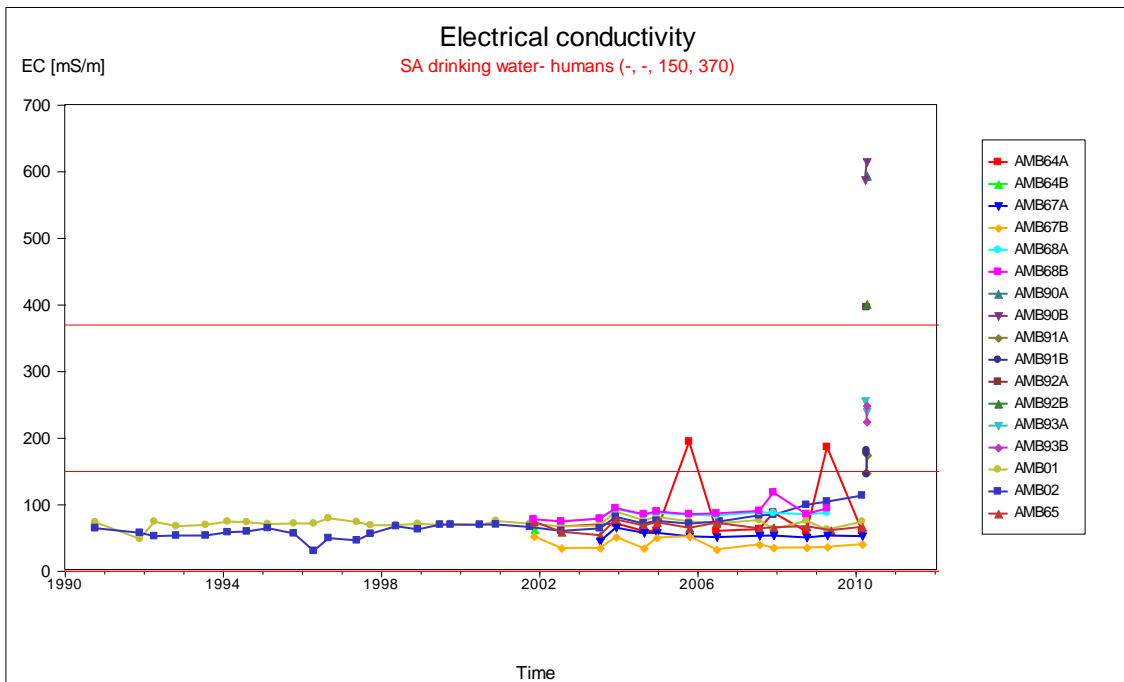
Figure 47. EC concentration of boreholes drilled to determine the extent of the pollution plume.
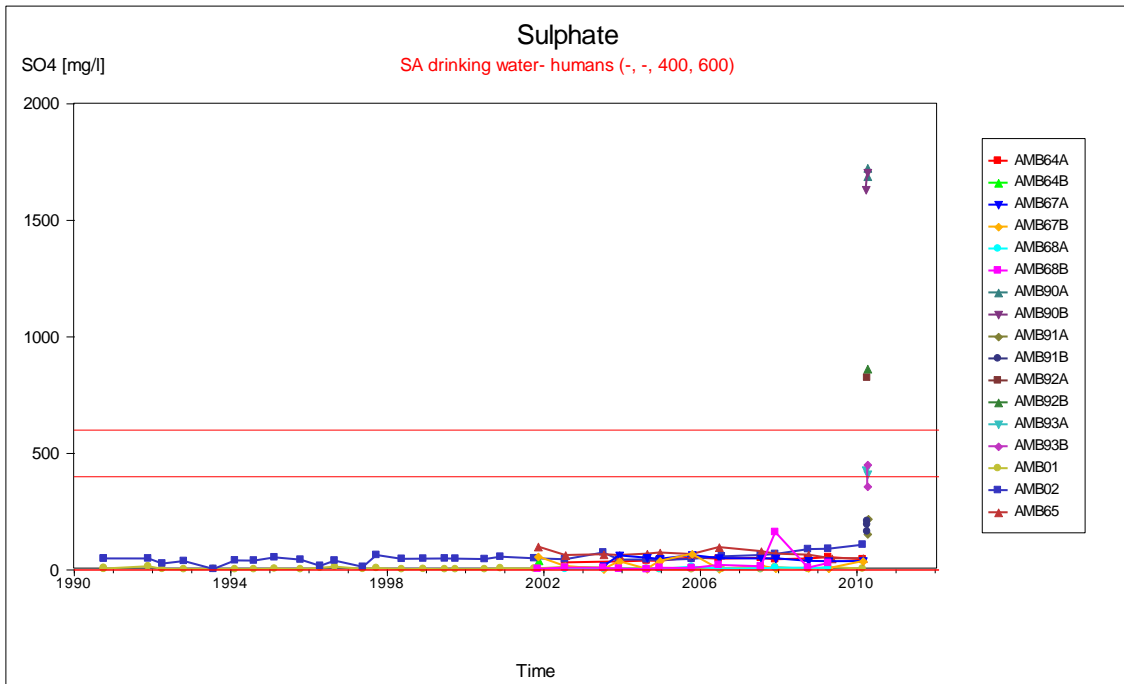
Figure 48. SO^4 concentration of boreholes drilled to determine the extent of the pollution plume.
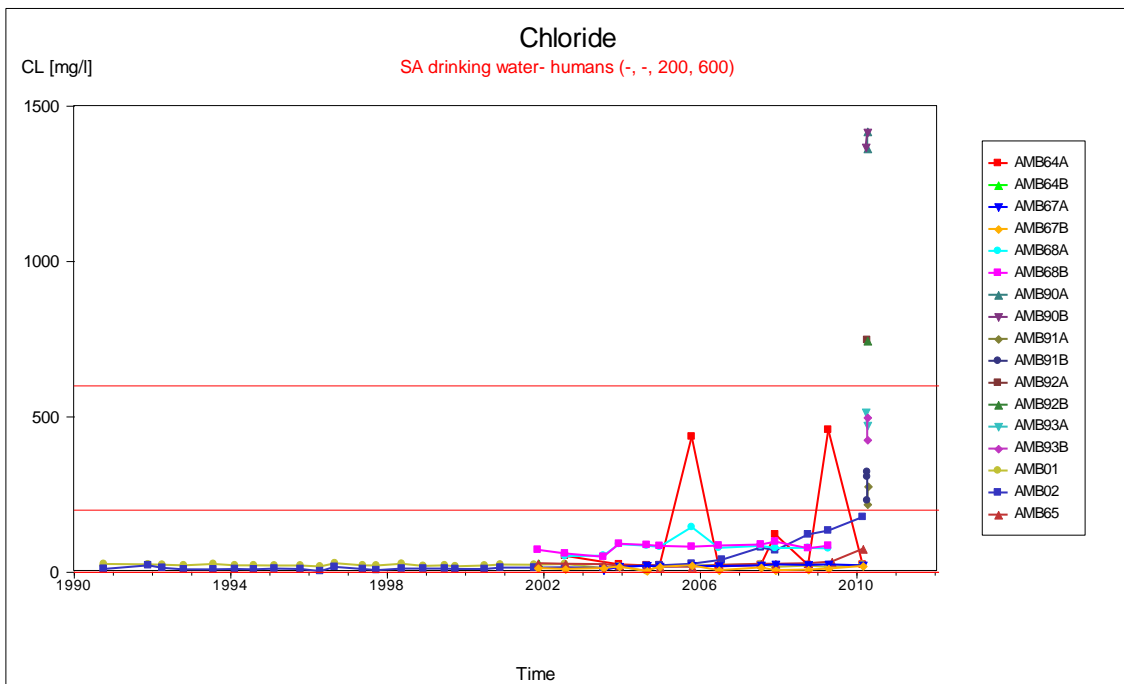
Figure 49. Cl concentration of boreholes drilled to determine the extent of the pollution plume.
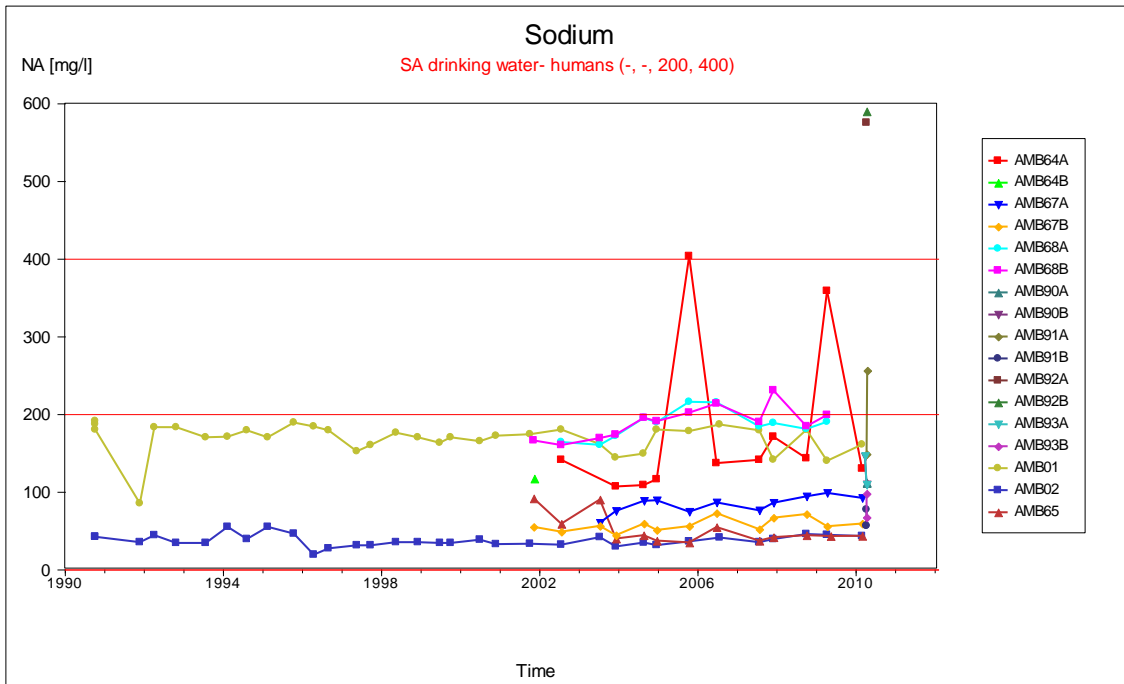
Figure 50. Na concentration of boreholes drilled to determine the extent of the pollution plume.
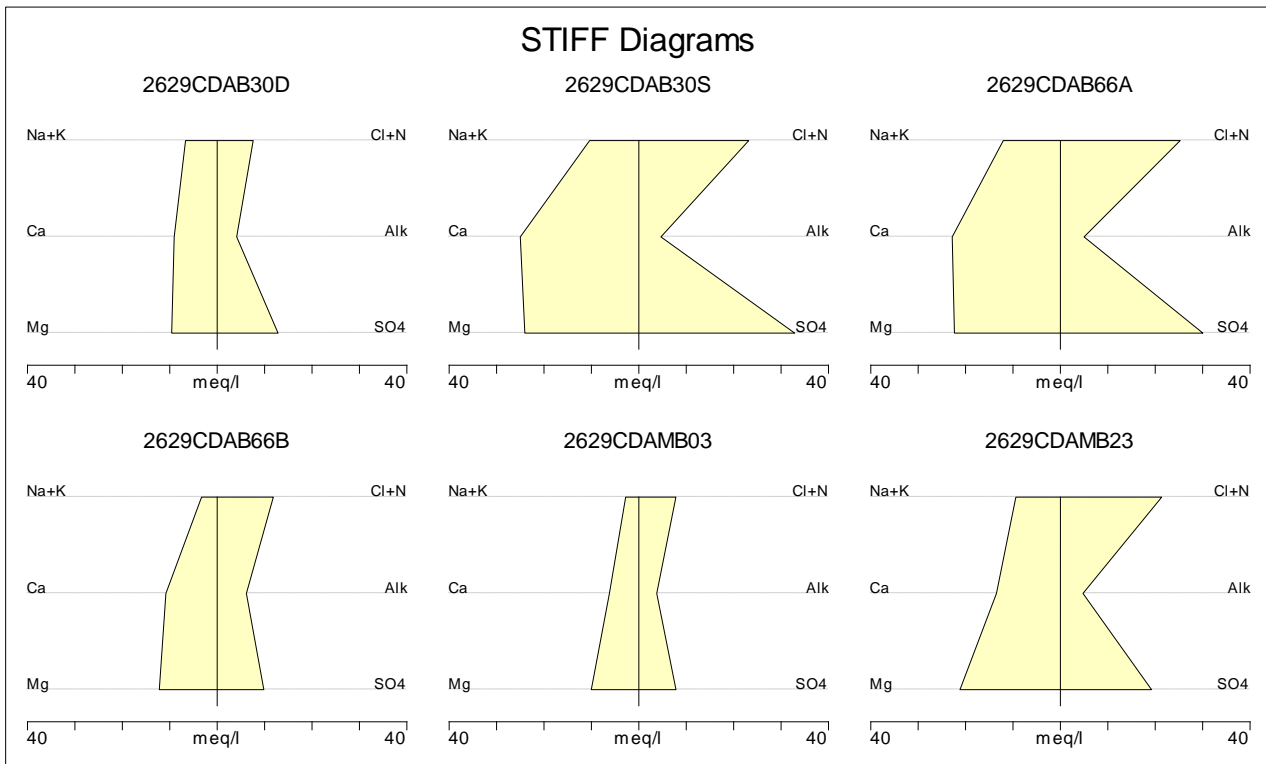
Figure 51. Stiff diagrams of destroyed boreholes covered by ashing operations.
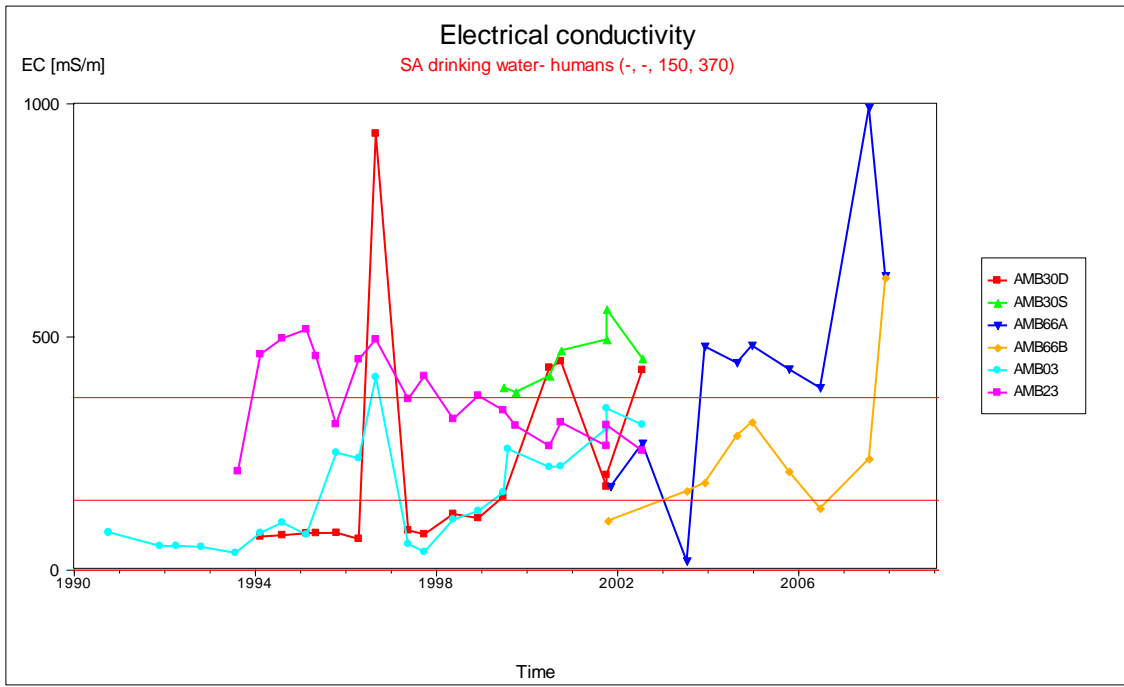
Figure 52. EC concentration of destroyed boreholes covered by ashing operations.
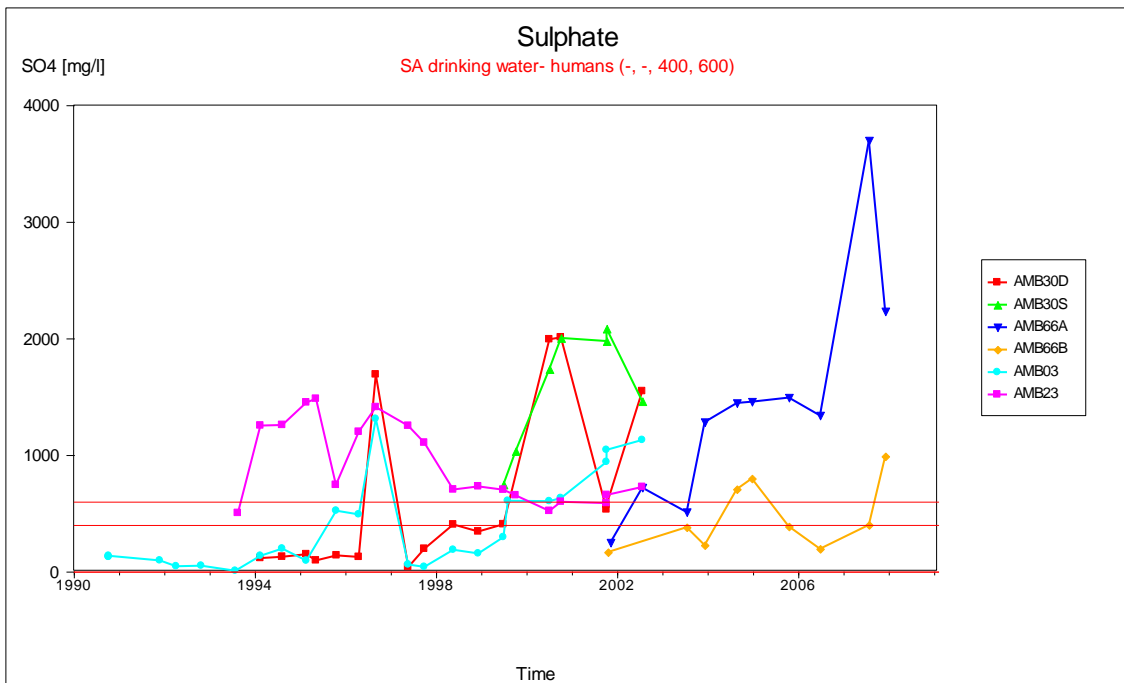
Figure 53. SO^4 concentration of destroyed boreholes covered by ashing operations.
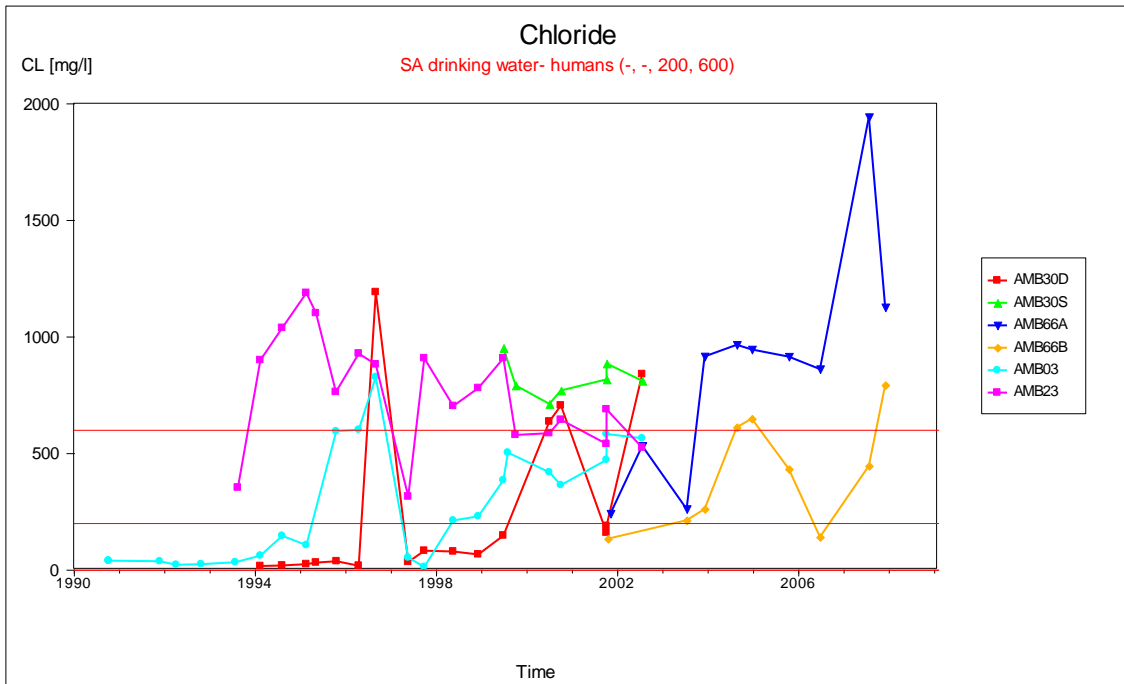
Figure 54. Cl concentration of destroyed boreholes covered by ashing operations.
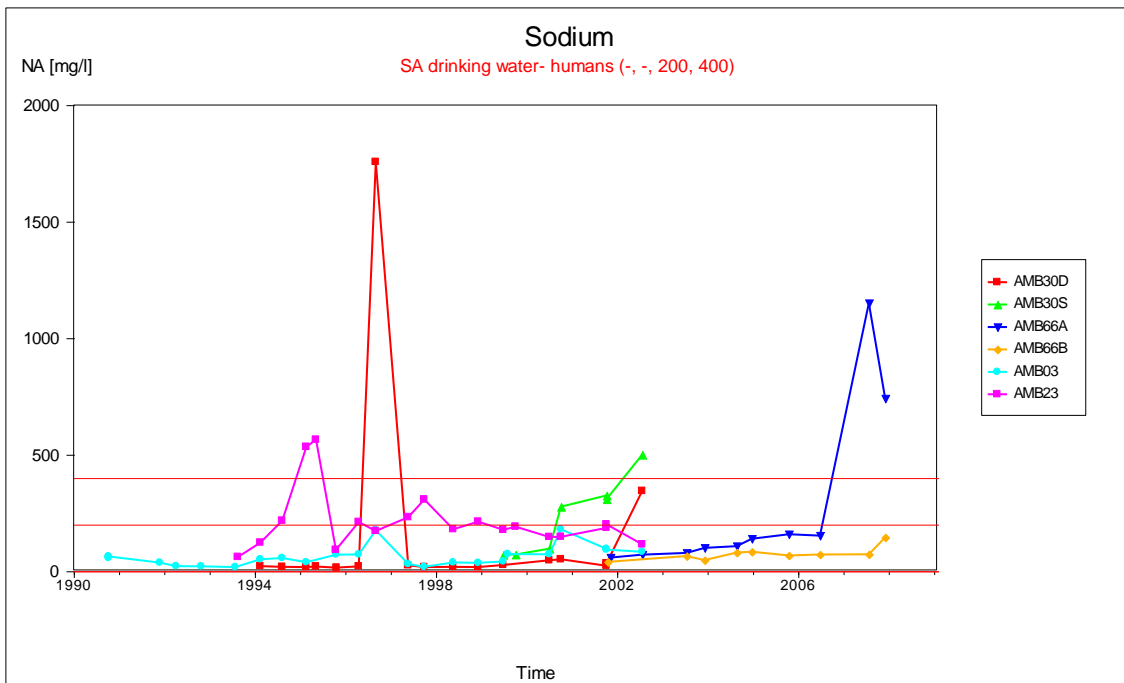
Figure 55. Na concentration of destroyed boreholes covered by ashing operations.

From the data that has been collected for this study, as well as for previous studies, it is clear the ash stack at Tutuka Power Station is contaminating the groundwater. Data has been re-evaluated, along with new data from pump tests. It was found that pollution has penetrated into the deep aquifer, as can be seen in the double piezometer borehole curves.

From Table 5 it is concluded that the shallow and deep aquifers in the direct vicinity of the ash stack are polluted and that a cut-off trench to a depth of 5 m will not be sufficient to intercept the

spreading of the pollution plume. The contamination of the deep aquifer, >40 metres below ground level, negates the trenching option, as the depth is excessive.

The observed chemistry of perched aquifer water is to be expected when the leaching characteristics of the pile and brine water constituents are considered. Laboratory testing undertaken by Rudolph, van Niekerk, and Associates (1993) suggests that Na, SO_4 and Cl ions will leach from the pile, and thus these ions can be expected to be predominant in any groundwater perched within the ash. However, the brine water irrigated at the site is also of Na-SO_4 or Na-Cl type, and thus any excess that percolates from the ground surface to the perched water table will influence groundwater chemistry. It is not possible, therefore, to distinguish between ion sources on the basis of major ion analyses alone in this instance.

From the above figures it is evident that the shallow perched aquifer is polluted underneath the ash stack and that pollution has reached the deep aquifer adjacent to the ash stack. This is due to the disposal of brine water on the ash stack which pollutes the shallow perched aquifer. Adjacent to the ash stack the recharge from rainfall dilutes the concentrations in the shallow perched aquifer. Deep aquifer contamination at borehole AMB24 is especially evident, as indicator element concentrations are tending towards equal values in the upper and lower aquifer. It may be expected that this pollution will therefore migrate in the deep aquifer, as well as in the shallow aquifer. From the newly drilled boreholes AMB90 and AMB92 contamination of the shallow perched aquifer as well as the deep aquifer is evident. These two boreholes are situated within 50 m of the ash dump and are much more polluted than the boreholes further downstream in the small valley south of the ash stack.

3.6.3   Spatial distribution of the current pollution plume

Contour maps have been constructed for contaminant levels around the ash dump. The general down gradient flow of the plume was calculated by interpolation (refer to Figure 56 and Figure 57) from the number of spatially distributed boreholes in the vicinity of the ash stack. The currently installed boreholes are optimally placed with regards to delineated geological features and possible preferred pathways. The physical position and extent of the plume can however only be exactly determined by drilling an evenly distributed number of boreholes on a grid. Needless to say, at an enormous cost. This is why numerical methods and modelling have been developed for estimation and prediction purposes. The fairly good confidence and precision of the numerical model (reflected in Figure 59 to Figure 61) is measured by the comparison of predicted values against recorded values.
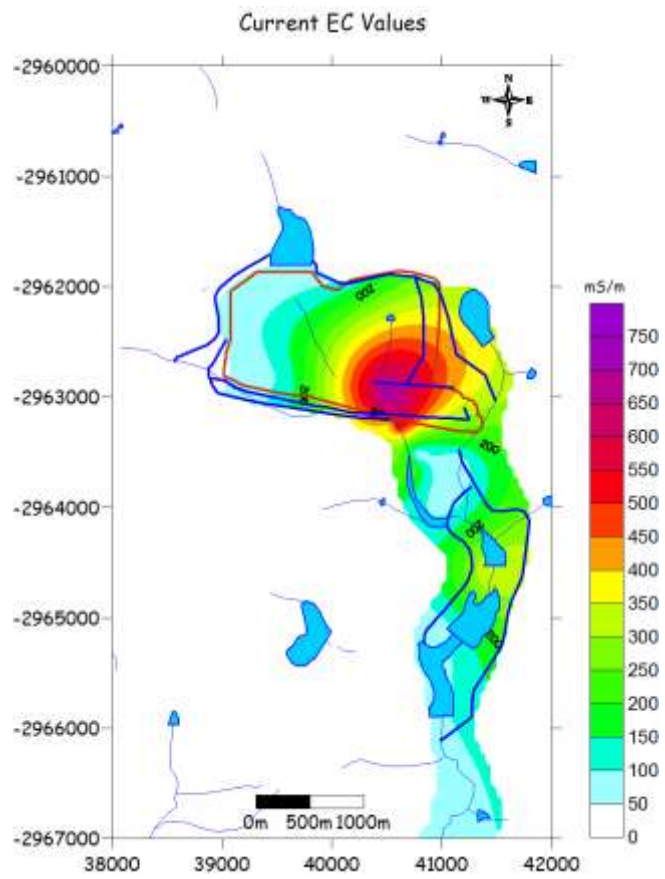
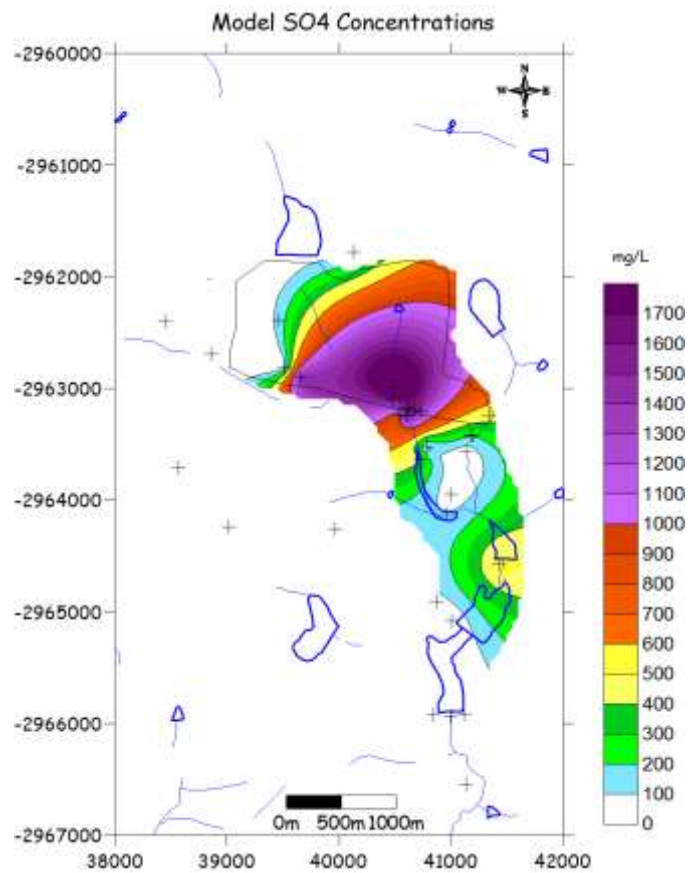*Figure 56. EC contours of the groundwater at the ashing area.*

Figure 57. SO₄ contours of the groundwater at the ashing area.

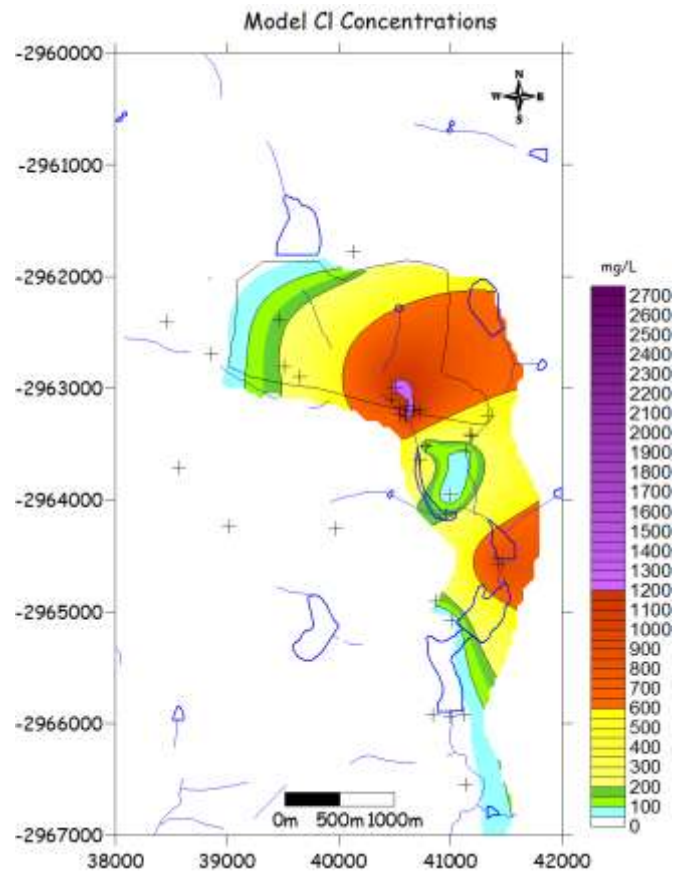*Figure 58. Cl contours of the groundwater at the ashing area.*

4   NUMERICAL MODEL

4.1   INTRODUCTION - NUMERICAL ENGINES USED

For this modelling exercise the computer software program Visual Modflow was used. Visual Modflow is an easy-to-use modelling environment for practical applications in three-dimensional groundwater flow and contaminant transport simulations, using the finite difference mathematical application.

The following numerical engines or methods for groundwater modelling were used. A broad explanation and discussion follows:

4.1.1   ModFlow and Modpath

For this numerical model the saturated groundwater flow - partial differential flow equation using the finite difference method:

$$\frac{\partial}{\partial x}\left(Kxx\frac{\partial u}{\partial y}\right) + \frac{\partial}{\partial y}\left(Kyy\frac{\partial u}{\partial y}\right) + \frac{\partial}{\partial z}\left(Kzz\frac{\partial u}{\partial z}\right) = Ss\frac{\partial u}{\partial t} \pm Q$$

where

$$u \quad = \quad \text{hydraulic head}$$

$$Q \quad = \quad \text{sources / sinks}$$

The equation describes the three-dimensional flow of groundwater through the substrata, calculating the water table-response. The equation may be solved analytically for simple problems, though for this study, piece-wise approximation of the equation is usually obtained through the finite difference method, because of the complexity of the problem. Once the water-level distribution is available over the whole area in question, seepage velocities and seepage directions can be calculated according to the following equation.

$$v = k(\partial h/\partial l)/n$$

where:

$$v \quad = \quad \text{seepage velocity (m/d)}$$

$$k \quad = \quad \text{Hydraulic conductivity (m/d)}$$

$$n \quad = \quad \text{effective porosity (\%)}$$

$$h/l \quad = \quad \text{groundwater gradient (m/m)}$$

The flow modelling is done based on the assumption that steady state has been attained for the water levels in the area. Realistically several of the factors should be varied over time, but currently the information available prevents these factors from being included.

4.1.2   MT3D-MS

Mass transport in the regions of the identified pollution sources will be simulated by means of the MT3D numerical engine. The engine simulates 3-D advective-dispersive transport of dissolved solutes in groundwater using the following equation:

$$\frac{\partial}{\partial \chi i}\left(Dij\frac{\partial C}{\partial \chi j}\right) - vi\frac{\partial C}{\partial \chi j} \pm Qc = \frac{\partial C}{\partial t}$$

where:

C   =   concentration

Dij   =   Dispersion

Qc   =   sources / sinks

Data Needed:

- Decartelisation in all directions $\partial xi, (\partial x, \partial y, \partial z)$

- Dispersivity: $D_{longitudinal}$, $K_{transverse}$

- Retardation, Decay, Transformations

- Boundary and Initial Conditions

4.2   FINITE DIFFERENCE MODELLING FOR THE ASHING AREA

A network – columns and rows was created with Visual ModFlow grid editor for the area under investigation. Each of the areas with its individual characteristics and own hydraulic parameters were allocated and zoned as a different colour. All the data obtained and interpreted for the conceptual model were used as input parameters for the flow and mass transport modelling. A single model has been constructed over the whole of the ashing area. Greater densities of elements have been introduced in areas where more detailed answers are required. Typically, these areas are around sensitive regions. This includes the ash stack, streams, dams and pans.

4.2.1   Groundwater flow directions and vectors

A map representing the local groundwater flow directions for the whole area has also been constructed (refer to Figure 30).

The general flow direction for the ashing area is from north to south towards the Wolwe Spruit. The flow of groundwater follows more or less the flow of the surface water drainage system.
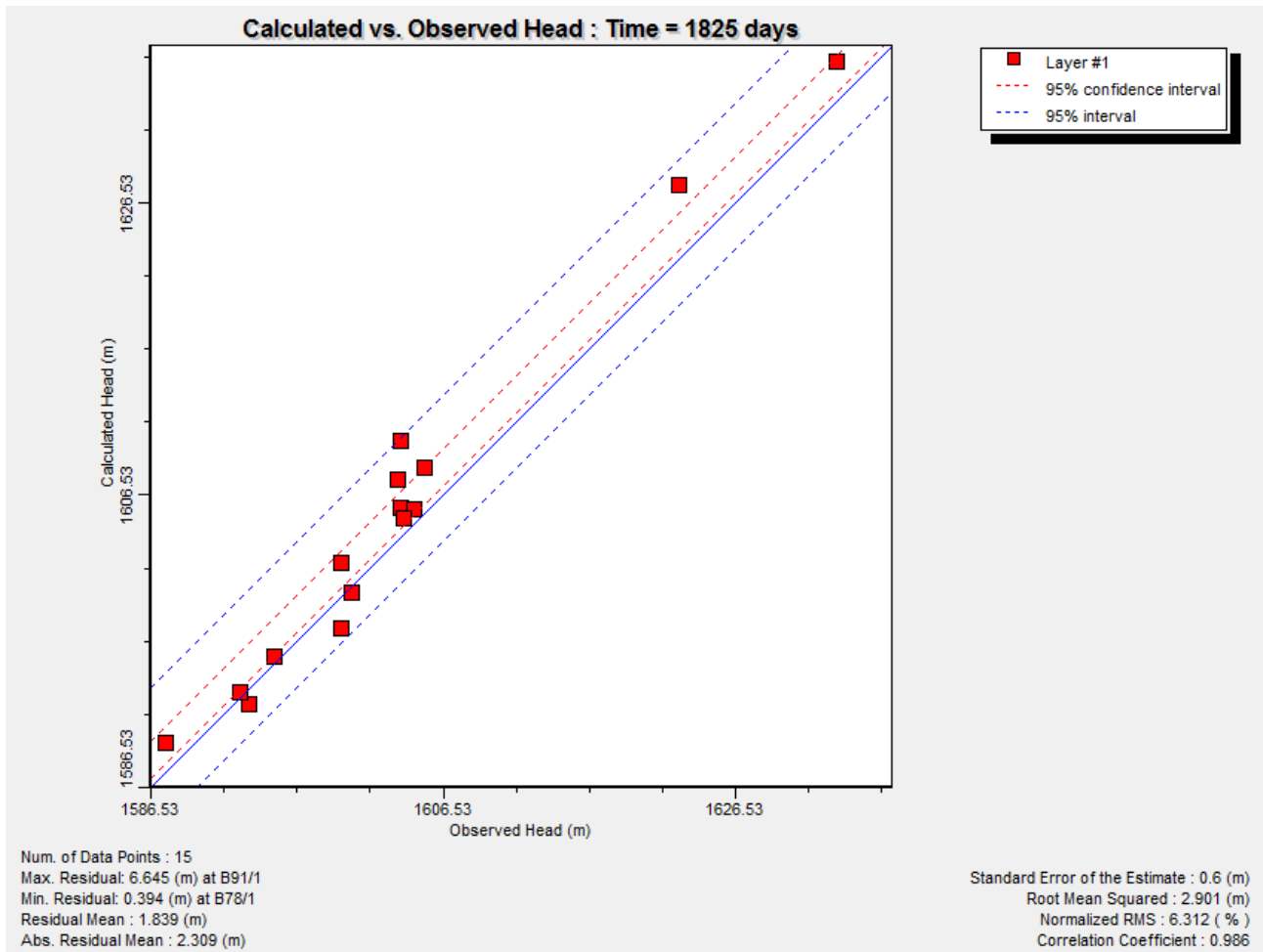
4.2.2   Calibration
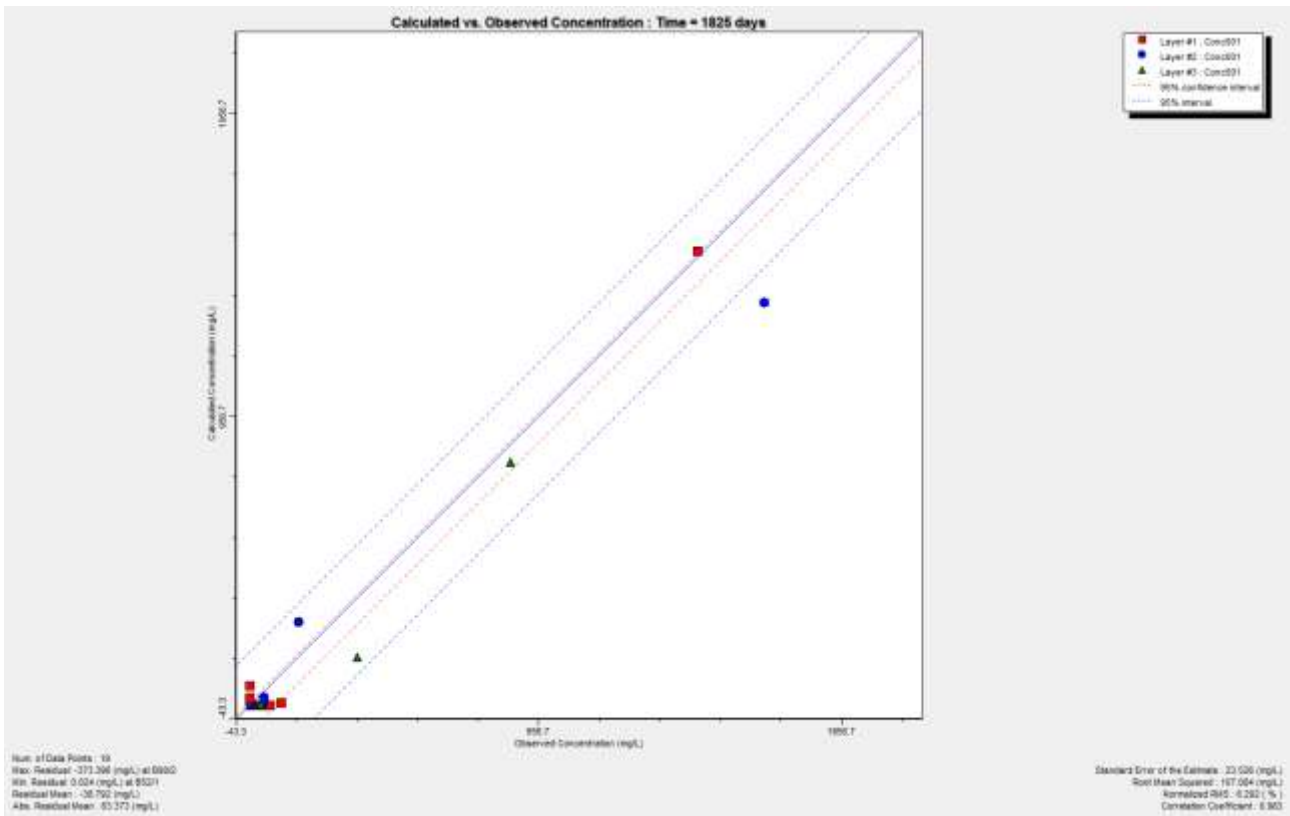

Figure 59. Water level calibration graph

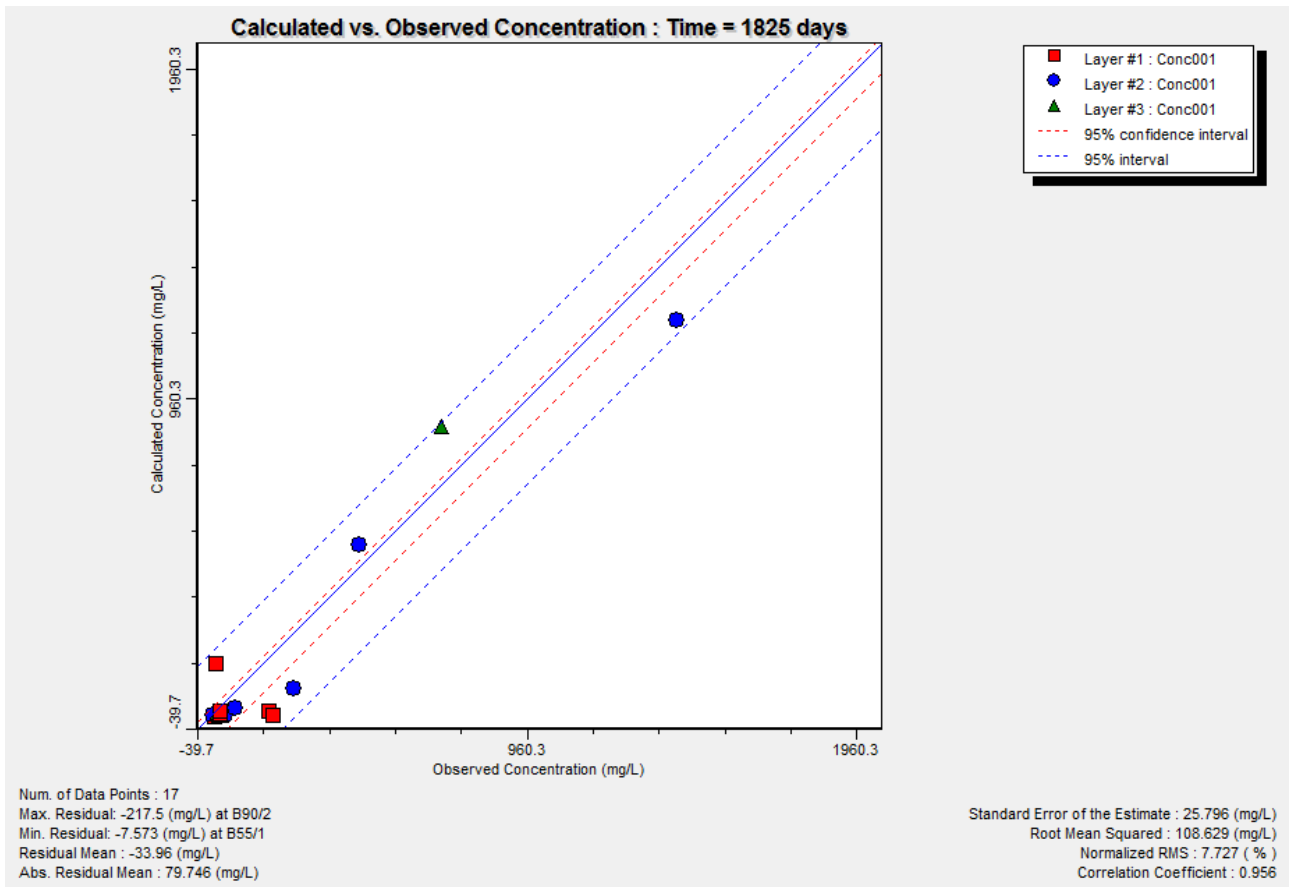*Figure 60. SO4 calibration graph*
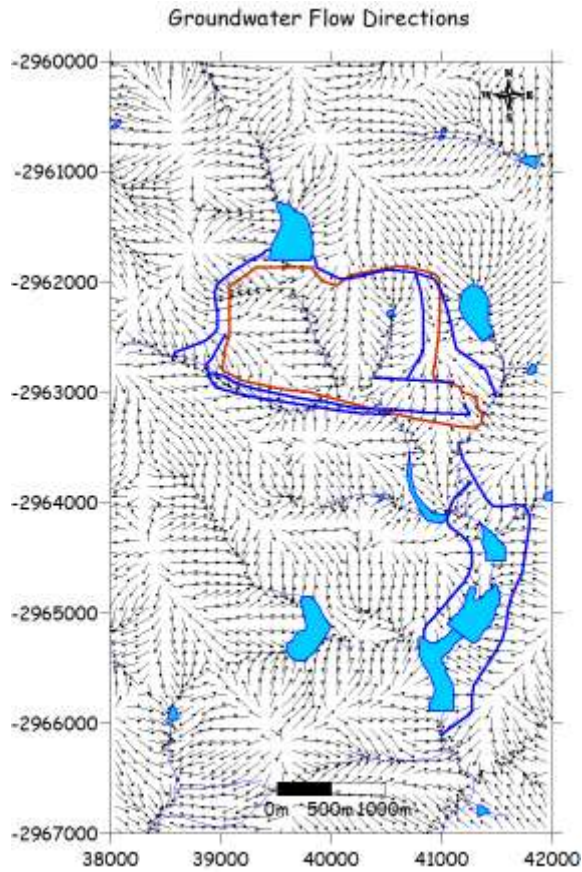

Figure 61. Cl calibration graph

Figure 62. Flow directions transient state - current situation.

4.3 LONG TERM IMPACTS

Sulphate was used as the indicator element for modelling purposes. It is introduced into the system either through oxidation of sulphides in ash stack or through the brine irrigation system. Sulphate is a convenient constituent to study the movement of pollution, because: sulphate is readily soluble, does not adsorb readily onto clay particles in soil or the aquifer and it does not decay over time. Apart from sulphates, sodium may also be considered, because sulphate usually has an attenuation factor in the order of 10.

Sulphate concentrations of several monitoring boreholes as well as chemistry data obtained from tests done on ash in-situ material were used to determine the different input concentrations. The following represents a model and estimates of sulphate concentration contours over time and with different scenarios.

The numerical modelling of the study area was done over different time periods with different scenarios. The time steps and scenarios are listed in Table 6. All possible influences from the identified pollution sources were incorporated.

Table 6. Different time steps and scenarios modelled.

Scenarios
Continuous brine irrigation and no abstraction. Brine irrigation is simulated by 20% recharge on the affected part the ash stack.
Continuous brine irrigation and abstraction to intercept pollution plume with 11 low yielding boreholes (0.8 l/s each to total approximately 760m^3/day). Brine irrigation is simulated by 20% recharge on the affected part the ash stack.
Brine irrigation is stopped in 2011 and no abstraction is taking place.

The following figure indicates the sulphate concentration contours for the regional pollution plume that was used as initial concentrations in the model. The calculated data for the different simulation time steps was export to the interpolation program "Surfer" for contouring purposes. Figure 63 indicates the simulation for the current situation.
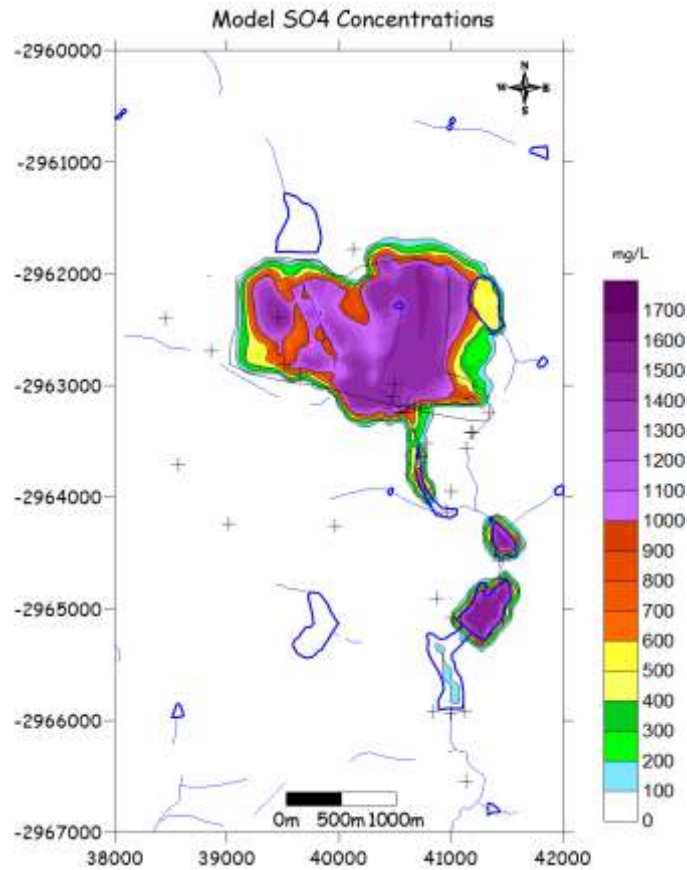
4.3.1   SO4 pollution plumes

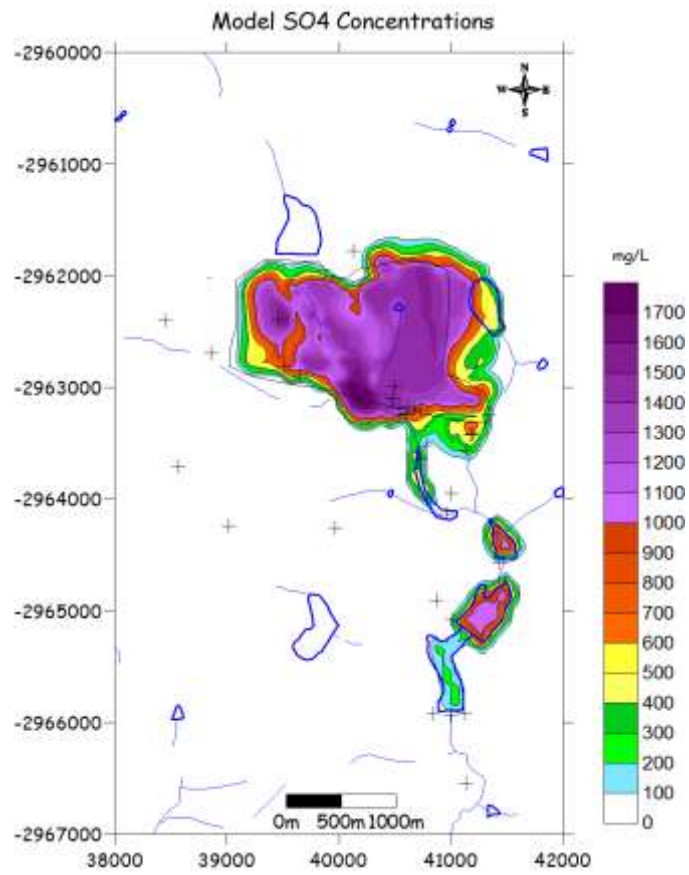*Figure 63. Simulated SO4 contours 2010 (Continued brine irrigation, no abstraction)*

Figure 64. Simulated SO4 contours 2011 (Continued brine irrigation, no abstraction)
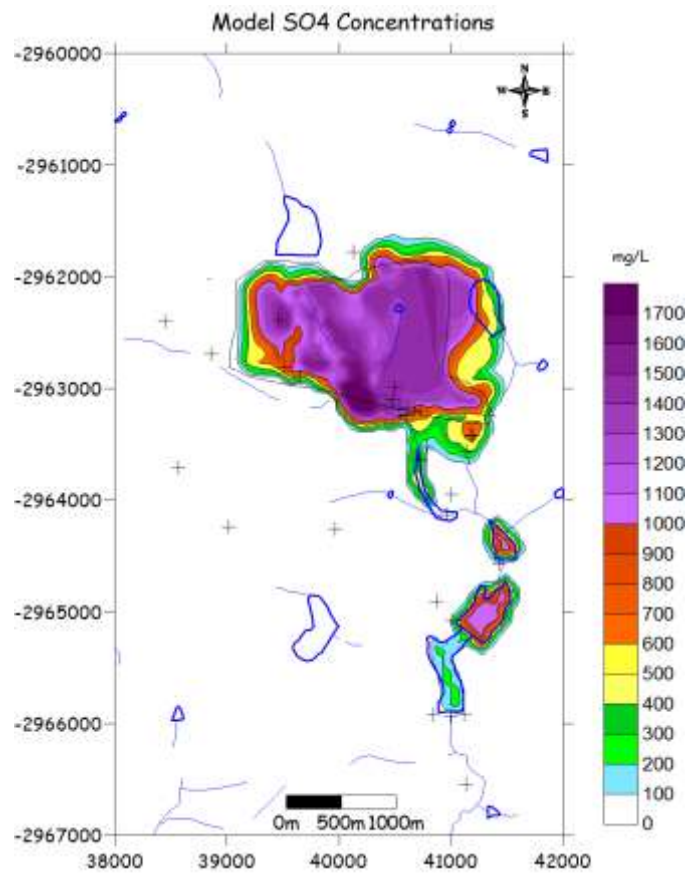
Figure 65. Simulated SO4 contours 2012 (Continued brine irrigation, no abstraction)
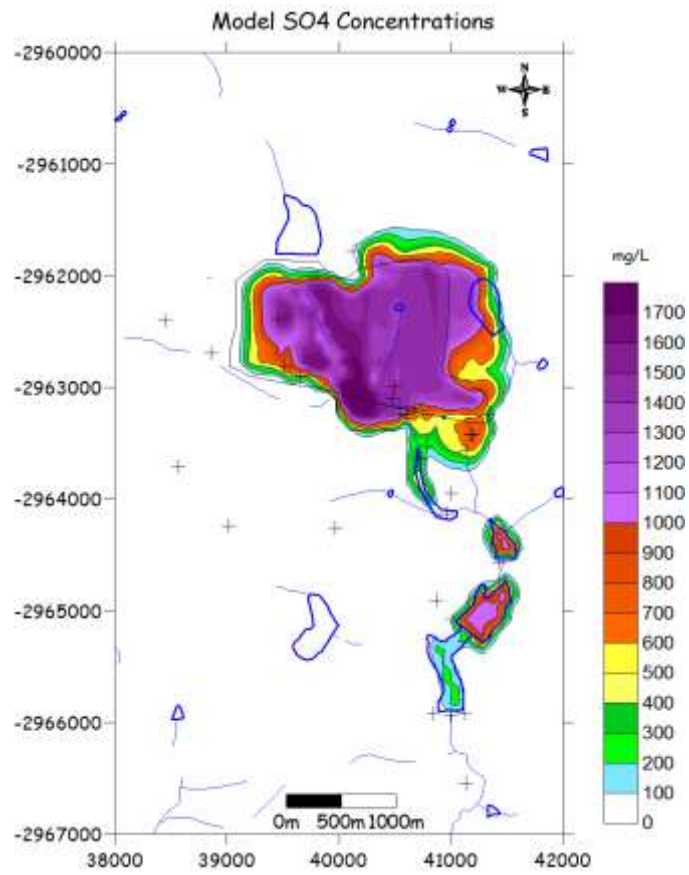
Figure 66. Simulated SO4 contours 2015 (Continued brine irrigation, no abstraction)
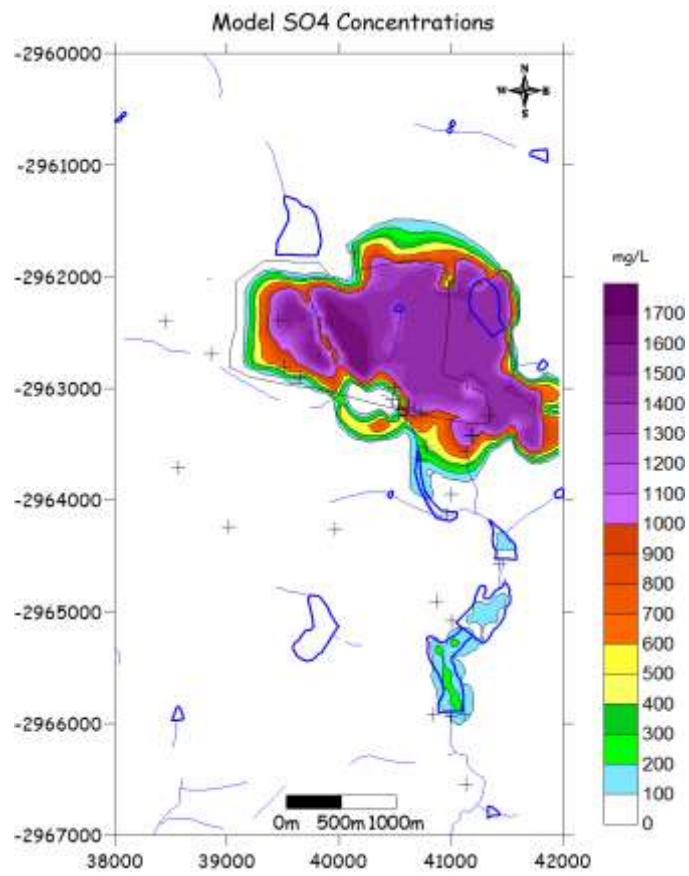
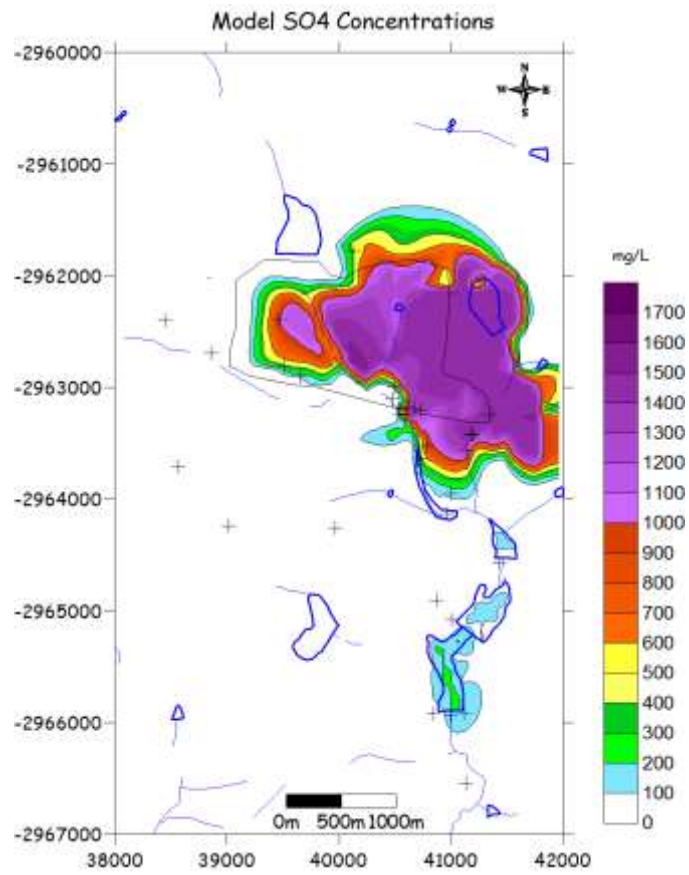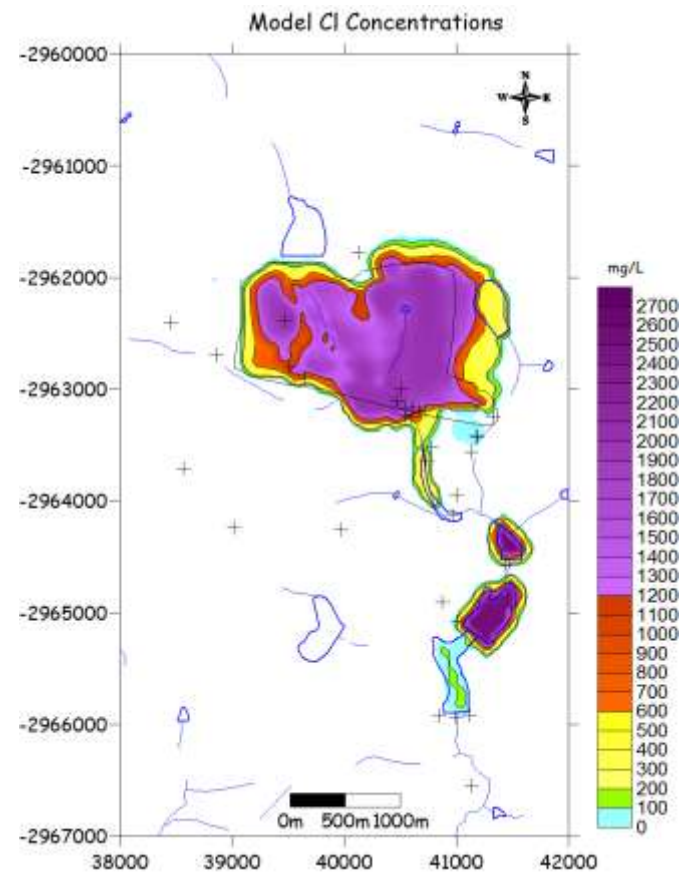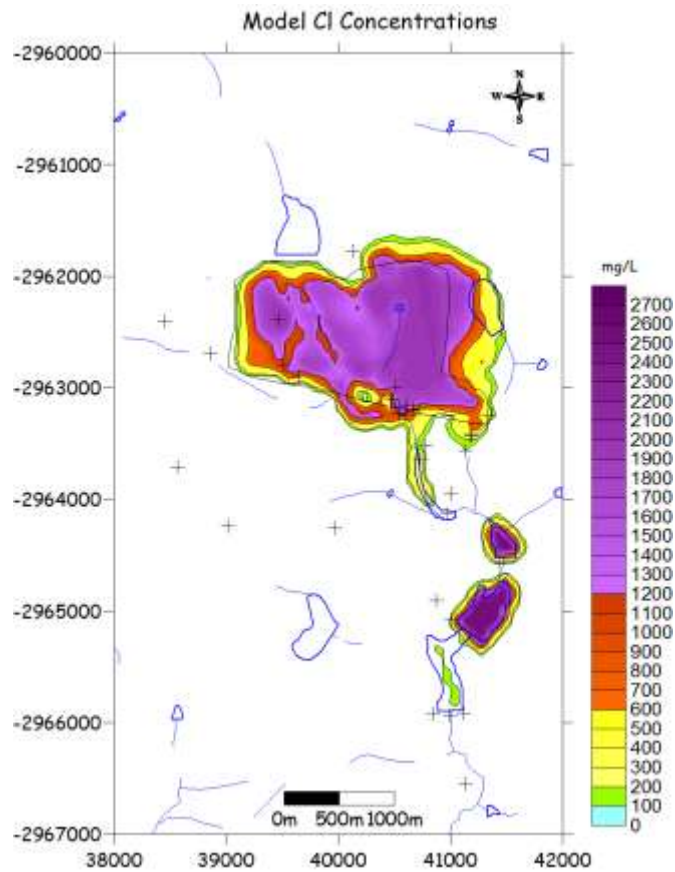*Figure 67. Simulated SO4 contours 2020 (Continued brine irrigation, no abstraction)*

Figure 68. Simulated SO4 contours 2030 (Continued brine irrigation, no abstraction)

Figure 69. Simulated Cl contours 2010 (Continued brine irrigation, no abstraction)

Figure 70. Simulated Cl contours 2011 (Continued brine irrigation, no abstraction)
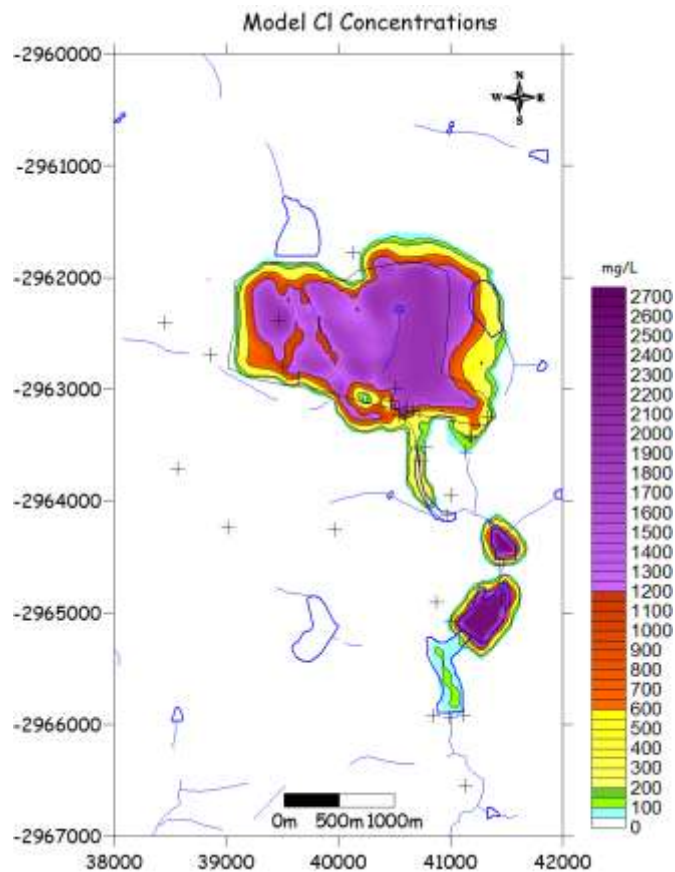
4.3.2 Cl pollution plumes

Figure 71. Simulated Cl contours 2011 (Continued brine irrigation & plume abstraction)
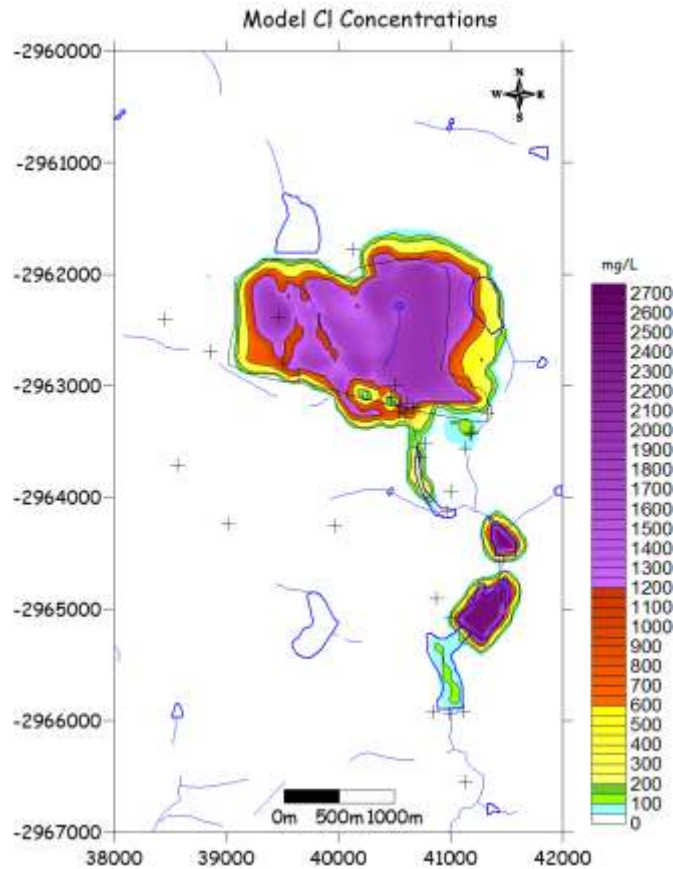
Figure 72. Simulated Cl contours 2011 (No brine irrigation, no abstraction)
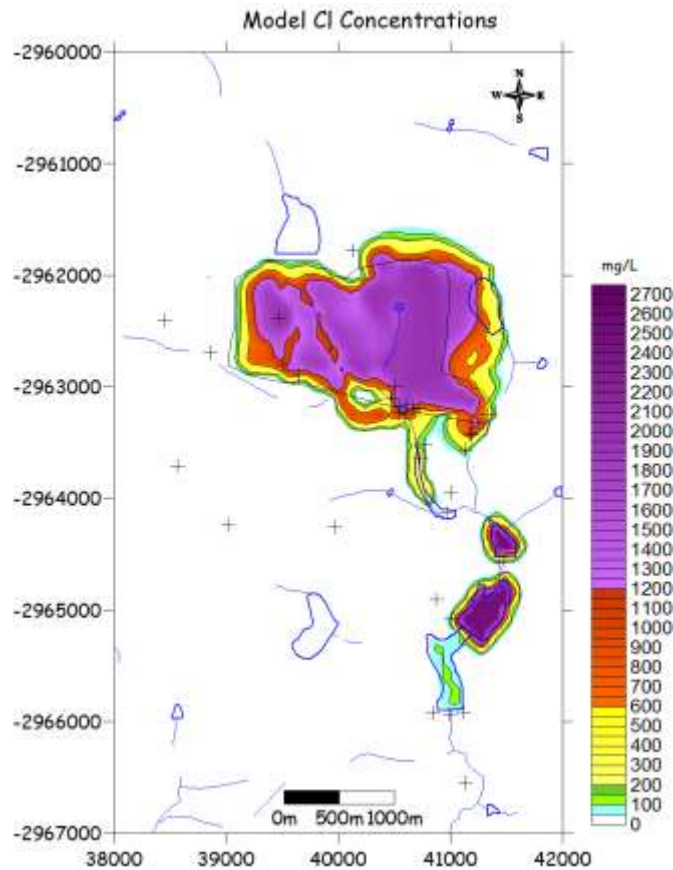

Figure 73. Simulated Cl contours 2012 (Continued brine irrigation, no abstraction)
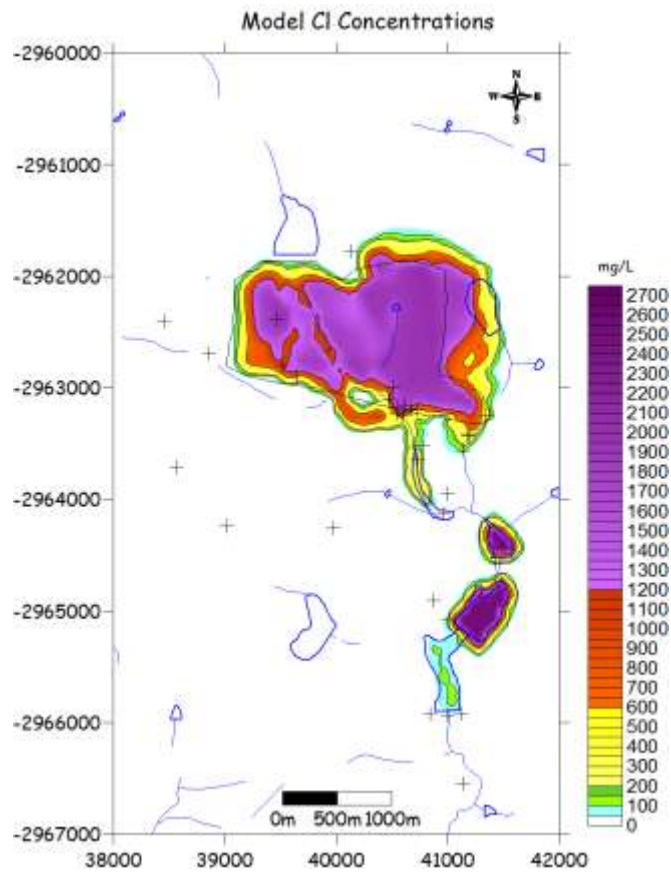
Figure 74. Simulated Cl contours 2012 (Continued brine irrigation & plume abstraction)

Figure 75. Simulated Cl contours 2012 (No brine irrigation, no abstraction)

Figure 76. Simulated Cl contours 2015 (Continued brine irrigation, no abstraction)

Figure 77. Simulated Cl contours 2015 (Continued brine irrigation & plume abstraction)
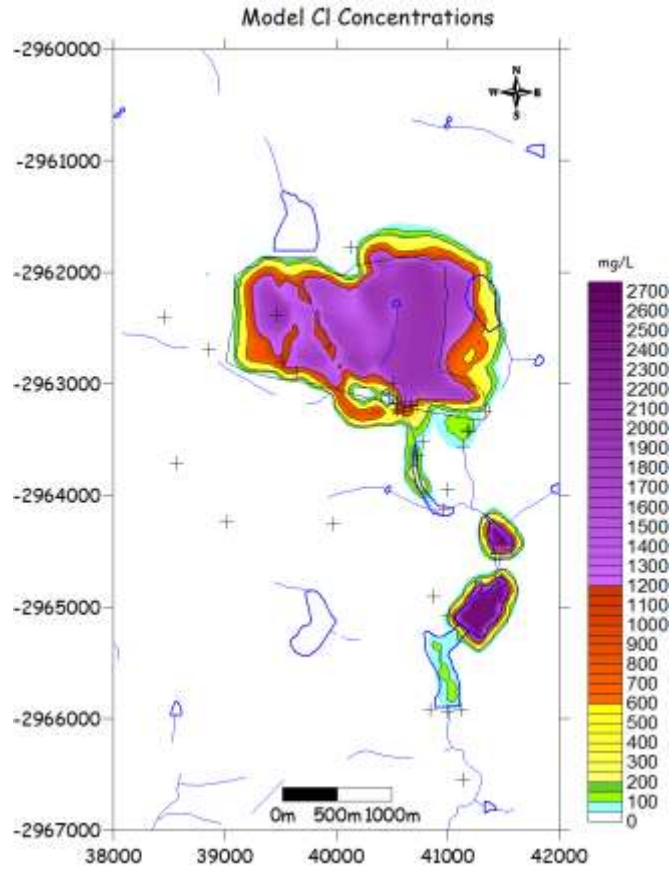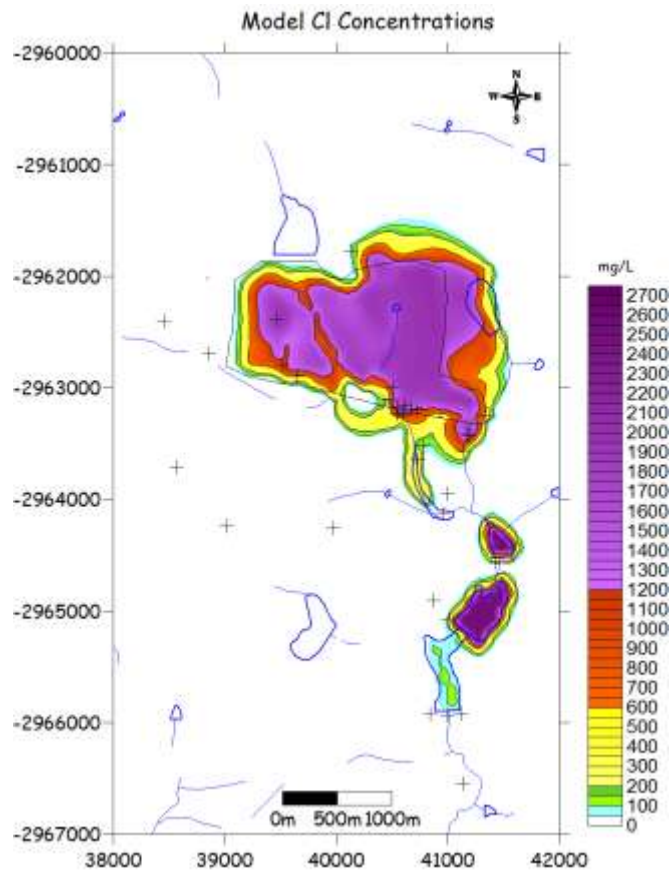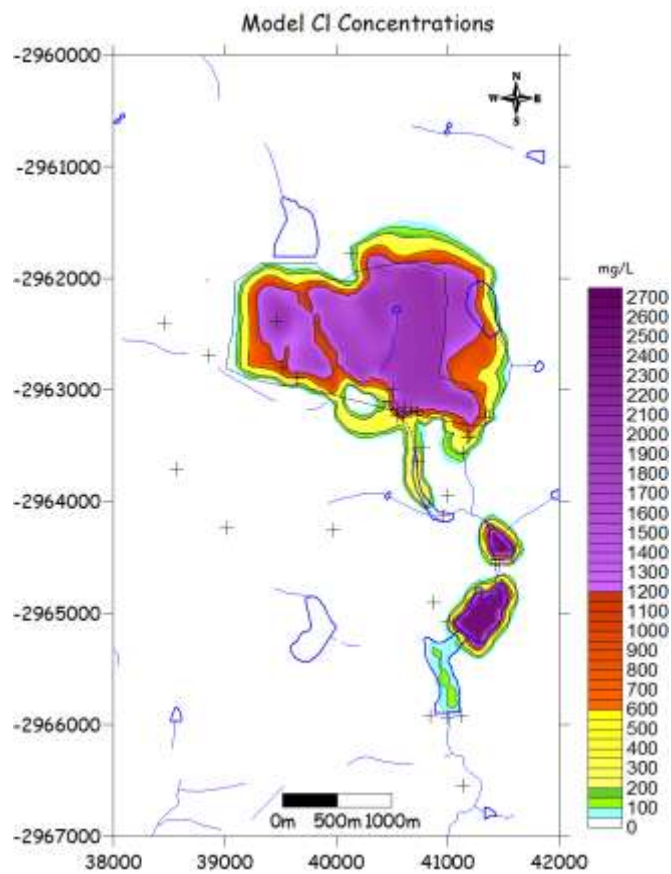
Figure 78. Simulated Cl contours 2015 (No brine irrigation, no abstraction)

Figure 79. Simulated Cl contours 2020 (Continued brine irrigation, no abstraction)

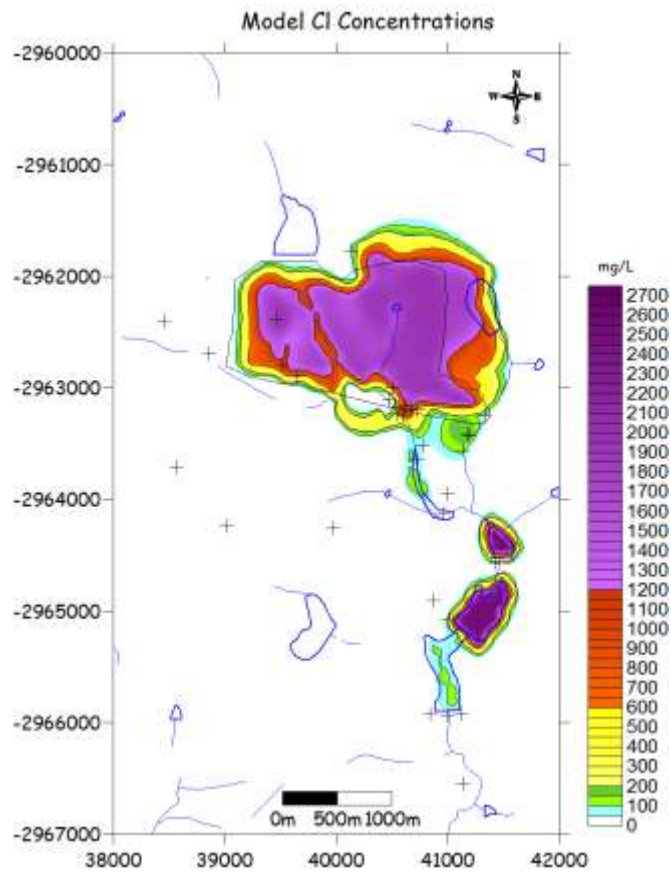*Figure 80. Simulated Cl contours 2020 (Continued brine irrigation & plume abstraction)*

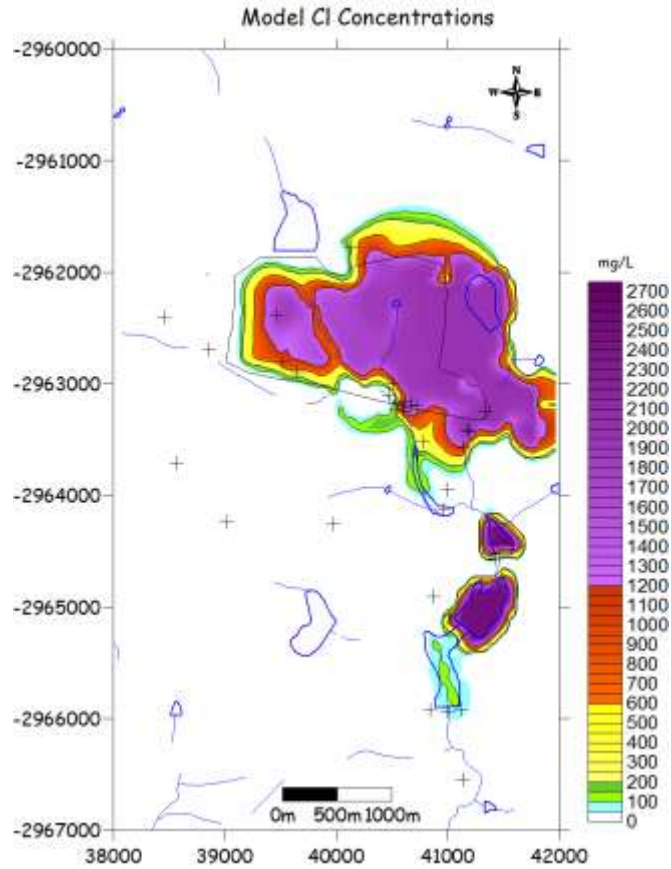*Figure 81. Simulated Cl contours 2020 (No brine irrigation, no abstraction)*

Figure 82. Simulated Cl contours 2030 (Continued brine irrigation, no abstraction)
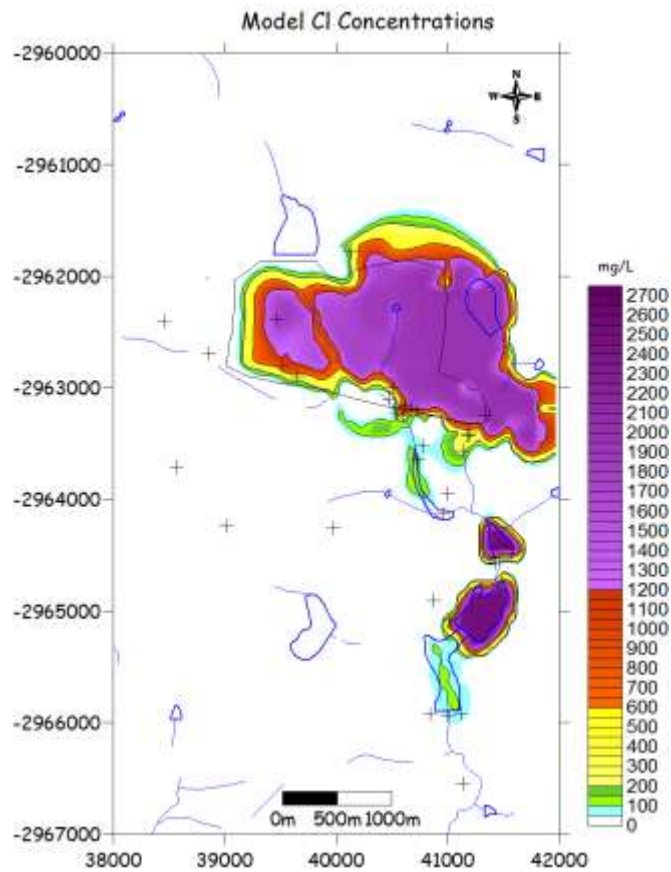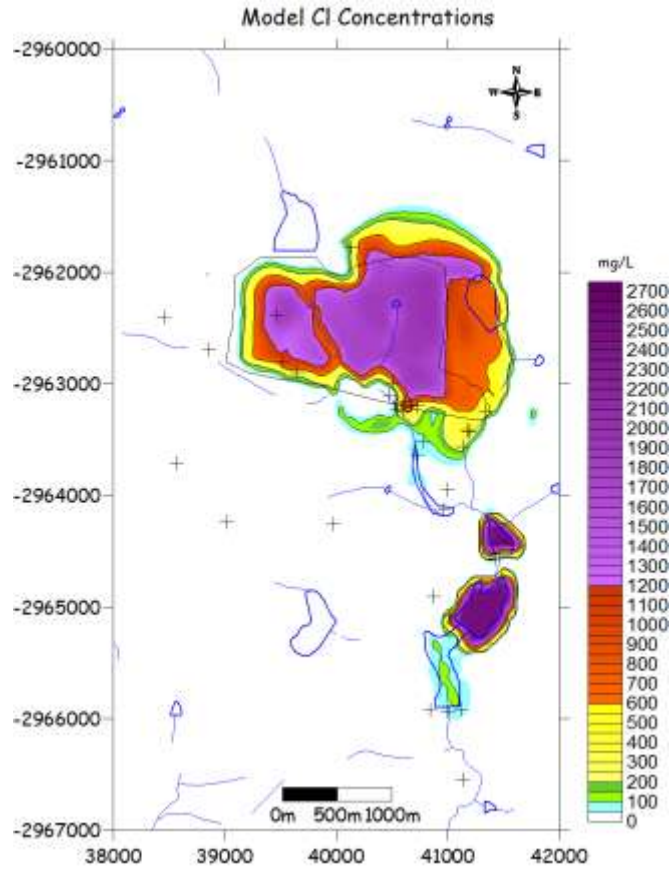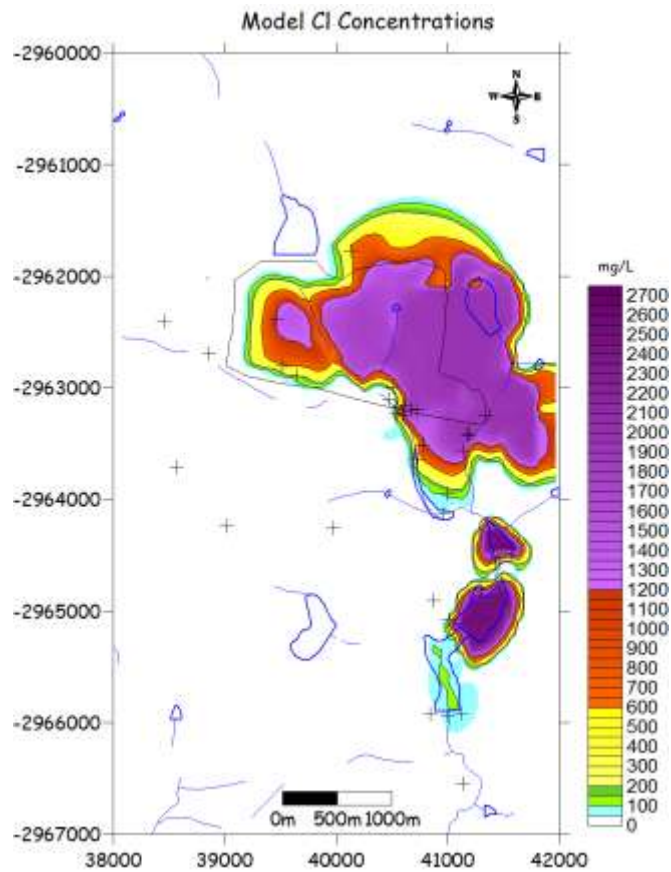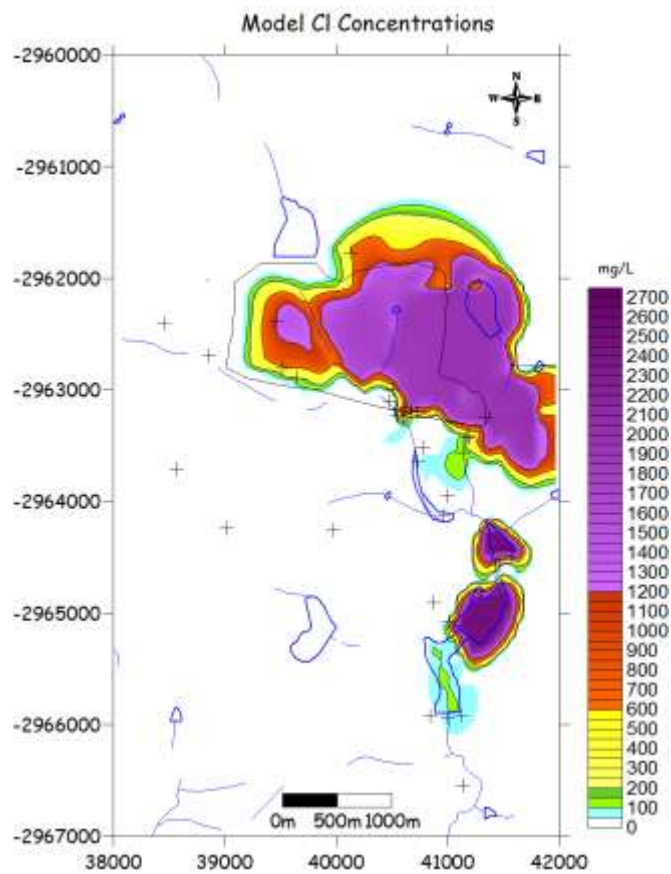

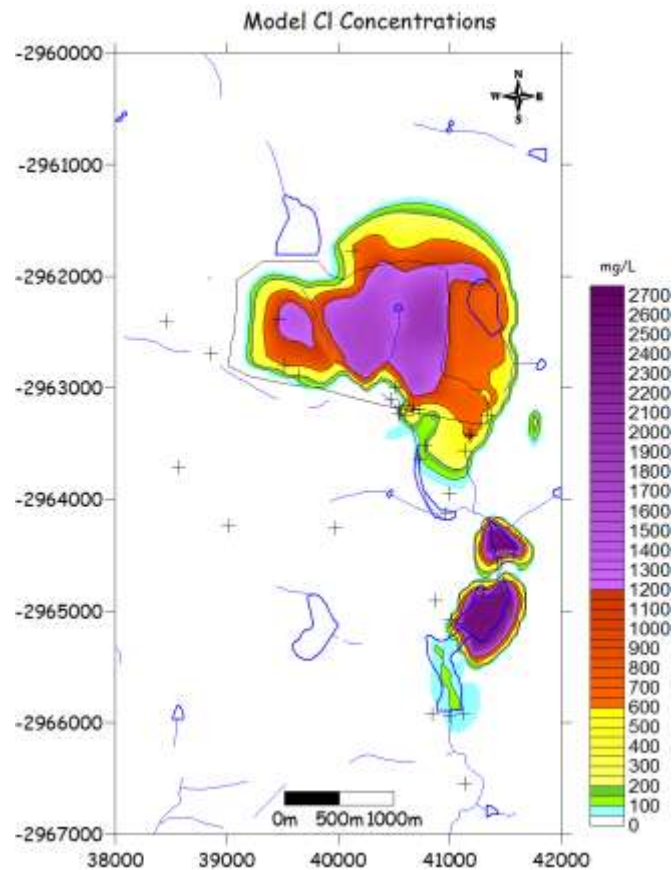*Figure 83. Simulated Cl contours 2030 (Continued brine irrigation & plume abstraction)*

Figure 84. Simulated Cl contours 2030 (No brine irrigation, no abstraction)

4.4   DISCUSSION

The following conclusions have been made on the basis of site observations and interpretation of the modelled simulations:

- Initial SO^4 and Cl concentrations were awarded as input parameters for no brine irrigation simulations. The recharge used for this simulation was 21 mm/year for the undisturbed and rehabilitated areas and 140 mm/year for the un-rehabilitated areas on the ash stack.

- Constant SO^4 and Cl concentrations were awarded as input parameters for continuous brine irrigation simulations. The recharge used for this simulation was 21 mm/year for the undisturbed and rehabilitated areas, 140 mm/year for the un-rehabilitated areas and 651 mm/year for the areas under irrigation on the ash stack.

- It is evident from the figures above that the ashing activities have a definite impact on the valley south of the ash stack. Migration of pollutants towards the eastern side and the Wolwe Spruit is now more prominent than before. Slightly reduced impacts are observed near AMS15 and the newly drilled boreholes AMB90 and AMB92. This can mainly be attributed to the fact that the front stack has proceeded so far to the east into the natural drainage of the Wolwe Spruit and with the saturated part of the ash stack (due to excessive brine water irrigation) no longer primarily above the natural drainage valley in the centre part of the ash stack.

- The impact and extend of the simulated pollution plume seems to be localised to the area around the ash stack. This finding is further supported by close inspection of the historical data and chemical analyses. Time graphs and MMAC plots indicate impacts of various

magnitudes. However, these results rather indicate sporadic impacts from surface water spillages. This localization of the plume can mainly be attributed to the geological formation (doleritic sill) underlying the ash stack and the area to the south of the as stack.

- Different abstraction rates from 9 dummy boreholes, as well as from the two newly drilled boreholes AMB90 en AMB92 on the south and south-eastern side of the ash stack were used to simulate the interception of the pollution plume. Sufficient interception is simulated with a total of 8.8 L/s ($760m^3$/day).

- The simulated period between 2020 and 2030 indicates that the system will improve if no irrigation will be taking place and that the system will become cleaner by a process called natural attenuation. This process is mainly driven by the following factors:
  - Dilution of the pollution plumes by rainfall recharge;
  - Fresh groundwater entering the system;
  - Surfacing of pollution plumes in the streams, dams and fountains, thus being removed from the groundwater system.

- Reverting back to a dry system by stopping of brine irrigation simulated by the model indicates a better improvement of the overall state than pumping, and is thus highly recommended.

- Decommissioning of power generation activities in future times will have therefore a definite turn around impact on pollution plume migration.

5 CONCLUSIONS AND RECOMMENDATIONS

5.1 <u>CONCLUSIONS</u>

From the data that has been collected during this study, as well as from previous studies, it is clear that contamination of the groundwater is taking place within the direct vicinity of the ash stack.

Data has been re-evaluated, along with new data from pump tests. It was found that some pollution has penetrated into the deep aquifer, as can be seen in the double piezometer borehole curves. This indicates that there are fractures in the dolerite along the recurring block type drainage patterns or natural streams, which is structurally controlled. This permits the contaminant to travel to the deep aquifer system in these areas.

The initial project was therefore aimed at intercepting of the pollution plume by mainly abstracting water from two newly drilled boreholes to the south of the ash stack.

When evaluating groundwater levels, it is clear from the boreholes in the ash stack that the phreatic level of the water within the western part of the ahs stack becomes lower as the brine irrigation progresses to the east. The time and progress at which this lowering occurs is currently not well documented due to the limited number of boreholes in the ash stack. For the same reason, the influence of the streams on the natural water table below the ash stack is also not recorded. From the graphs it is also evident that the water table is at the bottom or below the ash stack and that very little water exists in the ash stack itself where the brine irrigation has stopped. Due to this the leaching of pollutants from the ash is limited as soon as excessive irrigation stops. From the conclusions drawn from the moisture retention testing dust suppression may continue as long as over irrigation does not occur.

It is evident from the numerical model simulations that steady state conditions and cleaning of the system, will be reached after several years if no brine irrigation is taking place regardless of the amount of natural recharge on the ash stack. Signs of this are already visible in the older parts to the west of the front stack. Decommissioning of power generation activities in future times will have therefore a definite turn around impact on pollution plume migration.

Analyses of the pump tests that were conducted between the 27th of March and the 10th of April 2010, indicate some hydraulic conductivity between boreholes B93 and B67, as well as between boreholes B90 and B92. Dewatering of the aquifer system to the south of the ash stack along the small tributary of the Wolwe Spruit from two abstraction boreholes are however not practical due to the following geological constraints:

- The area underneath the ash stack consists of a shallow weathered zone of soils and clayey material (of varying thickness between approximately 1 to 3 meters) followed by interlaminated shales and sandstones (also of varying thicknesses between 1 to 10 meters). The shale and sandstone layer is followed by a dolerite sill (once again varying in thicknesses of between 10 to 40 meters). The same geological formations of shale and sandstone encountered above the dolerite sill are found beneath the sill.

- Water strikes generally occur at the top and bottom of the sill within a relative thin or narrow fracture zone (so called baked zone).

Due to the geology, large drawdown curves will not be achieved as dewatering of the thin layers will only occur within the direct vicinity of the abstraction boreholes. This dewatering would however occur concentric and will thus not only abstract polluted water, but will inevitably and undesirably draw some clean water from areas down gradient of the boreholes. The pump and treat scenario will therefore not be feasible as a sustainable abstraction rate from the aquifers may not be achievable.

Although Time graphs and MMAC plots of certain chemical parameters in groundwater within a few meters of the ash stack and the natural drainage system to the south of the ash stack indicate impacts of various magnitudes, these results rather indicate sporadic impacts from surface water spillages within the natural drainage system to the south of the ash stack. Furthermore it is not indicated by these time graphs that the pollution plume is migrating southwards as one does not find increasing trends in pollution indicator element concentrations at boreholes further away from the ash stack and natural drainage system.

5.2   RECOMMENDATIONS

The following recommendations are based on the preceding findings:

- As long as it is not evident that the pollution plume is migrating south, monitoring should be continued quarterly.

- Within the current monitoring program, not only water from selected boreholes to the south of the ash stack, but from all of the boreholes to the south of the ash stack must be analysed for $Cr6^+$ at least once a year.

- If any increasing trends in pollution indicator element concentrations become evident, further investigations must be undertaken to determine the extent and possible pollution interception.

- All excessive brine irrigation must be stopped as soon as possible (in line with the commissioning of the brine disposal propject) and dust suppression should be continued by making use of water from the dirty water dams.

- Further studies and research regarding the analyses methods of $Cr6^+$ and the chemical processes (conversion to $Cr3^+$ and retention factors of $Cr6^+$) within the specific chemical environment and site conditions at Tutuka must be undertaken.

- With the advances of the ash stack to the east and south, it is recommended that additional boreholes be drilled through both the new and old parts of the ash stack in order to determine and monitor the water levels in and below the stack. Water levels should be recorded in order to establish trends in the drying process of the ash stack.

- Additional boreholes must also be drilled to the east of the currently advancing ash stack in order to establish current groundwater qualities and to serve as future monitoring boreholes. Should the spreading of the pollution plume towards the Wolwe Spruit become evident, further investigations for containing the plume must be undertaken.

- The continuation of proper management of the dirty / clean water separation system south and east of the ash stack is of utmost importance to limit the spreading of pollution along the natural drainage system of the Wolwe Spruit. Ponding and standing water increases the seepage of pollutants into the groundwater.

Louis J van Niekerk (Pr.Sci.Nat.)